

# Composite Fibrin Scaffold for Skeletal Muscle Regeneration

A Major Qualifying Project Report

Submitted to the Faculty

of

Worcester Polytechnic Institute

in partial fulfillment of the requirements for the

Degree of Bachelor Science

By

---

Alexandra Burr

---

Anthony Campagna

---

Janine Fatal

---

James Lin

---

Elizabeth van Zyl

Advisors:

---

Professor George Pins

---

Professor Jeannine Coburn

April 27, 2017

# Table of Contents

Table of Contents .....	1
Authorship .....	3
Table of Figures .....	5
Table of Tables .....	7
Acknowledgements.....	8
1.0 Introduction.....	9
2.0 Literature Review.....	14
2.1 Volumetric Muscle Loss (VML).....	14
2.1.1 Current Treatment Methods for VML.....	15
2.1.2 Clinical Need .....	17
2.2 Skeletal Muscle.....	18
2.2.1 Structure and Properties.....	18
2.2.2 Skeletal Muscle Regeneration.....	20
2.3 Tissue Engineering Scaffolds.....	24
2.3.1 Current Scaffold Technology.....	26
2.3.2 Biophysical and Biochemical Cues in Scaffolds .....	34
2.3.3 Controlling the Release of Growth Factors.....	42
2.4 Summary and Need.....	47
3.0 Project Strategy.....	48
3.1 Stakeholders.....	48
3.2 Initial Client Statement .....	49
3.3 Constraints .....	50
3.4 Objectives .....	51
3.5 Quantitative Analysis of Objectives .....	55
3.6 Functions and Specifications .....	57
3.6.1 Function 1: Fabricated with over 90% success and require under 2 hours user labor .....	57
3.6.2 Function 2: Promotes Cellular Viability .....	58
3.6.3 Function 3: Prolongs Degradation to Preserve Partial Structural Integrity for Two Weeks .....	59
3.6.4 Function 4: Promotes Nuclear Alignment Along Fibrin Threads at Angles <10 Degrees Relative to the Thread.....	60
3.6.5 Function 5: Releases 10 ng of FGF-2 over a period of two weeks .....	60
3.7 Engineering Standards .....	61
3.8 Revised Client Statement.....	63
4.0 The Design Process.....	64
4.1 Needs Analysis.....	64
4.2 Design Alternatives.....	65
4.2.1 Fabrication Optimization Means.....	66
4.2.2 Cellular Survival Means.....	67
4.2.3 Prolong Degradation Means.....	72
4.2.4 Promote Aligned Myogenesis Means .....	74
4.2.5 Controlled Release Means .....	78
4.3 Means Evaluation.....	83
4.4 Feasible designs .....	85
4.5 Final Design.....	90
5.0 Design Verification.....	90

5.1 Composite Fabrication Optimization .....	91
5.2 Cellular Viability .....	96
5.3 Degradation Study .....	100
5.4 Alignment analysis.....	103
5.5 Release Characterization.....	107
5.6 FGF-2 Functional Assay .....	110
6.0 Final Design and Validation .....	111
6.1 Overview of Composite Fabrication .....	111
6.2 Impact Analysis of Device.....	117
6.2.1 Economic Impact .....	117
6.2.2 Environmental Impact.....	118
6.2.3 Health and Safety Impact.....	119
6.2.4 Societal Impact.....	120
6.2.5 Political Impact .....	120
6.2.6 Ethical Impact .....	121
6.2.7 Manufacturing Impact.....	121
6.2.8 Sustainability.....	121
7.0 Discussion.....	122
8.0 Conclusions and Recommendations .....	124
References.....	127
Appendices.....	136
Appendix A: Gantt Charts .....	136
Appendix B: Constraints Test for Developed Means .....	140
Appendix C: Pairwise Comparison Charts of clients, users, and design team.....	141
Appendix D: Summary of Pairwise Comparison Charts .....	166
Appendix E: Weighted Sub-Objectives .....	177
Appendix F: Means Evaluation Matrix.....	180
Appendix G: Standard Curve for Cell Viability Assay.....	181
Appendix H: Experiment Protocols .....	182
Fibrinogen and Thrombin Aliquot Preparation.....	182
User Manual for LACEY .....	185
Fibrin Composite Scaffold Fabrication Protocol .....	210
Resazurin Cell Viability Assay Protocol .....	211
Laser Thickness Measurements .....	212
Human FGF-2 Standard ABTS ELISA Protocol.....	212
EDC/NHS Crosslinking with Heparin Protocol.....	215
Glycine Quenching Protocol.....	215
Loading of FGF-2 Protocol.....	215
Instron Testing Protocol.....	216
Alignment Analysis Protocol .....	222
Degradation Analysis Protocol .....	227
Appendix I: Raw Data Table for Alignment Analysis.....	230

# Authorship

1.0 Introduction	Anthony Campagna, James Lin
2.0 Literature review	All
2.1 Volumetric Muscle Loss (VML)	Janine Fatal
2.1.1 Current treatment methods for VML	Janine Fatal
2.1.2 Clinical need	Alex Burr
2.2 Skeletal muscle	Janine Fatal
2.2.1 Structure properties	Alex Burr, James Lin
2.2.2 Skeletal muscle regeneration	Janine Fatal
2.3 Tissue engineering scaffolds	James Lin
2.3.1 Current Scaffold Technology	Elzani van Zyl
2.3.2 Biophysical and Biochemical Cues in Scaffolds	James Lin
2.3.3 Growth factor delivery	Anthony Campagna
3.0 Project strategy	Alex Burr
3.1 Stakeholders	Alex Burr
3.2 Initial client statement	Alex Burr
3.3 Constraints	Alex Burr
3.4 Objectives	Alex Burr
3.5 Qualitative analysis of objectives	Janine Fatal
3.6 Functions and Specifications	All
3.7 Engineering Standards	James Lin
3.8 Revised client statement	Alex Burr
4.0 The Design Process	Alex Burr
4.1 Needs Analysis	Anthony Campagna
4.2 Design Alternatives	Elzani van Zyl, Anthony Campagna
4.2.1 Fabrication Optimization Means	Anthony Campagna
4.2.2 Cellular Survival Means	Elzani van Zyl
4.2.3 Prolong Degradation Means	James Lin
4.2.4 Promote Myogenesis Means	Elzani van Zyl
4.2.5 Controlled Release Means	Anthony Campagna
4.3 Means Evaluation	Anthony Campagna, Elzani van Zyl
4.4 Feasible Designs	Alex Burr, Janine Fatal
4.5 Final Design	Alex Burr
5.0 Design Verification	Anthony Campagna
5.1 Composite Fabrication Optimization	Alex Burr
5.2 Cellular Survival	Alex Burr, Janine Fatal
5.3 Degradation Study	James Lin
5.4 Alignment Analysis	Elzani van Zyl
5.5 Release Characterization	Anthony Campagna
5.6 FGF-2 Functional Assay	Anthony Campagna
6.0 Final Design and Validation	All N/A

6.1 Fabrication of Composite	All
6.2 Impact Analysis	James Lin
7.0 Discussion	All
8.0 Conclusions and Recommendations	All

# Table of Figures

Figure 1: Histologic sections showing collagen fibers within regenerated muscle tissue stained using hemtatoxylin and eosin (H&E) and Masson’s Trichrome. (Li, 2014). .....	16
Figure 2: Satellite cell specification during the its development and activation, proliferation, and differentiation during a muscle injury (Yoseph, 2015).....	20
Figure 3: Segments B, C, and D in the figure show the proliferation of satellite cells, their fusion into immature myofibers, and their fusion with existing healthy fibers. Segments E, F, and G show the inhibition of this process due to fibroblast infiltration and collagen formation, which occurs in VML as a result of destruction of the basal lamina. (Grasman, 2015). .....	24
Figure 4: Biophysical and Biochemical cues which make up the synthetic niche for satellite cells for regeneration (Cezar, 2015).....	25
Figure 5: Current clinically successful GFs, showing that some are multifunctional.....	42
Figure 6: Temporal drug release mechanisms. (Uhrich, 1999).....	44
Figure 7: Release profile of GFs FGF-2 (○), TGF-β1 (●), BMP-2 (Δ), and VEGF (▲) from a gelatinous hydrogel into PBS. (Yamamoto et al., 2001). .....	45
Figure 8: Cumulative release of FGF-2 from fibrin gels prepared at different fibrinogen concentrations (Group V, fibrinogen, 9.4 mg/ml (○); Group II, fibrinogen, 94.3 mg/ml (●); Group VI, fibrinogen, 188.6 mg/ml (▼)) with thrombin (NIH U/ml) in the presence of heparin (166.7 μg). The values represent the mean ± S.D. (n = 5). (Jeon, 2005).....	47
Figure 9: Project objective and sub-objective tree .....	52
Figure 10: Diffusion drive release of FGF-2 .....	79
Figure 11: Degradation induced FGF-2 release .....	81
Figure 12: Immobilization of FGF-2 using heparin.....	82
Figure 13: Polymer encapsulation for controlled release.....	83
Figure 14 Film with Microthreads, FGF-2 immobilized using heparin and EDC/NHS crosslinking.....	85
Figure 15: Film with microthreads, FGF-2 incorporated and released with degradation and UV crosslinked .....	86
Figure 16: Gel with microthreads, FGF-2 immobilized using heparin and EDC/NHS crosslinked .....	87
Figure 17: Gel with microthreads, FGF-2 released with degradation and UV crosslinked .....	88
Figure 18: Film with microthreads and patterned surface, FGF-2 released with degradation and EDC/NHS crosslinked .....	89
Figure 19: Final Design .....	90
Figure 20: Experimental design of cell viability assay .....	97
Figure 21: Results from cell viability assay from all 3 trials .....	98
Figure 22: Overall results from cell viability assay .....	99
Figure 23: An example showing potential differences in degradation based on time for the composites that are crosslinked vs uncrosslinked.....	101
Figure 24: Experimental layout for degradation study where UNX = uncrosslinked composite and EDC/NHS = crosslinked composite using EDC/NHS solution .....	102
Figure 25: Average area remaining over the course of 14 days for crosslinked and uncrosslinked samples .....	103
Figure 26: Cartoon depiction of the composite scaffold and the regions (outlined in red) that were imaged for each sample .....	104
Figure 27: A depiction of ideal nuclear alignment along the thread for an imaged region. The nuclei closest to the thread would be quantified at 0 degrees and the angle increase as they move farther away from the thread.....	105
Figure 28: Angle frequency for composite samples .....	106
Figure 29: Angle frequency for film samples .....	106

Figure 28: FGF-2 loading methods.....	108
Figure 29: Burst release profile from scaffold .....	109
Figure 30: Extended release profile from scaffold.....	110
Figure 32: Blending applicator set up as described in steps 2 - 4. ....	113
Figure 33: Syringe pump set up .....	114
Figure 34: Extrusion head with pipette tip and polyethylene tubing set up.....	114
Figure 35: Teflon pan inserted into frame on corner notches indicated by red arrows.....	114
Figure 36: Shoe frame placed into machine over Teflon pan. ....	115
Figure 37: Fibrin microthreads stretched and being dried .....	115
Figure 38: Full year Gantt chart.....	136
Figure 39: A-Term detailed Gantt chart.....	137
Figure 40: B-Term detailed Gantt chart.....	138
Figure 41: C-term detailed Gantt Chart .....	139
Figure 42: MP Biomedical Certificate for Fibrinogen.....	187
Figure 43: Blending applicator set up as described in steps 2 - 4. ....	190
Figure 44: Syringe pump set up .....	191
Figure 45: Extrusion head with pipette tip and polyethylene tubing set up.....	191
Figure 46: Teflon pan inserted into frame on corner notches indicated by red arrows.....	192
Figure 47: Pouring HBS into Teflon pan .....	192
Figure 48: Inverted shoe frame .....	193
Figure 49: Inverted shoe frame with shoes placed into shoe sliders, yellow arrows indicating sloped edges, red arrows indicating roughened edges.....	194
Figure 50: Clip securing shoe in shoe slider. ....	194
Figure 51: Top view of clips securing shoes into shoe sliders.....	195
Figure 52: Reverted shoe frame with shoes secured in place. ....	195
Figure 53: Shoe frame placed into machine over Teflon pan. ....	196
Figure 54: Clips flush against shoe sliders.....	196
Figure 55: Squeegee pieces in place on top of extruded threads. ....	202
Figure 56: Squeegee pieces in place on top of extruded threads. ....	203
Figure 57: Emergency stop button highlighted by red square. ....	204
Figure 58: Extruded threads using 45 degree cut in tubing. ....	208

# Table of Tables

Table 1: List of the many biochemical cues natural in the body and their function (Horsley, 2004).....	39
Table 2: Some of the GFs currently being researched with success and the actions they perform (Whitaker, 2001).....	40
Table 3: Project constraints.....	50
Table 4: Main objective definitions .....	52
Table 5: Sub-objective definitions: user friendly.....	53
Table 6: Sub-objective definitions: cost efficient .....	53
Table 7: Sub-objective definitions: robust scaffold mechanical properties .....	54
Table 8: Sub-objective definitions: reproducible composite fabrication .....	54
Table 9: Sub-objective definitions: promote myogenesis.....	54
Table 10: Sub-objective definitions: promote angiogenesis .....	54
Table 11: Sub-objective definitions: promote innervation.....	54
Table 12: Scores of main objectives by category.....	56
Table 13: Weights of main objectives.....	56
Table 14: Ranked objectives by percentage.....	64
Table 15: Means for each function .....	66
Table 16: Pros and cons for fibrin gel to promote cellular survival.....	67
Table 17: Pros and cons for fibrin film to promote cellular survival.....	69
Table 18: pros and cons for fibrin microthreads to promote cellular survival.....	70
Table 19: Pros and cons for fibrin gel with microthreads to promote cellular survival.....	71
Table 20: Pros and cons for fibrin film to promote cellular survival.....	71
Table 21: Pros and cons of chemical crosslinking to allow for isomorphous degradation .....	73
Table 22: Pros and cons of UV crosslinking to allow for isomorphous degradation.....	73
Table 23: Pros and cons of protease inhibitors to allow for isomorphous degradation .....	74
Table 24: Pros and cons for fibrin microthreads to promote aligned myogenesis.....	75
Table 25: Pros and cons for patterned surfaces to promote aligned myogenesis.....	76
Table 26: Pros and cons for fibrin microthreads and peptide ligands to promote aligned myogenesis.....	77
Table 27: Pros and cons for fibrin microthreads and patterned surfaces to promote aligned myogenesis ..	77
Table 28: Pros and cons for patterned surfaces and peptide ligands to promote aligned myogenesis.....	78
Table 29: Pros and cons for diffusion to allow for controlled release .....	80
Table 30: Pros and cons of a degradation driven system to allow for controlled release .....	81
Table 31: Pros and cons of immobilization using heparin to allow for controlled release .....	82
Table 32: Pros and cons of polymer encapsulation to allow for controlled release.....	83
Table 33: Summary of means evaluation.....	84
Table 34: Morphology chart 1 .....	86
Table 35: Morphology chart 3 .....	87
Table 36: Morphology chart 4 .....	88
Table 37: Morphology chart 5 .....	89
Table 38: Results from acetyl slide coating experiment .....	92
Table 39: Results for alignment method experiment .....	93
Table 40: Results from acetyl slide coating experiment .....	94
Table 41: Results for alignment method experiment.....	95
Table 42: Results from rinse time and volume experiment .....	95
Table 43: t-test p-values.....	100

# Acknowledgements

The team would like to acknowledge all of those that made our project successful and possible: the Biomedical Engineering (BME) Department for funding and overseeing our project, our advisors Dr. George Pins and Dr. Jeannine Coburn for advising our project and helping it be successful, and Meagan Carnes for helping the team in the lab and providing user feedback. Additionally, thank you to Joanna Santos and Megan Chrobak for providing additional assistance in the lab and feedback, as well as the BME department head, Kristen Billiar.

# 1.0 Introduction

As military technology advances, modern warfare has caused more devastating injuries to soldiers on the battlefield. In parallel with the advancements in modern warfare, the survival rate of critically wounded soldiers has improved with better trauma wound care (Devore, 2011). As more soldiers survive their combat wounds, they must face the consequences of devastating functional and morphological skeletal muscle tissue damage. During the most recent military operations, Operation Iraqi Freedom and Operation Enduring Freedom, an estimated 82% of the soldiers injured on the battlefield suffered from at least one musculoskeletal extremity wound (Devore, 2011). These combat wounds can cause volumetric muscle loss (VML) where severe muscle damage results in inadequate functional recovery. Furthermore, there are many more causes of VML other than wound trauma, such as accidents including car crashes, sports injuries, and burns (Eckardt, 2003).

Skeletal muscle accounts for 40% of the adult human body's mass, and as robust as it is in terms of responding to physiological changes, can be damaged by an injury which can affect its ability to remodel, repair, and regenerate (Yin, 2013). Skeletal muscle is composed of myofibers, neurons, vasculature networks, and connective tissue (Yin, 2013). The innate skeletal muscle regeneration capacity is directed by satellite cells (SCs) or skeletal muscle stem cells (Yoseph, 2015). Quiescent SCs become activated during injury to reconstruct muscle tissue (Tedesco, 2010). However, when skeletal muscle is damaged significantly, native SCs and their microenvironment are compromised, hindering the body's natural ability to direct regeneration (Yoseph, 2015).

Current solutions for the treatment of VML consist of autologous tissue transfers from other healthy regions of the patient's body to the injury site. Despite being the most common

treatment method, these grafts can result in failure, scar tissue formation and necrosis (Eckardt, 2003). For these wounds to be treated more effectively and consistently an alternative solution must be developed.

Myofibers are the structural and functional element of skeletal muscle, and each one is encased by a basement membrane where SCs reside (Sanes, 2003). VML results in the destruction of the basement membrane, causing the wound site to lose the necessary cues provided naturally by this layer (Yin, 2013). The lack of basement membrane impairs muscle regeneration since SCs no longer have guides or cues that promote migration and alignment (Tedesco, 2010). Additionally, the lack of muscle tissue is coupled with a lack of structural support for cellular growth at the wound site.

SCs are considered the initial guides that trigger muscle regeneration. Researchers have investigated how the niche, or biological environment of SCs may guide their performance (Yoseph, 2015). The SC microenvironment consists of extracellular matrix (ECM), vascular and neural networks, growth factors (GFs), and cytokines (Yoseph, 2015). By understanding their niche, tissue engineers may be able to develop therapies to successfully treat VML. The goal of these tissue engineered strategies is to provide auxiliary cues, often using natural chemicals, to signal the body to regenerate the damaged or missing muscle tissue.

Biomimetic scaffolds are engineered to mimic the endogenous SC niche to induce the activation of SCs from surrounding tissue for muscle regeneration at the wound site. (Bae, 2012; Cezar, 2015; Yin, 2013). By implanting an engineered scaffold, it can act as a source of nutrients and delivery vehicle for GFs, provide topographical cues for cellular alignment, as well as provide temporary structural support at the injury site (Ahmed, 2008; Cornwell, 2007). Another

benefit of tissue engineered scaffolds is its 3D structure that has been shown to induce cell differentiation, similar when in native ECM (Chen, 2015).

A promising material for biomimetic scaffolds is fibrin, the polymerized product of the glycoprotein fibrinogen and the enzyme thrombin (Cornwell, 2007). Fibrin is advantageous because of its modular and tunable capabilities (Grasman, 2012; Grasman, 2015). Fibrin is also an important factor in wound healing and tissue repair (Cornwell, 2007). Fibrin's matrix facilitates tissue regeneration by promoting migration, adhesion, and proliferation of cells while directing cell signaling via integrin-based mechanisms (Clark, 2001). For instance, fibrin microthreads, fibrin extruded into long thin threads, have been used for the restoration of VML defects in the skeletal muscle of mouse models (Page, 2011). The fibrin microthreads were created because they are similar to the hierarchical cable-like structure of skeletal muscle fibers (Grasman, 2015; Page, 2011). GFs can be incorporated into fibrin to facilitate controlled release to enhance skeletal muscle regeneration (Grasman, 2015) Although fibrin has advantageous properties, some limitations include rapid scaffold degradation and the GF release is still too rapid and not able to sustain its release for effective skeletal muscle regeneration (Grasman, 2015)

The goal of the project was to make progress towards the development of a fibrin-based scaffold to treat VML in a clinical setting. Specifically, the project aims were to create a platform technology using a fibrin composite scaffold that will release growth factors in a controlled manner while being user friendly, easy to handle and providing structural support. Finally, it will allow for further development by future MQP groups to expand, layer or potentially stack the composite for a full-thickness model.

The project involved designing, developing and testing a tissue engineered scaffold for the regeneration of skeletal muscle tissue. A series of Gantt charts, Appendix A, were used to

track the team's progress. The design team worked with the clients and users to develop a set of objectives and constraints for the scaffold. From the initial set of objectives, the design team interviewed clients and users and reviewed current literature to refine and expand the objectives to encompass the project goals. A list of constraints were utilized, Appendix B, in order to limit the project's scope. Additionally, the team defined sub-objectives for each of the main objectives. The sub-objectives were defined to further clarify the important aspects for the project.

Once the objectives were finalized, the clients, users and designers conducted comparison analysis to determine the most important scaffold properties. It was determined that developing a scaffold that **promoted myogenesis**, was **reproducible**, had **robust properties**, and was **user friendly** were the most important features for the scope of the project. The design team then used these prioritized objectives to develop a series of needs, or requirements of the scaffold, which were translated into the five primary scaffold functions:

1. Fabricated with over 90% success and require under 2 hours user labor
2. Promotes cellular viability without significant difference between composite and positive control
3. Slows degradation to preserve partial structural integrity for two weeks
4. Promotes nuclear alignment along fibrin threads at angles <10 degrees relative to the thread
5. Releases 10 ng of FGF-2 over a period of two weeks

After functions were developed to satisfy the needs, different possible solutions were researched to carry out the functions, known as means. The means were then ranked based on the priority objectives to see which would be the best at accomplishing their specific function. Once the means were ranked, a series of feasible designs were created by identifying the highest

ranked combinations of means for each function. After doing an analysis of all the possible designs, a final design of a fibrin film with fibrin microthreads, controlled release of FGF-2 loaded to the surface using heparin immobilization, and chemically crosslinked was evaluated to have the highest success rate.

Once the final design was selected, experimentation was conducted to optimize the design. Initially, feasibility studies were performed to test different steps of the protocol and try to maximize the number of usable scaffolds during production and reduce user labor time. These tests were successful and allowed the design team to move forward with validating that it was user friendly, easy to handle and required little user labor. The scaffold was analyzed for release of FGF-2 using an ELISA (Peprotech) to monitor release kinetics of the GF from the scaffold. Additionally, an aresazurin assay was used to characterize cell viability, Hoechst stain to allow for visualization of cellular alignment along the threads and a protocol was developed to analysis the degraded area of scaffold over time to study crosslinking efficacy.

Through these experiments, the team was able to conclude that the scaffold allows for controlled release of FGF-2 over 14 days with and without heparin immobilization to the surface. The scaffold was able to promote cellular viability just as well as a positive control tissue culture plate without a significant difference. The incorporation of fibrin microthreads increased cellular preference for alignment compared to cells placed on a film scaffold. Finally, chemical crosslinking of the composite preserved 94% of the composite area after 14 days with cells seeded on the scaffolds and left in media. Overall, the composite scaffold is a successful structurally supportive, user friendly scaffold that delays degradation and releases growth factor for two weeks while promoting cellular viability and alignment.

The major aim of this project was to create a functional composite scaffold that can be developed into a full-thickness scaffold in the future. Further characterization and modification

of the scaffold components are required before moving forward with creating a functional composite scaffold. For instance, the experiments that would need to be completed, is a functional assay of the composite loaded with growth factor and cells to quantify cell differentiation and observe myotube formation, as well as long-term experiments to test the scaffold over the 3-6 week long repair phase. Once the components are optimized, future work with the fibrin-based scaffold could focus on the creation of a full-thickness scaffold. The scaffold will also need to be further characterized and tested in-vivo. Although this scaffold is for skeletal muscle regeneration after traumatic injury, in the future, it may be possible extended to other skeletal muscle loss such as aging, disease, or inactivity.

## 2.0 Literature Review

The literature review includes an overview of volumetric muscle loss (VML), including the causes, prognosis, and current treatment methods. By identifying insufficiencies in the current treatments, the need for a tissue engineered scaffold becomes clear. The properties and natural regeneration of skeletal muscle tissue were also reviewed to further understand and identify important aspects of the process. By further understanding the process of skeletal muscle regeneration, endogenous cues can be incorporate into a tissue engineered scaffold to improve regenerative capabilities. This chapter is a review of current technologies in research that explore scaffolds as a solution along with their advantages and disadvantages.

### 2.1 Volumetric Muscle Loss (VML)

Each year, VML injuries that occur as a result of combat injuries, car accidents, sports injuries, tumor ablation procedures, and reconstructive surgeries affect 5.8 million Americans

and account for 20 billion dollars in health care expenses (ASPS, 2015). This type of injury is characterized by extensive musculoskeletal damage that hinders functional regeneration. VML injuries usually involve the loss of 20% or more volume of muscle in a particular area of the body (Turner, 2013). The majority of combat wounds are extremity injuries, 53% of which involve VML (Owens, 2008). Additionally, 64% of all soldiers who are considered unfit for continued duty are those with VML (Owens, 2008; Masini, 2009). Although these injuries are not always life-threatening, they can severely impact the quality of life of patients. Chronic pain for the remainder of a patient's life often occurs due to the large-scale loss of the muscle tissue. Significant loss of muscle tissue results in limited functional regeneration and the formation of nonfunctional scar tissue. The destruction of the basement membrane, which normally contains GFs, SCs, and other biochemical cues, results in inhibited regeneration (Turner, 2012).

### 2.1.1 Current Treatment Methods for VML

If VML injuries are acute, physical therapy may be sufficient (Dziki, 2016). However, in most cases surgical intervention is required. The current gold standard for the treatment of VML is autologous tissue transfer, in which several studies have been performed with *in vivo* models and *in vitro* models. This is a surgical procedure in which muscle tissue is removed from a healthy area and grafted onto the site of the injury (Eckardt, 2003). This procedure has many limitations because it is complicated, time consuming, and does not consistently achieve functional muscle regeneration (Äärimaa, 2004). Additionally, 10% of these surgeries result in infection or tissue necrosis (Eckardt, 2003). Many patients with a tissue graft experience chronic pain for years after the surgery, which in some cases can be so severe that patients request amputation (Huh, 2011).

To understand how debilitating VML injuries are, *in vivo* models were used to study the viability of tissue grafts in repairing muscle function. In a study of quadriceps grafts in rats,

significant loss of muscle function was observed, with the injured legs exhibiting 55% less strength than the uninjured control legs, four weeks after the injury (Li, 2014). Extensive fibrosis was observed that resulted in scar tissue formation. Muscle contractility measurements showed an extreme reduction in strength. In Figure 1, the control images show that collagen fibers are not present in healthy muscle tissue. The lack of organization of the extracellular matrix (ECM) due to the orientation of the autograft inhibited functional recovery of the muscle, which is consistent with much of the literature that suggests that structural alignment is necessary for functional recovery. In addition, peripheral nerve damage caused severely hindered muscle function, highlighting the importance of innervation in muscle regeneration (Li, 2014).

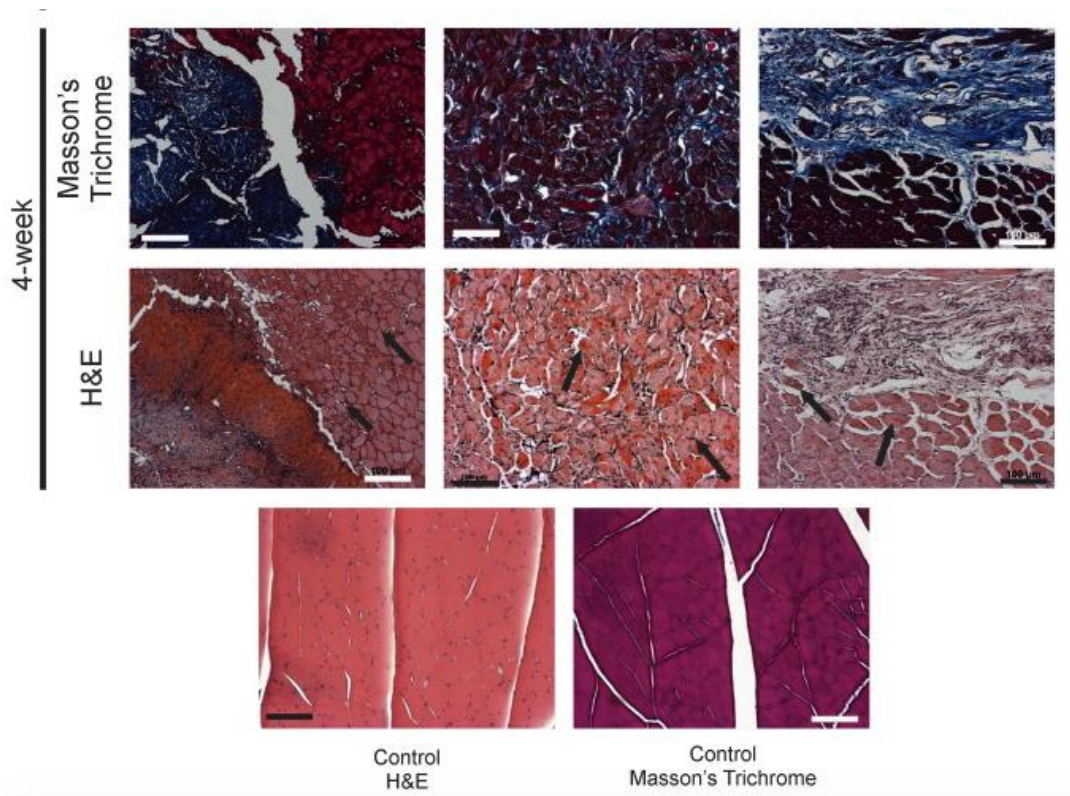


Figure 1: Histologic sections showing collagen fibers within regenerated muscle tissue stained using hemtatoxylin and eosin (H&E) and Masson's Trichrome. (Li, 2014).

Garg et al. performed a study in a rat “open fracture” model with VML. Male Lewis rats were divided into four experimental groups: Sham-operated, Osteotomy, VML injury, and Osteotomy + VML injury (Garg, 2015). The sham group was uninjured, the Osteotomy group had a piece of the tibia surgically removed, the VML injury group had tibialis anterior (TA) muscle injury, and the Osteotomy + VML injury group had both. Persistent functional deficits were found as well as increased stiffness due to scar tissue formation in the groups with VML. It was shown that VML resulted in weak repair tissue that persisted even after bone healing. The maximal force was significantly decreased in the Osteotomy + VML injury group and the VML injury group only compared to the Osteotomy only group and the uninjured sham. It was also found that the severity of muscle functional deficits was dependent on the length of the muscle and the joint angle (Garg, 2015). This study among many others shows that VML is a severely debilitating injury that requires either physical therapy, which does not correct muscle deficit, or surgical muscle transfers, which lack in restored function, indicating a need for a better and more reproducible way of treating VML (Dziki, 2016; Garg, 2015).

### 2.1.2 Clinical Need

Although current studies have furthered the understanding of VML, they have not resulted in a standardized or consistent strategy to address VML or restored muscle function (Li, 2014). Moderate success has been achieved but the persistence of functional deficits in the injured area highlight the need for an improved treatment of VML that promotes functional regeneration of muscle tissue.

In addition to the lack of functional muscle or healing occurring with physical therapy or orthotics, there are many limitations as mentioned above with the current treatment strategies. Current autologous transfer procedures involve the possibility for donor site morbidity and may

not provide an environment that is favorable for tissue reconstruction or angiogenesis (Dziki, 2016). Due to the numerous adverse effects of these current treatments for VML, they result in muscle function deficiency weakness and overall reduced quality of life. Because of the inability of current VML solutions to restore skeletal muscle function, there exists a need for a solution that induces muscle regeneration.

## 2.2 Skeletal Muscle

In order to assess the best solutions for VML, there needs to be an understanding of the structure and functions of native skeletal muscle, and more importantly, how the natural repair process takes place. A treatment method will need to mimic and function similarly to the highly aligned, innervated, and vascularized native tissue in order to signal the appropriate biochemical and biophysical cues for regeneration. An emphasis will be placed on recreating the processes and environment that occur during the repair phase of native muscle regeneration.

### 2.2.1 Structure and Properties

Skeletal muscle consists of highly innervated, and vascularized myofibrils that are aligned for contraction. The somatic motor neurons innervate the tissue branch to affect a number of muscle fibers. For skeletal muscle contraction to occur there needs to be an action potential signaled to the somatic motor neuron which controls several individual muscle fibers. These muscle fibers are multinucleated because of fusion between the myoblast cells. Resting directly above the myofibers are the motor units that consists of a somatic motor neuron and neuromuscular junctions to the myofibers, which facilitates contraction. These motor units are the endings to axons that originate from the spinal cord and are controlled by the central nervous system. Because a somatic motor neuron can stimulate many muscle fibers at once, it allows

contraction of the entire muscle to occur synchronously. This is also facilitated by the alignment of the muscle fibers and ability to contract in the same longitudinal direction (Fox, 1996).

Surrounding the muscle fibers is the ECM made up of structural proteins including collagen (type I-IV) and elastin, and specialized proteins including fibronectin, various laminins and integrins, and proteoglycans. Within muscle tissue, a basement membrane encases each myofiber and provides structural support. The basement membrane, or basal lamina, is mainly composed of collagen and laminin proteins which are cross-linked together in a network of glycoproteins and proteoglycans (Sanes, 2003). Heparin sulfate proteoglycans modulate growth factor activity and protect them from denaturation and proteolytic degradation. They also collaborate with other components of the ECM to define the structure of the basement membrane (Sarrazin, 2011).

Another important property of muscle tissue is vascularization. Within the ECM, the vasculature providing oxygen and nutrients to the muscle fibers and other cells located within the tissue. Compared to tissue such as bone, muscle tissue is highly vascularized (Sanes, 2003). Overall, it is important that muscle tissue consists of highly aligned myofibers that are innervated and vascularized to function properly.

Another important component of skeletal muscle are the SCs beneath the basal lamina. SCs serve as myogenic precursors for muscle growth and repair. Specifically, SCs that express the transcription factor paired box 7 (Pax7) are required for skeletal muscle regeneration in response to injury (Cezar, 2015). SCs exhibit properties similar to archetypal stem cells and are essential in forming the basal origin of adult muscle regeneration. (Collins, 2005). The mechanism of how SCs function is shown in Figure 2. SCs are dormant until injury occur, at which point they are activated by growth factors such as HGF and FGF-2 to initiate muscle regeneration (Collins, 2005). SCs guide myogenic regulatory factors (MRF) such as MyoD,

Myf5, Myogenin, and MRF4 which further promote SC proliferation. The proliferation of SCs is followed by differentiation and fusion to form multinucleated myofibers that allow for highly functional skeletal muscle (Yoseph, 2015).

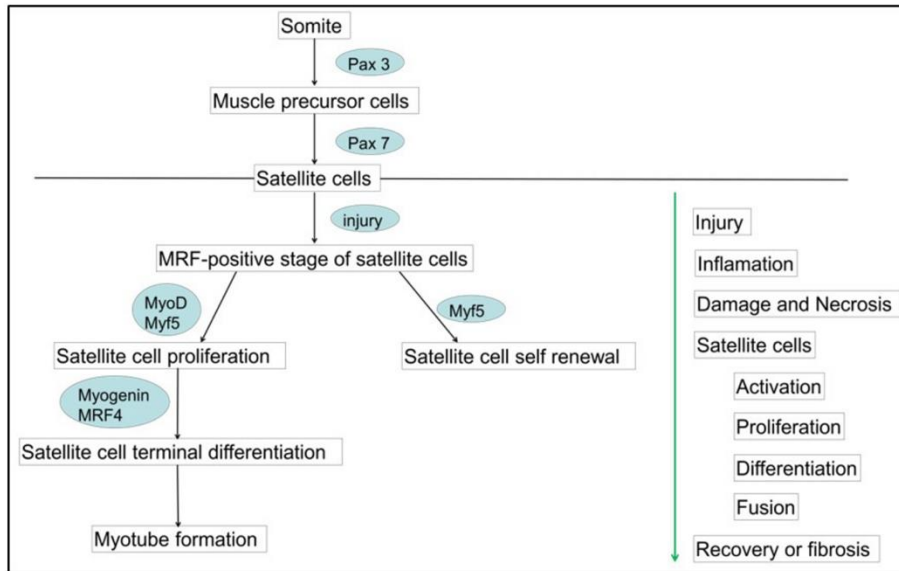


Figure 2: Satellite cell specification during its development and activation, proliferation, and differentiation during a muscle injury (Yoseph, 2015)

Numerous studies have since revealed that the proliferation and differentiation of SCs during muscle regeneration is profoundly influenced by innervation, vasculature, GFs, hormones, nutrition, and the extent of the injury (Bae, 2012; Yoseph, 2015). By mimicking the biological environment or niche, SCs can function better and effectively regenerate injured muscle tissue.

### 2.2.2 Skeletal Muscle Regeneration

Skeletal muscle has the innate capability of natural repair, which requires a complex, stepwise process and the coordination of a variety of cell types. However, this process, as described below, can only occur naturally in response to minor muscle damage from injuries such as small lacerations, contusions or sports-related tears (Cezar, 2015). When extensive damage has occurred due to severe trauma from vehicular accidents and combat injuries, factors

such as poor cell migration, and rapid death hinder the natural process. The three sequential, overlapping main phases of muscle regeneration are the inflammatory phase, the repair phase, and the remodeling phase (Cezar, 2015).

During the inflammatory phase, the body breaks down and removes damaged tissue. Plasma membrane dissolution resulting from muscle fiber necrosis activates the complement cascade. Inflammation occurs as neutrophils migrate to the injury site within two hours to degrade damaged myofibers after necrosis has taken place (Tidball, 2010). The peak neutrophil concentration occurs between six and twenty-four hours. Myeloperoxidase (MPO) is released by these neutrophils and induces damage of the muscle membrane. Through the production of free radicals, neutrophils target the damaged debris from the membrane for phagocytosis (Nguyen, 2005). Necrotic myofibers are engulfed via phagocytosis by pro-inflammatory M1 macrophages, which become the primary cell type at the injury site within two days (Tidball, 2010). Anti-inflammatory M2 macrophages begin to replace M1 macrophages over the next three to seven days and increase myoblast proliferation and differentiation through the secretion of interleukin 10 (IL-10), preparing the injury site for the next stage of regeneration, the repair phase (Deng, 2012).

The repair phase has a duration of three to four weeks and is characterized by satellite cell activation, proliferation, and migration, and is further broken down into two sub-phases. The first sub-phase is the recruitment and proliferation of SCs, which is triggered by the release of various growth factors such as hepatocyte growth factor (HGF), the only GF that brings SCs back into the cell cycle, from the ECM of muscle fibers, which triggers stimulation of satellite cell proliferation and chemotaxis (Tatsumi, 2004). Other GFs that are involved in signaling proliferation are insulin-like growth factor-1 (IGF-1), vascular endothelial growth factor (VEGF), fibroblast growth factor-2 (FGF-2), fibroblast growth factor-6 (FGF-6), and platelet-

derived growth factor (PDGF) (Tatsumi, 2004). These GFs are also present in the second sub-phase, the differentiation phase (Ciciliot, 2010). As SCs proliferate, they typically migrate in a longitudinal direction along the myofibers (Charge, 2004). When SCs activate and reenter the cell cycle, they express myogenic factor 5 (Myf5), commit to myogenic differentiation, then express myogenic differentiation factor-1 (MyoD) (Cooper, 1999). A major issue in VML is that the basal lamina is ruptured, and the SCs lack the guidance to direct this cell migration and myogenic differentiation (Jarvinen, 2005).

The second subphase of the repair phase, the differentiation phase, is characterized by the differentiation of SCs into mature muscle fibers. Myogenesis occurs as myoblasts produce myogenin and begin to fuse together to form myofibers (Cornelison, 1997). Myogenesis is stimulated by IGF1 and IGF2 (Menetrey, 2000). IGF1 and IGF2 stimulate the proliferation and differentiation of myoblasts, which promote myofiber formation as more myoblasts are able to fuse together. Due to increased availability of insulin-like growth factor receptor-1 (IGRF1) in skeletal muscle, IGF1 has more of an influence in skeletal muscle regeneration than IGF2 (Smith, 1999). The significance of IGF1 in regeneration has been determined by neutralizing IGF1, which inhibited regeneration (Lefaucheur, 1995). Furthermore, IGF1 has been injected into aged rats, to enable the restoration of satellite cells to proliferate (Chakravarthy, 2000). Temporal expression of another growth factor, HGF, for 48-72 hours in the proliferation phase has been shown to inhibit the differentiation phase (O'Reilly, 2008). For functional regeneration, vascularization and innervation must occur simultaneously to the process of myogenesis. IGF1 has been shown to induce sprouting of nerves during the repair phase, which is crucial for functional muscle contractility. At the same time, HGF and IGF2 promote angiogenesis through paracrine signaling (Christov, 2007). Another factor that has been shown to be crucial for angiogenesis, which is crucial for skeletal muscle regeneration, is FGF-2 (Kim,

2010). FGF-2 has also been shown to facilitate myogenesis by recruiting additional satellite cells from the quiescent stage, thus increasing the number of proliferating satellite cells (Yablonka-Reuvini, 1997).

The final stage of skeletal muscle regeneration has the longest duration, on the order of three to six months, called the remodeling phase. Once myofibers are formed in the repair phase, they are able to further mature during the remodeling phase, as they fuse with the existing muscle at the site of the injury (Turner, 2012). Infiltration of fibroblasts, which can start as early as the inflammatory phase, continues into the remodeling phase and replaces damaged connective tissue. Fibroblastic infiltration is crucial for regeneration, but too much fibroblastic activity leads to increased collagen deposition, which remodels into non-functional scar tissue (Jarvinen, 2005). This is often seen in large injuries such as VML, whereas smaller injuries are typically able to recover without the formation of scar tissue. The destruction of the basal lamina by VML is another reason for increased scar tissue formation because the loss of biochemical signaling for satellite cell infiltration results in much higher fibroblast infiltration and a lack of myoblast formation and is shown in Figure 3 (Jarvinen, 2005).

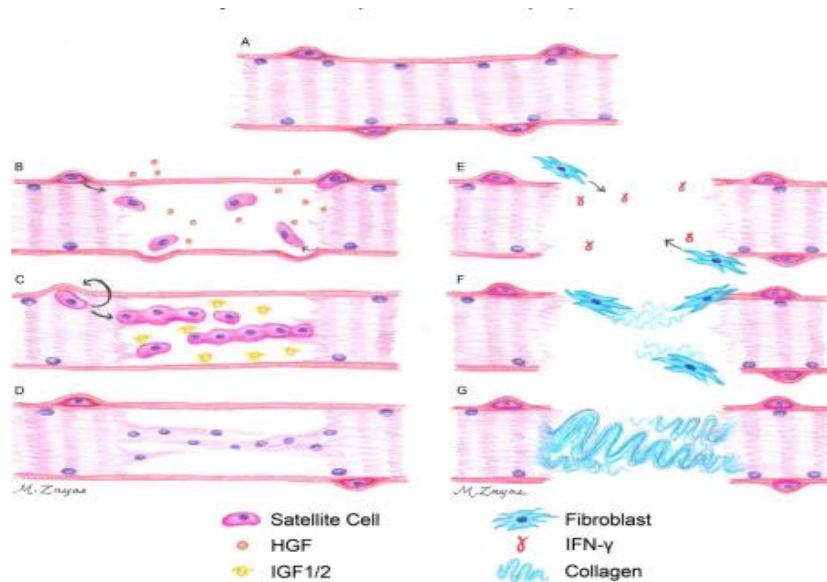


*Figure 3:* Segments B, C, and D in the figure show the proliferation of satellite cells, their fusion into immature myofibers, and their fusion with existing healthy fibers. Segments E, F, and G show the inhibition of this process due to fibroblast infiltration and collagen formation, which occurs in VML as a result of destruction of the basal lamina. (Grasman, 2015).

Throughout the entire process of muscle regeneration, there is a delicate balance between formation of healthy tissue and scar tissue that is determined by the relative infiltration of satellite cells and fibroblasts. VML injuries inhibit the full capacity of the innate repair process. In order to promote this process, intervention is necessary to assist the natural repair process.

## 2.3 Tissue Engineering Scaffolds

Tissue engineering has emerged as a promising solutions for the treatment of VML. Tissue engineering technology encompasses the use of tissue substitutes known as scaffolds for the functional reconstruction of damaged skeletal muscle. Scaffolds can be made from many different materials or combinations of materials, which can be modified for various applications. Benefits of using tissue engineered scaffolds include (Bian, 2008):

1. The ability to engineer custom tissue architecture for precise structural repair at the injury site.

2. The ability to precondition tissue implants to specific mechanically or metabolically demanding environments.
3. The ability to deliver molecules or cells upon implantation.
4. The ability to guide cellular functions.

When designing a scaffold, it is imperative to ensure that the microenvironment created by the scaffold incorporates cues that help signal the SCs to direct the body's natural regeneration. Some of the cues that help signal SCs and help them function are shown in Figure 4. For scaffolds to direct skeletal muscle regeneration it is imperative that they facilitate cell alignment, promote skeletal muscle formation, and stimulate vascularization and innervation (Grasman, 2015). Cell alignment is one of the most influential factors in regeneration. Other strategies to promote regeneration include the incorporation of GFs and peptide sequences within the materials of scaffolds (Grasman, 2015). These strategies involve incorporating cues that mimic the SC niche.

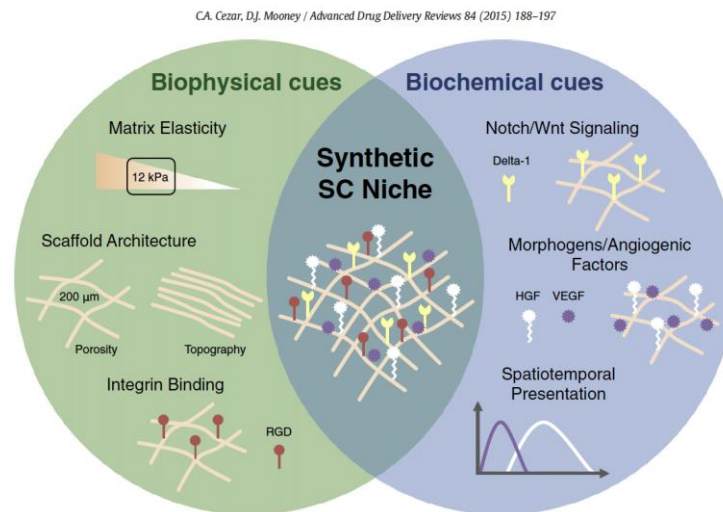


Figure 4: Biophysical and Biochemical cues which make up the synthetic niche for satellite cells for regeneration (Cezar, 2015).

### 2.3.1 Current Scaffold Technology

There are many factors to consider when developing an effective scaffold to promote the regeneration of skeletal muscle. The generally accepted considerations are biocompatibility, promotion of native tissue infiltration, promotion of cell alignment, 3D organization, and biodegradability (de la Puente, 2014). Both synthetic and natural materials have been investigated for use in tissue scaffolds. A major issue with synthetic polymers such as Polylactic Acid (PLA) and Polyglycolic acid (PGA) is that the mechanism by which they degrade forms acidic byproducts that increase pH (Sung, 2004). This can be harmful to the native tissue around the implanted scaffold and lead to scaffold failure (Sung, 2004). Natural materials such as fibrin breakdown through known mechanisms in the body (Page, 2011). Some of the current natural scaffold materials that are being researched include fibrin, alginate, decellularized extracellular matrix, and collagen (Borselli, 2010).

#### 2.3.1.1 Cellular and Acellular Scaffolds

Current research into implantable scaffolds for the regeneration of VML is divided into two categories: cellular and acellular scaffolds. Cellular scaffolds are seeded with cells before implantation, while acellular scaffolds are devoid of cells upon implantation. Cellular scaffolds allow the seeded cells to incorporate with the native tissue, while acellular scaffolds require host cells to migrate into the scaffold (Burg, 2000). Scaffolds with seeded autologous cells may decrease the amount of foreign body response produced but can be very costly and time consuming due to the culture time needed (de la Puente, 2014). An additional limitation of cellular scaffolds is the size of the implant due to oxygen diffusion limitations (Corona, 2016). Acellular scaffolds provide an off the shelf treatment option for VML. The scaffold can be manufactured and packaged without needing to provide a strictly controlled sterile environment

or worry about cell apoptosis on the scaffold (Badylak, 2016). Fibrin, alginate, decellularized extracellular matrix, and collagen scaffolds can all be manufactured with or without cells upon implantation.

#### 2.3.1.2 Fibrin Scaffolds

Fibrin is produced by the polymerization of fibrinogen and thrombin, which forms naturally in the body in response to tissue damage, to create a protein mesh that acts as a support in blood clot formation. Because fibrin is produced in the body, it allows the scaffolds to be more readily accepted by the body. Cells bind readily to fibrin, and the scaffold can also be loaded with GFs (de la Puente, 2011). This allows fibrin to be used as a scaffold for drug delivery to the surrounding tissue. Fibrin scaffolds allow for the proliferation of cells throughout the scaffold, are degradable, and are eventually replaced by extracellular matrix that is produced by the native cells (Huang, 2005). Fibrin scaffolds can be produced in many forms such as gels and threads (Proulx, 2011).

Huang et al. studied the formation of functional muscle *in vivo* through the use of fibrin gels (Huang, 2005). Myoblasts were isolated from the left tibialis anterior muscle of rats, seeded into well plates, and after five days of cell culture, seeded onto a fibrin gel. After two days, myotube formation was observed, after five days the contraction of the gel was almost finalized, and after eight days the engineered structure was electrically stimulated. Upon stimulation, the engineered muscle produced length-tension trends that were characteristic of skeletal muscle. The engineered muscle, however, was only able to produce a fraction of the force that skeletal muscle is able to produce and the myotubes formed were only about a tenth of the size of native skeletal muscle (Huang, 2005).

Page et al. studied the regeneration of muscle defects through the use of fibrin microthreads seeded with adult human muscle-derived cells from discarded muscle flap tissue (Page, 2011). The fibrin threads were formed by mixing fibrinogen and thrombin and extruding the polymerized fibrin into threads (Page, 2011). Muscle defects were created in mice, and fibrin threads seeded with adult human muscle cells were placed into the wound. The alignment of the fibrin threads is thought to mimic the alignment in native muscle tissue. It was found that the fibrin microthreads were able to promote native muscle regeneration, cell migration, and reduce the amount of scar tissue formation. Tetanic intermittent and maximum force measurements were performed on uninjured mice, untreated injured mice, and fibrin thread treated injured mice. In the treated mice, almost 100% of native muscle strength was regained, while in untreated mice only 50% strength was achieved. Upon dissection and analysis of cell types in the affected region, it was found that the majority of the cells involved with the regeneration process were native muscle cells and not the exogenous cells that were implanted. This suggests that acellular microthreads may allow for the possibility of aided muscle regeneration (Page, 2011).

#### 2.3.1.3 Alginate Hydrogels

Naturally-derived alginate is a polysaccharide that is extracted from brown algae. The structure of the polysaccharide is a copolymer of guluronate and mannuronate (Lee, 2012). It is a lightly cross linked hydrogel that without surface modifications does not allow for cell infiltration and degrades through passive dissolution. This means that natural biological mechanisms such as phagocytosis and enzymatic cleavage do not facilitate degradation of alginate hydrogel. Therefore, modifications are needed to allow for controlled and predictable degradation. For this reason, alginate is predominantly used as a scaffold for GF delivery to target tissues, and a biocompatible structure for nanoparticles (Stilhano, 2016).

Borselli et al. studied the muscle regeneration effects of alginate gels loaded with angiogenic and myogenic GFs (Borselli, 2010). Hind limb ischemia was induced in mice and different test group materials were injected into the injury site. The various test groups evaluated were alginate gel, alginate gel loaded with VEGF, alginate gel loaded with IGF, alginate gel loaded with both VEGF and IGF, bolus injections, and a control group. The study found that alginate gel provided a suitable vehicle for drug delivery to the targeted muscle tissue. The test group that consisted of alginate loaded with VEGF and IGF produced muscle fiber diameters closest to that of native muscle. This test group also produced muscle regeneration that exhibited the maximum amount of strength produced across all test groups during a tetanic force test (Borselli, 2010).

Wang et al. developed a shape memory alginate scaffold that allows for minimally invasive cell and GF delivery. A modified, crosslinked alginate scaffold was produced to act as synthetic extracellular matrix. The scaffold was dehydrated and then rehydrated with a suspension of cells, GFs, or both. The seeded cells were found to proliferate and migrate through and out of the scaffold in clusters. The scaffold's surface properties were also found to be suitable for cell migration and proliferation. The degradation rate was determined to be beneficial for muscle regeneration as the degradation rate closely matched the rate of regeneration in damaged skeletal muscle. Although these tests were all done *in vitro*, they provide promising results for the use of alginate memory scaffolds in future research (Wang, 2012).

#### 2.3.1.4 Decellularized Extracellular Matrix

Decellularized ECM scaffolds are tissues harvested from mammalian origin and then decellularized (Wolf, 2012). They are comprised of collagen, elastin, laminin and

glycosaminoglycans, all of which naturally provide structure and support for cellular growth (Corona, 2016). The decellularized ECM not only provides structure, but also provides other factors that are responsible for triggering and controlling a range of cellular reactions, including VEGF, FGF-2, and cytokines (Gentile, 2014). All of these factors and biochemical cues allow the scaffold to assist in the migration and proliferation of target cells (Wolf, 2015). This is essential because of the scaffold's acellular nature. ECM scaffolds are also degradable, allowing the native tissue to replace the scaffold entirely as the macrophages break it down. The density of the scaffold is the determining factor for the degradation rate. Generally less dense ECM degrades in 60-90 days, while denser ECM degrades fully in 12-24 months (Badylak, 2016).

ECM can also be produced in a variety of formats. The major ones are 2D ECM sheets, powders, tube shapes, thermally responsive hydrogels, and whole decellularized organs. The format most used for VML research is whole decellularization of organ or tissue samples. This is mainly due to the mechanical properties of the whole decellularized tissue and the fact that the tissue maintains its native architecture (Crapo, 2011).

Many studies have been performed on the effectiveness of porcine urinary bladder ECM scaffolds as a treatment method for VML. Sicari et al. performed a study that consisted of ECM scaffold implantations into both rat and human patients with lower extremity VML. The study observed that in both cases, perivascular stems cells and initial formation of skeletal muscle in the affected area were present. In the human study, increased functionality was observed that was not achieved through physical therapy alone (Sicari, 2014). Clinical studies have been done to explore the ability of biologic scaffolds to be used as a surgical treatment for VML by providing a microenvironment that triggers a healing response. A murine model of VML was used to evaluate the spatial and temporal presence of skeletal muscle cells during tissue remodeling at the site of the skeletal muscle injury (Sicari, 2014). To create VML in the mouse model, an

excisional defect was made in the quadriceps of the hind limb. Untreated injuries were evaluated as a negative control six months after the injury and showed no signs of skeletal muscle formation. Mice that were treated with an ECM scaffold exhibited striated muscle cells six months after the injury. After these encouraging results in mice, clinical studies were done in five human patients who had experienced VML and exhausted all other treatment options. An acellular scaffold composed of porcine urinary bladder ECM was surgically implanted after removing scar tissue that had developed at the injury site. After surgery, each patient was put into a physical therapy program to promote functional recovery. Images were taken both before the surgery and six months post-surgery. Magnetic resonance imaging (MRI) showed formation of dense tissue after six months. Desmin and MHC positive cells were found, which are indicative of actively regenerating skeletal muscle cells. Additionally, postsurgical function was examined. Three out of five of the patients had 20% or greater improvement in muscle strength. The other two patients were considered nonresponders because although they reported an increased quality of life, functional deficits remained as they had lack of active movement (Sicari, 2014).

Corona et al. performed a similar study with less promising results (Corona, 2013). This study tested the use of ECM scaffolds on rats that had induced VML in both hind limbs, while only treating one with the scaffold. The study monitored the growth of muscle fibers and found that after six months, there was no indication that any mature muscle fibers were able to form across the muscle gap for the treated leg or the untreated leg. Fibrous masses were observed in both legs; however, the leg that was treated developed fibrous tissue to a lesser degree. Functionality increased but it was determined that this could not be due to muscle regeneration since muscle fibers were not formed (Corona, 2013).

More recently, Dziki et al. performed a cohort study with 13 patients implanted with

porcine ECM scaffolds (Dziki, 2016). At 24-28 weeks post-op a statistically significant average increase in strength of 37.3% was observed when compared to pre-op values. Also at 24-28 weeks, 12 out of the 13 participants were reported to have increased range of motion and functionality (Dziki, 2016). These varying results show that there is potential for an increase in muscle regeneration through the use of ECM scaffolds, but the exact mechanism of action may not fully be identified yet.

#### 2.3.1.5 Collagen Scaffolds

Collagen scaffolds are another type of scaffold made from natural materials found in mammalian tissue. Collagen is found naturally in bone, cartilage, and skin, providing structure to all of these tissue types. Collagen can be harvested from skin, tendon and cartilage and fabricated into collagen mesh, porous scaffolds, and sponges (Gómez-Guillén, 2011). These scaffolds are predominantly seeded with cells before implantation. For this reason, many scaffolds are fabricated with specific geometries to promote cell alignment for skeletal muscle formation. This is done through the creation of grooves and pores in the scaffold structure (Chen, 2015). Collagen is a degradable material that upon implantation would eventually be replaced by ECM which is secreted by the native cells in the region. Similar to decellularized ECM scaffold, the degradation rate for the collagen scaffolds are dependent on the density of the scaffold and the ease at which macrophages can penetrate the material (Kroehne, 2008).

Experimental studies done on the viability and effectiveness of collagen scaffolds at promoting cell alignment have provided promising results. Choi et al. conducted a study on the ability to produce self-aligned skeletal muscle through the use of electrospun collagen nanofiber meshes (Choi, 2008). The study used collagen fibers mixed in a 1:1 ratio with PCL and then electrospun to create a mesh. PCL is a biodegradable, flexible polyester polymer. The study

aimed to determine if the orientation of the electrospun mesh could influence the organization, proliferation and differentiation of seeded human skeletal muscle cells. It was found that mesh orientation had no effect on cell adhesion and proliferation, but the formation of myotubes was more consistently aligned in the organized mesh compared to that of the randomly oriented fiber control group. This increased alignment can potentially improve the muscle function and maturation of myofibers in the body (Choi, 2008).

Chen et al. performed a study that tested whether or not the geometry of a collagen scaffold influences the alignment of skeletal muscle myoblasts (Chen, 2015). In this study, lines of water were printed onto a liquid nitrogen cooled plate. The frozen lines that were produced provided a mold to cast the collagen matrix. This allowed for the production of a collagen scaffold that had clearly defined grooves. Rat skeletal muscle myoblasts were seeded onto the scaffold and cultured for 7-12 days. The grooved collagen scaffolds increased cell alignment. However, there was no observable difference observed in myogenic gene expression (Chen, 2015).

In a study by Kroehne et al., C2C12 myogenic cells were seeded onto collagen sponges and implanted into rat skeletal muscle tissue (Kroehne, 2008). Isometric contraction measurements were done before and after implantation. Between 14-50 days after implantation, the scaffold and surrounding muscle were analyzed. The implant region was observed to be redder in color than the surrounding tissue, which was determined to be due to an increase in vascularization. The force measurements were determined to be 5-20% of undamaged skeletal muscle tissue tetanic tension values. It was also determined that there were large regions of the scaffold where endogenous cells had not infiltrated. This means that the formation of muscle fibers was not supported by the host cells (Kroehne, 2008).

## 2.3.2 Biophysical and Biochemical Cues in Scaffolds

By incorporating cues that naturally occur during muscle regeneration into scaffolds, it is possible to induce a biomimetic microenvironment at the injury site to facilitate muscle regeneration. As mentioned, the cues can be either biochemical or biophysical (Cezar, 2015). Biophysical cues are considered as adhesive and mechanical signals, presented by material carriers that dramatically affect cell survival and ultimately participate in regeneration (Cezar, 2015). Whereas biochemical cues are considered as growth factors, cytokines, and signaling ligands that signal host cells (Cezar, 2015). The creation of an ideal synthetic niche for SCs has seen clinical success for improving survival, engraftment, and fate control of delivered cells. Incorporating a variety of cues is difficult; therefore a few key cues deemed imperative for adhesive, mechanical, and soluble microenvironment cues are chosen in particular (Cezar, 2015).

### 2.3.2.1 Biophysical Cues – Surface topography

Biophysical cues such as adhesive signals incorporated into scaffolds are crucial for an effective scaffold. Topography, the surface features of scaffolds, will greatly affect cell behavior by facilitating cell alignment as well as differentiation and gene expression. Patterns on the surface of the scaffold have been studied with great success (Gilbert, 2010). Patterning can be incorporated in two-dimensional (2D) or three-dimensional (3D) and has been shown to guide alignment of muscle myoblasts and myotubes which lead to the formation of pre-patterned cell sheets. Issues with 2D microprinting include limited thickness which can lead to less alignment of myotubes, also harvesting the cell sheets is cumbersome. 3D microprinting has seen greater success of alignment of myotubes due to greater thickness and processability (Chen, 2015).

Getting cells to adhere to the scaffold via the guidance is an obstacle that must be overcome to maximize effectiveness. Cell types that are known to be adherent to a positive

control or tissue culture plate, may not adhere to the biomaterial surface. The surface of scaffolds can be altered at a nanoscale to greatly influence cell contact guidance. Small features on the nanoscale level like columns, protrusions, pits and nodes were shown to promote cell adhesion. Janson et al. was able to prove the importance of nanotopography by performing a study to show that increasing the size of the small features results in a decrease in cell adhesion (Janson, 2015).

Chen et al. investigated how 3D porous collagen scaffolds fabricated via 3D microprinting affected cell behavior (Chen, 2015). The microgrooves were concave to imitate the basement membrane for engineering skeletal muscle tissue. Microgrooves on the scaffolds were shown to promote cell alignment once the activated SCs adhered to the microgrooves. Afterwards, the SCs divided to produce SC-derived myoblasts that further proliferated before differentiation further and fusing to form myotubes. These then matured further into myofibers (Chen, 2015).

#### 2.3.2.2 Biophysical Cues – RGD Ligand

The incorporation of adhesive cues that mimic natural binding in the satellite niche has been researched in skeletal muscle regeneration. For instance, by covalently modifying alginate hydrogel scaffolds with RGD-containing cell adhesion ligands it mimicked adhesive cues for myoblast cells (Rowley, 1999). RGD is a tripeptide, Arginine-Glycine-Aspartic acid, which is the sequence found in proteins. The binding of integrins to the RGD ligands mediates both cell-cell and cell-substratum interactions (D'Souza, 1991). Rowley et al. were able to get myoblasts to adhere to RGD-modified alginate surfaces (Rowley, 2002). The adherence of myoblasts allowed for further proliferation, and the fusion into multinucleated myofibrils (Rowley, 1999). *In vitro* RGD density, affinity, and nanoscale distribution were shown to regulate skeletal myoblast proliferation and differentiation (Boontheekul, 2008; Rowley, 2002).

### 2.3.2.3 Biophysical Cues – Porosity

When regeneration occurs, fibroblast activity leads to scar tissue formation. Ideally fibroblastic activity should be controlled to ensure proper collagen deposition. Fibroblasts deposit collagen which eventually forms into scar tissue and inhibits the full recovery of functional skeletal muscle tissue. Typically, pores that range in the size of 5-15  $\mu\text{m}$  favor fibroblast ingrowth (Annabi, 2010). By incorporating pores and controlling the sizes, the fibroblastic activity can be greatly optimized.

Another benefit of porous scaffolds is that without an intrinsic vascular system, the maximum thickness of engineered tissue is approximately 150-200  $\mu\text{m}$  (Annabi, 2010). This maximum thickness can be attributed to the insufficient oxygen and nutrient transport within the deeper areas of the biomaterial (Annabi, 2010). Therefore, scaffolds are generally highly porous with interconnected pore networks to facilitate nutrient and oxygen diffusion as well as waste removal. Open porous and interconnected networks are essential for cell nutrition, proliferation, and migration for tissue vascularization and formation of new tissue.

The porous surface may also help improve the mechanical stability of the implant by mechanical interlocking between the scaffolds and surrounding tissue (Loh, 2013). As a result, the porosity and pore size of the scaffold should be taken into account for the intended application. The pore size needs to be large enough to allow the release of GF and endogenous SCs to infiltrate the scaffold but still allow for necessary mechanical stability (Loh, 2013). Incorporating porosity into a scaffold is a delicate balance as the degree of porosity will have a substantial effect on the mechanical properties, specifically with the decrease in scaffold elasticity or stiffness. It is imperative to not alter the scaffold elasticity because it has been shown to induce cellular differentiation (Engler, 2006; Gilbert, 2010).

#### 2.3.2.4 Biophysical Cues – Scaffold Elasticity

The mechanical properties of scaffolds also impact their success in muscle regeneration. Mimicking native muscle tissue elastic modulus, has been shown to induce cellular differentiation (Engler, 2006; Gilbert, 2010). The elastic modulus of native skeletal muscle tissue ranges from 8-17 kPa when at rest (Engler, 2006). When skeletal muscle is in contraction, the elastic modulus can be as high as 11,200 kPa (Caiozzo, 2002). Engler et al. were able to determine that SCs commit to the different lineages of muscle cells based on matrix elasticity (Engler, 2006). By having a scaffold with a similar elastic modulus, better SC engraftment and niche repopulation *in vivo* occurs. Matrix elasticity is another concern, and it has been shown to help regulate SCs self-renewal in culture. Gilbert et al. were able to culture SCs on soft hydrogel substrates that mimicked the elasticity of muscle 12 kPa (Gilbert, 2010). Great success was shown in regulating SCs to self-renew *in vitro* and extensively contributed to muscle regeneration when the hydrogels with SCs were implanted into mice. (Gilbert, 2010). The self-renewing proliferation of SCs is multifunctional and maintains the cell population, but also provides numerous myogenic cells. The myogenic cells proliferate, differentiate, fuse and lead to new myofiber formation that have functional contractility (Yin, 2013).

#### 2.3.2.5 Biophysical Cues – Degradation

In addition to the scaffold providing stability, the scaffold degradation should match the timing of the regeneration process. The ideal mechanism of healing would allow for the synchronization of scaffold degradation with the replacement of native tissue, which makes the resorption rate of the scaffold important (Sung, 2004). For a muscle scaffold, the scaffold should be fully degraded at the end of the repair phase (Turner, 2011). By following the timeline of the repair phase – three to six weeks – it allows for the scaffold to provide support for the wound site

while new myofibers repopulate (Sung, 2004). By degrading within this timeframe, it allows for the replacement by natural tissue produced from cells (Sung, 2004).

There are many factors that affect degradation such as hydrophobicity, molecular weight, crystallinity and many *in vivo* processes that need to be considered. Typically, degradable polymers will break down or erode by surface erosion, bulk erosion or a combination of the two (Ulery, 2011). Surface erosion is characterized by the rate of polymer degradation being much greater than the rate at which water diffuses into the bulk of the material leading to it degrade almost entirely at its surface (Ulery, 2011). Bulk erosion is the opposite, water diffusion is much faster than degradation leading to degradation occurring throughout the bulk of the material (Ulery, 2011). These two distinctions are important in determining which material is best for a desired application.

The degradation products of the biomaterial scaffold are also an important consideration. Some materials may produce toxic byproducts, which can be detrimental to the surrounding tissue. For instance, polymers like PLA and PGA degrade by hydrolysis of the ester bonds, which produces acidic byproducts (Sung, 2004). The acidic byproducts make a more acidic environment which can lead to tissue necrosis (Sung, 2004).

#### 2.3.2.6 Biochemical Cues – Growth Factors

The aforementioned cues are just some of the biophysical cues that scientists have successfully incorporated into scaffolds. Although incorporating physical cues is important, the incorporation of chemical cues paired with physical cues allows for greater effectivity.

Biochemical cues help the body signal and facilitate muscle regeneration. Biochemical cues can be membrane proteins, intracellular proteins or extracellular factors such as GFs. Within the body are a plethora of biochemical cues that naturally occur; Table 1 lists some of the

currently known cues. These cues are important to regeneration of tissue because they signal for cellular activity.

Table 1: List of the many biochemical cues natural in the body and their function (Horsley, 2004).

<i>Molecule name</i>	<i>Effect on</i>
<b>Membrane proteins</b>	
Integrins (VLA-4, $\beta$ 1), integrin receptor VCAM-1	Myoblast fusion
Nephrin	Myotube accretion
K <sup>+</sup> ion channel, T-type Ca <sup>2+</sup> channel	Intracellular Ca <sup>2+</sup>
Epidermal growth factor receptor	Myoblast differentiation
Protein GRP94	Myoblast fusion
ADAM 12, Calveolin-3	Myoblast fusion
Notch receptor	Satellite cell regulation
Mannose receptor	Myotube accretion
<b>Intracellular proteins</b>	
Calpain, Calmodulin	Myoblast fusion
Calcineurin	Myoblast recruitment
AMPKinases	Protein catabolism
NFATC(1,2,3)	Gene activation
Yap	Hippo signaling
MAP Kinases	MEF2, stress signaling, activator mTORC1
TSC1-TSC2	mTORC1 inhibitor
mTOR	Regulation protein anabolism
FoxO/Smad	Protein catabolism
<b>Extracellular factors</b>	
PGE 1, PGF2 $\alpha$ , arachidonic acid	Myoblast fusion
IL-4, IL-6, LIF	Myoblast fusion, satellite cells
Ca <sup>2+</sup>	Signaling pathway
Cathepsin B	Autophagy
IGF-1, Insulin, Androgen, GH	Protein anabolism
Myostatin, glucocorticoids	Protein catabolism
NO	Regulation satellite cell, myoblast fusion

There has been clinical success with incorporating GFs into tissue engineering constructs to enhance muscle regeneration (Borselii, 2010, Cezar, 2015). For a scaffold, GFs are used to either replace the GF population that would naturally occur or supplement the surrounding tissue. The GFs' intended function for this application is to activate the removal of damaged tissue and synthesis of new muscle fibers which ultimately helps to restore functional contractile properties. Many GFs are present in the body and not all of them have been characterized. Table 2 is a summary of the current characterized GFs and their actions are shown.

Table 2: Some of the GFs currently being researched with success and the actions they perform (Whitaker, 2001).

Growth factor	Action	Use in tissue engineering	Delivery method	Reference
Platelet-derived growth factor (PDGF)	Endothelial cell proliferation	Angiogenesis Wound healing	Implanted EVA rods Alginate hydrogels PLLA, PLGA, PLA microspheres	Walsh et al (1995); Kim & Valentini (1997); Lohmann et al (2000); Park et al (2000a, b)
Fibroblast growth factor (FGF)	Cell proliferation	Bone and cartilage regeneration Nerve growth Endothelial cell proliferation Angiogenesis	Hydrogels PLGA Cross-linked fibrin and collagen Heparinized fibrin	Kang et al (1995); Fujisato et al (1996); Martin et al (1999); Shireman et al (1999); Chandler et al (2000); Hile et al (2000); Sakiyama-Elbert & Hubbell (2000b); Tabata et al (2000); Wissink et al (2000)
Nerve growth factor (NGF)	Axonal growth and cholinergic cell survival	Neurite extension in central and peripheral nervous systems	PLGA/poly(caprolactone) encapsulation	Krewson & Saltzman (1996); Cao & Shoichet (1999); Sakiyama et al (1999); Saltzman et al (1999); Benoit et al (2000)
Epidermal growth factor (EGF)	Cell proliferation	Migration and differentiation of neural stem cells Wound healing	Surface immobilization on polymers PLGA microspheres Photoimmobilization	Mooney et al (1996b); Chen et al (1997); Haller & Saltzman (1998); Watanabe et al (1998); von Recum et al (1999)
Vascular endothelial growth factor (VEGF)	Endothelial cell proliferation	Angiogenesis	Alginate hydrogels PLGA-PEG microspheres Heparinized fibrin	Weatherford et al (1996); King & Patrick (2000); Lee et al (2000); Murphy et al (2000b); Sheridan et al (2000)
Bone morphogenetic protein-2 (BMP-2)	Cell proliferation	Bone regeneration	Hydrogels PLGA	Hollinger & Leong (1996); Boden (1999); Whang et al (2000)
Transforming growth factor- $\beta$ (TGF- $\beta$ )	Extracellular matrix (ECM) production	Bone and cartilage regeneration Stimulates ECM synthesis	Surface immobilization EVA rods PLA Chitosan	Nicoll et al (1995); Kim & Valentini (1997); Chenite et al (2000); Lind et al (2001); Mann et al (2001)

Vascular endothelial growth factor (VEGF) has been proven to initiate blood vessel formation, or angiogenesis to return normal levels of tissue perfusion within three weeks in the thigh and leg muscles of ischemic rabbit hind limbs (Borselli, 2010). VEGF plays a role in myogenesis by helping improve muscle contractility (Bae, 2012). Another feature of VEGF is its ability to protect tissue from hypoxia and tissue necrosis, making VEGF a desirable and multifunctional GF (Sahni, 2000).

Fibroblast growth factor 2 (FGF-2) is a GF that helps facilitate myogenesis, angiogenesis, and innervation (Bae, 2012). This multifunctional GF requires prolonged exposure to cells to sustain vessel maturation for angiogenesis. The presence of FGF-2 has been shown to increase endothelial cell migration and proliferation (Bae, 2012). FGF-2 helps enhance myogenesis

because its natural function in the body is to stimulate SC proliferation (Bae, 2012). The requirement of prolonged exposure presents an issue for delivery, since FGF-2 acts as an inhibitor for the next step of the differentiation phase (Velleman, 2008).

Nerve growth factor (NGF) helps facilitate innervation of the newly formed muscle tissue, axonal growth, cell survival as well as angiogenesis and skeletal muscle fiber remodeling (Whitaker, 2001). NGF belongs to the neurotrophin family which functions to enhance peripheral nerve regeneration (Sakiyama-Elbert, 2000). Diao et al. was able to transfect NGF and show that it promoted NGF and VEGF protein expression which further facilitated angiogenesis and type I muscle fiber expression (Diao, 2016). *In vivo*, NGF has been added to nerve guide tubes, leading to a limited increase in nerve regeneration, highlighting the need for a delivery system to release NGF (Sakiyama-Elbert, 2000). Maintaining NGF release over a long duration is difficult and requires a delivery system that provides prolonged release. Sakiyama-Elbert et al., were able to develop a heparin-containing fibrin-based matrix to enhance neurite extension by controlling the rate at which NGF was delivered (Sakiyama-Elbert, 2000).

Insulin-like growth factor 1 (IGF1) is another multifunctional GF that has been studied with great interest. Its ability to protect cells from apoptosis and to mute the inflammatory response has led to IGF1 being heavily researched (Borselli, 2010). This GF is active during all stages of regeneration, and it leads to the activation and proliferation of SCs, therefore enhancing muscle fiber regeneration to form highly functional muscle tissue (Borselli, 2010).

Current research has focused on multifunctional GFs and their combined delivery effects is summarized in Figure 5. For instance, the combined delivery of VEGF and IGF1 led to parallel myogenesis, angiogenesis, and as a result innervation (Borselli, 2010). As SC activation and proliferation are stimulated, the presence of IGF1 mutes the inflammatory response, and

protects the cells from apoptosis. Borselli et al. were able to get highly functional muscle tissue to form by combining the temporal and spatial delivery of VEGF and IGF1 (Borselli, 2010).

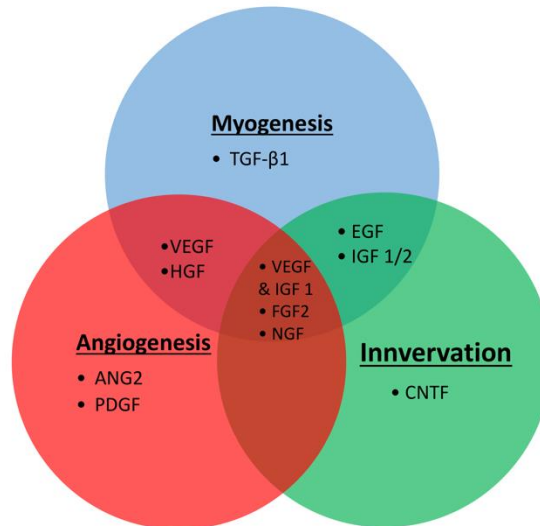


Figure 5: Current clinically successful GFs, showing that some are multifunctional

Native GF release is time and location sensitive since and they have short half-lives and do not act in an endocrine fashion (Lee, 2011). Direct injection of GFs may lead to severe side effects due to the abnormally high initial concentration (Lee, 2011). It is vital that the release of the GFs from a tissue engineered scaffold is controlled and models that of natural muscle tissue. The spatial and temporal complexity of endogenous GF release provides a significant new drug delivery challenge of mimicking endogenous release profiles.

### 2.3.3 Controlling the Release of Growth Factors

As mentioned previously, the biochemical cues, specifically GFs, involved in the regeneration of muscle tissue are very important to ensure the regeneration of functional skeletal muscle tissue. Due to the way in which these GFs react with the wound site, it is also important

that these factors are only released during certain phases, and also that a proper dosage is delivered throughout the healing process (Drury, 2003).

In addition to releasing these biochemical cues over an extended period, it is often desired to control the spatial distribution of drugs release. For certain GFs, such as the VEGF, delivery of a large amount to a single area can be very toxic towards the patient and possibly cause further issues, such as the development of tumors (Drury, 2003). In addition to facilitating the transport of drugs to a certain area and avoiding toxicity, being able to control the release profiles of these drugs will in turn increase their effectiveness and require less chemicals.

In order to mimic natural GF delivery to cells in-vivo engineers have developed different methods using polymers and other materials, which can control the release of GFs or other drugs at a wound site (Uhrich, 1999; Yamamoto, 2001). The methods developed have been categorized into either temporal or distribution control, each have been successful under specific conditions (Uhrich, 1999). The temporal release of a drug, as seen in Figure 6, is defined as a type of release that is controlled via the properties of a polymer. For example, the release profile of the drug can be limited by the degradation of the polymer, delayed dissolution, or by the drug's ability to diffuse through the polymer's membrane. Alternatively, controlled drug release known as distribution control consists of the placement of the drug directly at the site and is beneficial for the treatment of tumors. This method is focused on the targeted-area application of the drug, as well as the sustained release (temporal release) of the compound.

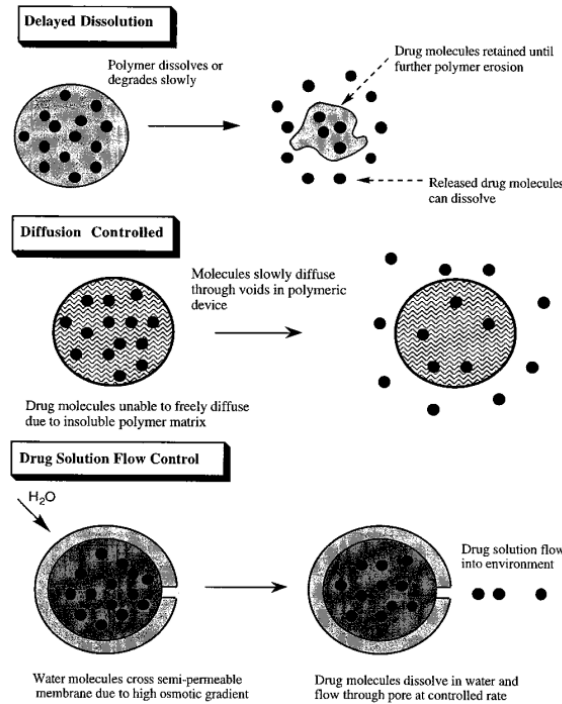


Figure 6: Temporal drug release mechanisms. (Uhrich, 1999)

GFs have a very short half-life and therefore if not protected, will degrade quickly (Yamamoto, 2001). This raises problems for the regeneration of muscle tissue, as certain GFs, such as FGF-2, required prolonged exposure to the cells during this process to achieve full maturation (Bae, 2012).

An early example of the controlled release of GFs was achieved by Yamamoto et al. in 2001 using a gelatinous hydrogel. In this study, a series of GFs relevant to regenerative medicine were selected - FGF-2, TGF- $\beta$ 1, BMP-2, and VEGF - and were sorbed into the hydrogels (Yamamoto, 2001). This approach of GF controlled release used the degradation of the hydrogel to control the release rate. For the *in vitro* experiment, the hydrogels were placed into varying ionic PBS solution baths. The GF concentration within the ionic solution was recorded each hour (Figure 7). It is evident that the amount of GF released throughout the experiment was dependent on the ionic solution strength, except in BMP-2 which was relatively constant. The release rate of the growth factors depended on its affinity to the hydrogel, making this a more effective

method of control for certain factors, such as FGF-2 and TGF- $\beta$ 1, than others, such as BMP-2 (Yamamoto, 2001).

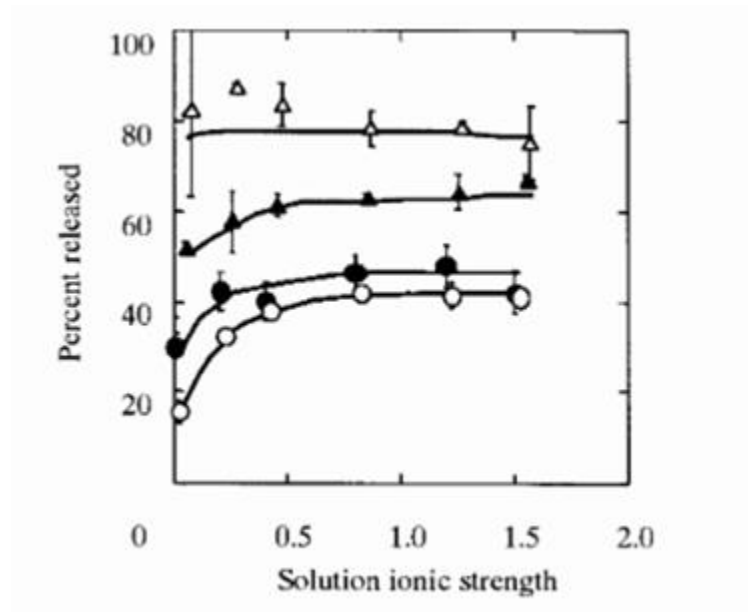


Figure 7: Release profile of GFs FGF-2 (○), TGF- $\beta$ 1 (●), BMP-2 ( $\Delta$ ), and VEGF ( $\blacktriangle$ ) from a gelatinous hydrogel into PBS. (Yamamoto et al., 2001).

In addition to the release profiles from the gelatin hydrogels, Yamamoto et al. observed the absorption of the GFs into the gel. It was determined that BMP-2 and VEGF absorbed less into the gel than their counterparts, FGF-2 and TGF- $\beta$ 1. This was predicted to be due to the differences in chemical structure and charge (Yamamoto, 2001). Therefore, there are a limited amount of compatible GFs and delivery vehicle combinations.

As well as using an entire scaffold as the delivery vehicle, studies have been performed using polymeric systems to delay the release rate of growth factors. These polymeric systems can encapsulate the desired protein or drug and due to either electrostatic interactions or pore size limitations the molecules will be encapsulated for longer, temporarily inhibiting the activity. In the study performed by Gu et al., VEGF was encapsulated into alginate microbeads in the presence of  $\text{CaCl}_2$  and the release rate was observed over two weeks (Gu, 2004). The objective of the study was to determine the most efficient method of encapsulating VEGF to delay its

release. The alginate bead compositions were altering, both with and without  $\text{CaCl}_2$ , and additionally different mediums, PBS and BSA, were used as the bulk liquid. It was determined that in order to sustain the release of the VEGF from the alginate beads, the electrostatic interactions would need to be overcome, and  $\text{CaCl}_2$  was used to do so at varying concentrations. It was observed that in the presence of 0.1 M  $\text{CaCl}_2$  and when placed in a PBS bath, the alginate microbeads were capable of sustaining a release rate of 6 ng/ml/day for over two weeks, which opens up possibilities for this technology to be incorporated into various tissue engineering constructs (Gu, 2004).

Controlled release studies have also been performed by altering the composition of a composite scaffold to create more affinity, resulting in an extended release time. In a study performed by Jeon et al., fibrin gels with varying fibrinogen (9.4-188.6 mg/ml), thrombin (3.3-66.66 mg/ml) and heparin (0-166.7  $\mu\text{g}/\text{mL}$ ) compositions were loaded with FGF-2 and the release kinetics were observed (Jeon, 2005). The goal of this study was to determine to what degree the release kinetics could be controlled in such a gel. In this study, it was observed that increasing the concentration of fibrinogen in the gel would extend the release through diffusion of FGF-2 out of the gel. In addition to increased fibrinogen concentrations, the addition of heparin to ionically bond the FGF-2 was also utilized to extend the release kinetics. The best combination observed was using 188.6 mg/ml of fibrinogen, 166.7 mg/ml of thrombin and 166.7  $\mu\text{g}$  of heparin, which resulted in approximately 55% cumulative release over 14 days (Figure 8).

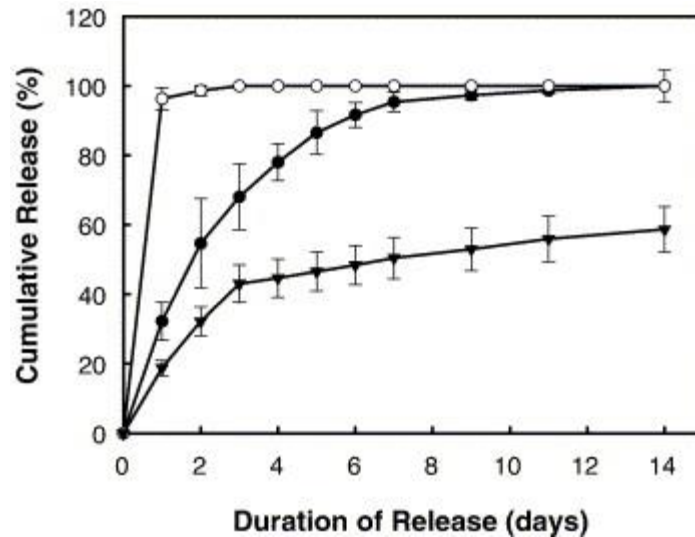


Figure 8: Cumulative release of FGF-2 from fibrin gels prepared at different fibrinogen concentrations (Group V, fibrinogen, 9.4 mg/ml (○); Group II, fibrinogen, 94.3 mg/ml (●); Group VI, fibrinogen, 188.6 mg/ml (▼)) with thrombin (NIH U/ml) in the presence of heparin (166.7 μg). The values represent the mean ± S.D. (n = 5). (Jeon, 2005).

## 2.4 Summary and Need

As discussed, there is a need for a technology that promotes functional skeletal muscle regeneration for VML patients. Currently, autologous tissue transfer is insufficient in regenerating functional muscle and the surgery often results in graft failure. There are many tissue-engineered scaffolds that have been explored as a solution for functional tissue regeneration in applications such as VML and others. While many make strides towards a viable solution, there is still a need for a scaffold that both mitigates foreign body response and scar tissue formation as well as can provide structural support and promote myogenesis for functional muscle regeneration.

One solution that has been explored in Pins' lab is the use of fibrin microthreads as a scaffold that can be implanted directly into the wound bed (Grasman, 2015). This scaffold showed promise in its ability to regenerate functional muscle without scar tissue formation, but is lacking in its ability to serve as a vehicle for controlled growth factor release. The growth factor loaded to the fibrin microthreads was released after only three days which is not sufficient to

provide release throughout the three to six week long repair phase (Grasman, 2015). Because of this, a need exists to develop a scaffold that is capable of controlled growth factor release throughout the repair phase. The following sections will detail how the project design addressed the concern.

## 3.0 Project Strategy

The project strategy chapter outlines the engineering design process and how it was applied to the project for designing a composite scaffold for skeletal muscle regeneration. To do this, the design team compiled the information from the initial client statement, client interviews, project objectives, constraints and the revised client statement. Processes and insight on the process were utilized from two sources that outline design process approach: *Engineering Design: A Project Based Introduction* by Clive L. Dym and Patrick Little and *Biodesign: The Process of Innovating Medical Technologies* by Paul G. Yock, Stefanos Zenios and Josh Makower (Dym & Little, 2000; Yock, 2015).

### 3.1 Stakeholders

To create a successful design, the team needed to consider all of the stakeholders in the project which include the design team, the clients, and users. The clients' opinions are very important as they are the ones funding the project, the users are the ones that will need to utilize the device and the design team are the ones who must be able to apply the design process and find a feasible solution. The design team considers the constraints they have created while trying to satisfy the clients' and users' objectives.

The clients for this project include Dr. George D. Pins and Dr. Jeannine M. Coburn, and Meagan Carnes and Joanna Santos are the users. The design team includes Alexandra Burr, Anthony Campagna, Janine Fatal, James Lin and Elizabeth van Zyl. The project objective was given to the team by Dr. George D. Pins and Dr. Jeannine M. Coburn because of the need for aligned myogenesis and vascularization to occur in a tissue engineered construct that graduate students Meagan Carnes and Joanna Santos are creating as a solution for volumetric muscle loss. The need exists for a composite scaffold to be created because even though fibrin microthreads have shown to be successful in promoting functional muscle regeneration from implantation in a wound site (Grasman, 2015) the microthreads alone are difficult to handle and degrade too quickly to be an appropriate vehicle for the growth factor delivery necessary to impact regeneration. The goal is to provide these users with a reproducible composite scaffold that promotes functional skeletal muscle regeneration through the release of growth factors for at least two weeks.

### 3.2 Initial Client Statement

The initial client statement given to the team was:

*“Design and characterize an implantable composite fibrin scaffold with controlled release of growth factors to promote regeneration of skeletal muscle tissue.”*

To best accomplish this goal, the team would need to combine a successful composite scaffold fabrication technique with a GF loading method. The team needed to identify and prioritize a set of design objectives and constraints. The objectives and constraints then needed further refining throughout the process as the stakeholders’ needs were more critically examined.

This led to a final set of objectives and constraints which allowed the team to plan a comprehensive project strategy and design process.

As previously mentioned, there have been attempts to create a scaffold in Pins' lab, but there is need to create a composite that is able to release the growth factor throughout the repair phase, as well as be more user friendly and easy to handle, as expressed by the stakeholders. The current method for fibrin microthread bundles have been noted as being difficult to work with by users.

### 3.3 Constraints

To complete the project for MQP requirements in a lab at WPI, there are certain criteria that have to be met. Some of the potential criteria were identified as constraints because they would limit the ability for the project to continue. The constraints and definitions can be found in Table 3.

*Table 3: Project constraints*

<b>Constraint</b>	<b>Definition</b>
Money	Budget of \$1300
Time	Must be finished by April 20th 2017
Availability	Materials must be available for Pins lab
Materials	Must not be cytotoxic or harm users
Sterility	Must be able to be sterilized by well-known techniques

The constraints provided the team with working limitations. They must be met to create the composite scaffold. First, the team had a budget through WPI of \$1300. Additionally, the team had until April 20th, 2017, project presentation day, to complete the project. The materials involved in the composite fabrication must be available to the members of design team and the users. Furthermore, the materials used for the scaffold must not be cytotoxic or harmful to the users during fabrication. Finally, for the *in vitro* studies, the team needs to make sure the fabrication process includes a method of sterilization that users are familiar with or are well-known and can be learned.

### 3.4 Objectives

The team initially developed a list of objectives and constraints based on the initial client statement. The team's initial objectives and constraints were also developed to encompass the needs and wants of the stakeholders. After user and client interviews, the team altered the set of objectives and constraints based on their priorities and timeline to guide the project goals and determine success.

The initial objectives were evaluated after the team received feedback from the users and clients. The team would focus on growth factor release for skeletal muscle regeneration so the objectives were broadened to reflect this potential. Therefore, instead of trying to achieve all three goals of angiogenesis, innervation and myogenesis, myogenesis would be considered the most important for this project. Additionally, the design team and the clients discussed the importance of a scaffold that provides structural support and is easier to handle than fibrin microthreads. Users expressed the difficulty of working with microthread bundles and the

limited ability to alter controlled release of growth factors from them. This mindset was used to strengthen and broaden our revised objectives which are outlined in the tree in Figure 9.

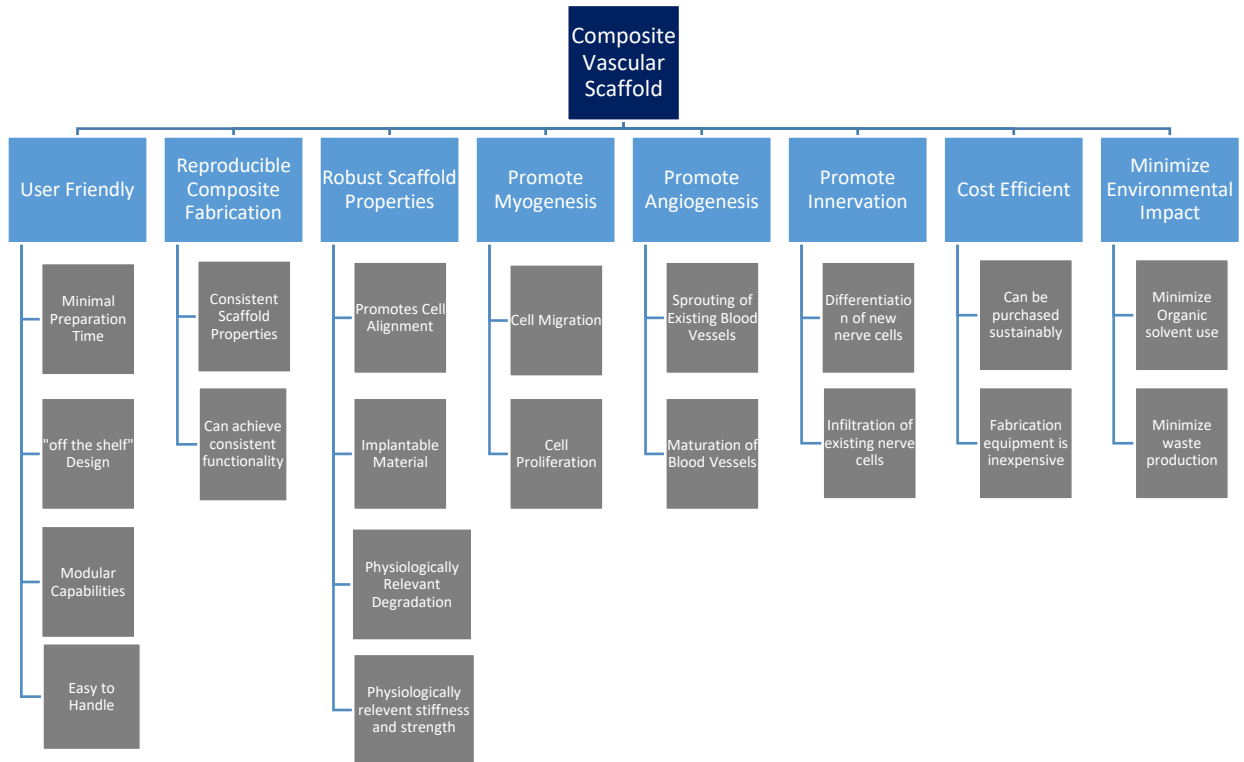


Figure 9: Project objective and sub-objective tree

The eight high-level objectives are user friendly, reproducible composite fabrication, robust scaffold properties, promote myogenesis, promote angiogenesis, promote innervation, cost efficient, and minimize environmental impact. These main objectives are defined as in Table 4 and are broken down further into sub-objectives which are defined in Tables 4-11.

Table 4: Main objective definitions

Initial Objective	Definition
User Friendly	Must be easy to use, easy to handle and have the potential for adapting to user needs (layers, size, etc)
Reproducible Composite Fabrication	Needs to be able to be continually produced at the same quality level and easy to fabricate
Robust Scaffold Properties	Needs to promote alignment as well as degrade and provide structural stability for the time span equivalent to the repair phase
Promote Myogenesis	Needs to promote processes involved with muscle regeneration
Promote Angiogenesis	Needs to promote processes involved with vascular regeneration

Promote Innervation	Needs to promote processes involved with nerve regeneration
Cost Efficient	Must cost a reasonable amount for the benefits it provides and can be produced with inexpensive equipment
Minimize Environmental Impact	Must considerably and reduce environmental impact through material selection and fabrication method

*Table 5: Sub-objective definitions: user friendly*

<b>Sub-objective Definitions: User Friendly</b>	
Minimal Preparation Time	Fabrication protocol needs to be simple and convenient for user
“off the shelf” Design	Some components are storable for later use and ready for incorporation into the composite
Easy to Handle	The scaffold must be easy to work with and allow user to perform experiments with it
Modular Capabilities	Protocol can easily be adapted to change size or number of layers in the composite

*Table 6: Sub-objective definitions: cost efficient*

<b>Sub-Objective Definitions: Cost Efficient</b>	
Consumables can be purchased sustainably	Materials required are available to the lab and are affordable for purchase over time, disposables and consumables are cheap
Fabrication equipment is inexpensive	Equipment required to produce scaffold is inexpensive and capable of being purchased by the user or is already available to the user

Table 7: Sub-objective definitions: robust scaffold mechanical properties

<b>Sub-Objective Definitions: Robust Scaffold Properties</b>	
Promotes Cell Alignment	Includes structural components that help to promote cell alignment
Physiological Relevant Degradation	Composite will degrade in vivo during the time span of the repair phase and function throughout it
Physiological Relevant Stiffness and Strength	Stiffness and strength of composite is comparable to native muscle tissue

Table 8: Sub-objective definitions: reproducible composite fabrication

<b>Sub-Objective Definitions: Reproducible Composite Fabrication</b>	
<b>**Precision**</b> Consistent Scaffold Properties	Thickness, incorporation, volume and other properties remain consistent each time it the scaffold is produced by following protocols
<b>**Accuracy**</b> Can achieve consistent functionality	Performance and success in achieving various objectives remains consistent. Accurate in the ability to achieve target goals

Table 9: Sub-objective definitions: promote myogenesis

<b>Sub-Objective Definitions: Promote Myogenesis</b>	
Cell Migration	Composite signals fibroblasts to the area to differentiate to myoblasts
Cell Proliferation	Composite is inductive and promotes cell proliferation in the area

Table 10: Sub-objective definitions: promote angiogenesis

<b>Sub-Objective Definitions: Promote Angiogenesis</b>	
Sprouting of existing blood vessels	Composite signals existing blood vessels from the healthy tissue to sprout to the scaffold site
Maturation of blood vessels	Blood vessels surrounding the impacted tissue mature and develop

Table 11: Sub-objective definitions: promote innervation

<b>Sub-Objective Definitions: Promote Innervation</b>	
Differentiation of new nerve cells	New nerve bundles develop at the site
Infiltration of existing nerve cells	Existing nerve endings growth and infiltrate the site

### 3.5 Quantitative Analysis of Objectives

To determine the most important objectives to drive the design specifications, a pairwise comparison was completed by the clients, users and design team. To complete the pairwise comparison charts, the stakeholders were asked which objective is preferable when placed next to another, causing them to prioritize. A score of "1" indicated that the objective in the column of the chart had priority over the objective in the row of the chart, a score of 0.5 indicated that were equal in priority, and a score of 0 indicated that the objective in the column of the chart had less of a priority than the objective in the row of the chart. Once the chart was complete, the scores in each row were added up to reach a score for each objective. The pairwise comparison charts for each stakeholder can be found in Appendix C. The design team completed the chart as a group.

The scores of the two clients and the two users were averaged for each objective to be used in the final scoring. An example of a summary table showing the averages for the clients, users, and design team is shown in Table 12 and a comprehensive table showing the summary of scores for all of the sub-objectives is found in Appendix D. Next, the objectives were weighted based on the total scores for each, using the equation in Table 12. The average of the clients' responses were multiplied by 0.4 as were the average of the users' responses. The design team's responses were multiplied by 0.2 in order to give more weight to the clients and users. An example of the final weighted objectives using the equation below is used in Table 13 for the main objectives and the remainder can be found in Appendix E.

$$\textit{Weight} = [(0.4 * \textit{average of users}) + (0.04 * \textit{average of clients}) + (0.20 * \textit{average of design team})]$$

Table 12: Scores of main objectives by category

	Clients	Users	Design Team	Total
User Friendly	3.75	3.75	2.5	10
Reproducible Composite Fabrication	5.25	6	6.5	17.75
Robust Scaffold Properties	5	5.75	6.5	17.25
Promote Myogenesis	9	5	4.5	18.5
Promote Angiogenesis	2.25	4	4.5	10.75
Promote Innervation	1.25	2	1	4.25
Cost Efficient	4.25	0.75	1.5	6.5
Minimize Environmental Impact	1.5	0.25	0.5	2.25

Table 13: Weights of main objectives

Main Objectives	Weight
Promote Myogenesis	6.5
Reproducible Composite Fabrication	5.8
Robust Scaffold Properties	5.6
User Friendly	3.5
Promote Angiogenesis	3.4
Cost Efficient	2.3
Promote Innervation	1.5
Minimize Environmental Impact	0.8

This shows that the main objectives the team focused on are for the scaffold to promote myogenesis, have reproducible composite fabrication, robust scaffold properties, and be user friendly.

## 3.6 Functions and Specifications

Specific functions were identified to determine whether or not the scaffold would be successful in achieving the objectives. For the first two objectives, user friendly and reproducible fabrication, a singular function was developed to optimize fabrication. The next objective, robust scaffold properties, was achieved by ensuring the scaffold promoted viability and prolonged degradation. Finally, to promote myogenesis, the functions that needed to be achieved were cellular alignment and controlled release throughout the repair timespan.

### 3.6.1 Function 1: Fabricated with over 90% success and require under 2 hours user labor

For two of the main objectives, user friendly and reproducible composite fabrication, the sub objectives included being easy to handle and reproduce along with being a supportive functional layer that could be modified for full-thickness solutions. To ensure this, the scaffold would need to be fabricated with 90% success and require under two hours user labor. This means that when scaffold are fabricated this way, 90% of them must be viable for experiments, without holes or incomplete incorporation with the frame. The composite needs to be much easier to handle and store than fibrin microthreads. To do this, the team would need to use the Pins' Lab protocols for fibrin microthreads and films and combine them while testing different variations for a composite scaffold. This could include altering different steps in the process or how the user interacts with the scaffold. Some variations that will be included are whether or not coating the material the gel is cast on is necessary, the best way to organize the

threads, the rinse times and volumes of water used for baths and which patterned surface shall be used. A similar approach would need to be done to ensure it could be fabricated in under two hours. A series of experiments needs to be completed that records the time taken for each step as well as the viability of the scaffolds using a particular method. This can be denoted by the number of usable scaffolds per batch which is typically five scaffolds per one milliliter polymerized fibrin.

### 3.6.2 Function 2: Promotes Cellular Viability

Primarily, the fibrin composite needs to not only be biocompatible, but must promote cellular growth. The composite needs to provide a stable environment for the cells with potential for muscle differentiation. The cell type to be used for the entirety of the experiments are C2C12 murine myoblasts because it is a relevant muscle progenitor cell line. The first step in doing that is providing an environment, with the composite that allows survival to be maintained. In addition, it must allow for cellular proliferation and adhesion onto the scaffold. The composite will maintain this stable environment for the duration of testing incubation which is simulated to be four days, as this should be sufficient to see multiple population doublings and be an indicator of long-term viability (Burattini, 2004). To test this, a viability assay can be performed using resazurin to show proliferation compared to a positive control after incubation. If the cellular viability is not compromised during this incubation period, it indicates that the scaffold is achieving this function. Similar results should be achieved when incubation time is extended to the entire three-week time span.

### 3.6.3 Function 3: Prolongs Degradation to Preserve Partial Structural Integrity for Two Weeks

Spatiotemporal degradation is necessary for treating VML to allow the native muscle fibers to integrate into the scaffold and eventually replace it. To successfully allow for tissue integration the scaffold should degrade slowly through the repair phase which takes three to four weeks (Tatsumi, 2004). This means that the time that the scaffold remains in the affected area should be equal to the time it takes to synthesize mature muscle tissue (Yannas, 2005). In order to accomplish this, the scaffold may need to be crosslinked to fortify the fibrin composite network to slow the degradation process (Page, 2011). In order to test that the scaffold is capable of remaining structurally intact for this time period, cells can be seeded on the surface and degradation can be measured by imaging the scaffolds at time points and identifying the degraded areas of the scaffold and quantifying them through imageJ. This will be used as a marker appropriate for measuring structural integrity. For exact quantification of this function, research and experiments would need to be conducted to test whether the composites degrade through bulk or surface degradation but that is outside the scope of this project due to time constraints. Newly created, and nondegraded scaffolds should be used to determine the degradation. Additionally, the same number of cells seeded on the surface are used across all experiments. The analysis will compare the percent area remaining of the scaffold and the team will mark success based on the percent area remaining after two weeks.

### 3.6.4 Function 4: Promotes Nuclear Alignment Along Fibrin Threads at Angles <10 Degrees Relative to the Thread

For the proper regeneration of functional muscle tissue, the scaffold needs to promote cellular alignment which will lead to the formation of myotubules (Bettadapur, 2016). As sub functions, the scaffold needs to allow for cellular signaling, migration, alignment and infiltration into and around the composite. In order to evaluate the success of this function, the C2C12 cells used will be fluorescently tagged using Hoechst, which stains the cell nucleus. Using a fluorescent microscope, these samples will be imaged at regions on the composite containing a thread for reference. Success will be achieved if the composite significantly improves cellular alignment compared to a plain film. This can be done by using imageJ to make the nuclei ellipsoidal and quantify how frequently the angles they are at align in response to a topographical cue such as the fibrin microthreads incorporated in the composite. Through histograms, the angles can be binned at intervals of 10 degrees and less than 10 degrees will be considered highly aligned cell nuclei. Therefore, the composite should significantly increase the frequency of nuclei aligned less than 10 degrees relative to the thread compared to a control scaffold. Significance can be quantified using an unpaired t-test between the <10 degree frequencies for each group.

### 3.6.5 Function 5: Releases 10 ng of FGF-2 over a period of two weeks

For the specific scope of the project, the design team and clients chose basic fibroblast growth factor (FGF-2) due to its ability to signal myogenesis, angiogenesis and innervation. While promoting myogenesis is the main objective for this function, it is advantageous to show proof-of-concept experiments with a growth factor that could be used in the future to promote all

three processes involved in regeneration. However, like other growth factors, FGF-2 has a short half-life (Lazarous, 1995). Therefore, if delivered in a bolus manner, such as an injection, the benefits and cues from the factor will not be as effective. For the specific scaffold being developed, a controlled release method must be utilized to allow for FGF-2 release over time to increase cellular activity. In order to determine the efficiency of the scaffold, release profiles can be used to monitor time versus amount of FGF-2 released from the scaffold. In order to accomplish this, an ELISA specific to the detection of FGF-2 is used. Samples will be compared to known standards in order to determine concentrations over time. To use concentrations that are relevant to the current research being done, the scaffold should be capable of releasing at least 10 ng of FGF-2 after being loaded (Makridakis, 2010). A successful growth factor release rate should sustain the release of the FGF-2 loaded into or bound to each scaffold throughout the desired release period, at least two weeks to match the repair phase.

### 3.7 Engineering Standards

Strict standards must be followed to ensure safety and functionality of the device. International Organization of Standardization (ISO) is a governing body that ensures that products are safe, reliable, and of good quality. The standard 10993-5:2009 is for assessing the biocompatibility of medical devices and materials, specifically, the cytotoxicity assessment in vitro. This standard is applicable for the device since it is designed to be implanted and in vitro experiments will be conducted. In the cell viability assay which will be done for the corresponding function, the results will also allow us to conclude that there are not cytotoxic to the cells if they sufficiently allow for proliferation that is comparative to a positive control.

American Society of Testing and Materials (ASTM) has formulated a standard guide for characterization and testing of biomaterial scaffolds used in tissue engineered medical products called ASTM F2150. The standard is a resource of currently available test methods for the characterization of the compositional and structural aspect of the scaffold. The test methods guide characterization of bulk physical, chemical, mechanical, and surface properties of a scaffold by describing test methods to determine, tensile, flexure, compressive, density, molecular weight, pore size and other characteristics. Degradation is a vital aspect of the scaffold and F2150 references F1635 which is a test method for characterizing degradation profiles of natural polymers such as fibrin. The standard also referenced ISO 10993 for additional guidance in the profiling of degradation. Specifically 10993-13 explains a test method for real-time degradation test in a simulated environment.

Since the device is designed to release FGF-2, drug release must follow strict standards. However based on ASTM F2211-13 there is currently no standard for the characterization and sourcing of GFs and methods for their assay. Also based on the ASTM F211 there is currently a need for guidance for development of *in vitro* assays to measure release of therapeutic proteins from matrices. The general consensus for evaluating drug release involve the following three methods sample and separate (SS), continuous flow (CF), dialysis membrane (DM) (D'Souza, 2014). The three methods are advantageous due to the ability to evaluate nano-sized dosage forms which is ideal for GFs (D'Souza, 2014). For the SS method entails having the drug delivery system be introduced into release media that is maintained at constant physiological conditions. The drug release can then be quantified by sampling the release media. The SS method provides a direct approach to monitor drug release that is the most simple. CF method monitors drug release by using an IV or flow-through cell apparatus. The method allows for drug release to occur as a result of buffer or media being constantly circulated through a column

containing the drug delivery system. The eluent can be collected and monitored to create a release profile. DM is considered the most versatile and popular of the three methods (D'Souza, 2014). This method involves physically separating the drug delivery system by using a dialysis membrane. The drug delivery system is introduced to a dialysis bag containing release media that is subsequently sealed and placed in a larger vessel containing release media. The drug will release and diffuse through the dialysis membrane to the outer compartment where it is sampled for analysis to create a release profile (D'souza, 2014).

Before any medical device can be implanted, it is vital that it is sterilized following the standard ISO 11737 to mitigate infection and other complications. This standard evaluates the amount of microorganisms that may be present, tests the sterility, and validates the sterilization process.

### 3.8 Revised Client Statement

From the weighted objectives and further specification from the clients and user, the team developed a revised client statement:

*“Design, develop, and characterize a **composite fibrin scaffold** composed of a patterned fibrin film with fibrin threads to provide topographical **cues for cellular alignment** that will guide myotube formation and myogenesis in an **easily reproducible** manner. The fabrication should be **user friendly**, and the composite should promote proliferation through the **controlled release of FGF-2** to the scaffold by adsorbing heparin and **prolonging scaffold degradation** in vitro for two weeks by chemically crosslinking with EDC/NHS solution.”*

This revised client statement will be used to ensure that the clients' and users' wants and needs are met with the various design specifications determined by the design team.

## 4.0 The Design Process

Once the team completely understood the background of the project and stakeholder's expectations, a project strategy was developed. This project strategy outlined a plan of action for the work needed to accomplish the project goals, starting with an analysis of the client, user, and designer's priorities, developing a series of functions, and determining means which would be capable of accomplishing these functions. Once all possibilities were determined, the success-rate of said means were then evaluated in terms of specifications, which lead to the final design.

### 4.1 Needs Analysis

As outlined in Chapter 3.5, all objectives were ranked based on their importance to the success of the project by the clients, Professor Pins and Professor Coburn, the users, Meagan Carnes and Joanna Santos, and the design team. The objectives are listed in order of importance based on percentage of the total points in Table 14.

*Table 14: Ranked objectives by percentage*

<b>Objective</b>	<b>Percentage</b>
Promote Myogenesis	38%
Reproducible Composite Fabrication	34%
Robust Scaffold Properties	33%
User Friendly	20%
Promote Angiogenesis	20%
Cost Efficient	13%
Promote Innervation	9%
Minimize Environmental Impact	5%

Once the main objectives were prioritized, the needs and wants of the project were developed. A need was defined as something that the stakeholders felt were integral to the success of the project. Based on the way in which the objectives were ranked, as seen in Table 13, the design team determined which objectives would be translated to needs. The top four ranked objectives, to **Promote Myogenesis**, to allow for **Reproducible composite fabrication**, to include **Robust scaffold properties**, and to create something **User friendly**. All the needs, which were determined by the design team in collaboration with the client's and user's rankings, were ultimately used to generate the functions of the scaffold.

A want was defined as something which was desired to be included, but would not be absolutely necessary. All of these lowly ranked objectives would improve the final, but without them, the team still would have created a successful product. Similarly, based on the way in which the objectives were ranked, as seen in Table 14, the design team determined which objectives would be translated to wants. The bottom four ranked objectives, to Promote angiogenesis, create a Cost efficient scaffold, to Promote innervation, and to Minimize environmental impact.

## 4.2 Design Alternatives

For each of the functions that the design group identified, a list of design alternatives (means) was identified. Means are different ways in which the scaffold material and modification options could fulfill each functional requirement. Each means was then compared to the list of constraints. If the means did not pass our constraints test then that specific means was no longer considered a viable option. Appendix B: Constraints Test for Developed Mean shows a list of our means and whether or not they passed the constraints test. Once it was determined whether

or not the means passed the constraint test, each means was looked into further and a list of pros and cons was developed for each. Table 15 shows the list of means for each function that passed the constraints test.

*Table 15: Means for each function*

<b>Promotes cellular viability</b>	<b>Prolongs degradation to preserve partial structural integrity</b>	<b>Promotes nuclear alignment</b>	<b>Releases FGF-2 over a period of two weeks</b>
Fibrin Film	Chemical Crosslinking	Fibrin Microthreads	Diffusion
Fibrin Gel	UV Crosslinking	Patterned Surface	Degradation
Fibrin Microthreads	Protease Inhibitors	Microthreads with Peptide Ligands	Polymer Encapsulation
Fibrin Gel with Microthreads	-	Patterned Surface with Microthreads	Immobilization using heparin
Fibrin Film with Microthreads	-	Patterned Surface with Peptide Ligands	

#### 4.2.1 Fabrication Optimization Means

The means for fabrication optimization were approached in a slightly different manner than the means for the following functions. Where listing multiple options for each function is possible for functions 2-5, the optimization means only include binary options. Therefore, they were just listed and tests during scaffold fabrication. The variables tested and adjusted during fabrication were the alignment method – manual alignment or using the vacuum alignment device, coating the casting platform – either coated according to the protocol used in Pins’ lab or left uncoated,

and finally the rinse duration and volume for the rinses after casting – ranging from 5 – 10 minutes and 15 mL to 25 mL per scaffold.

#### 4.2.2 Cellular Survival Means

##### *Fibrin Gel*

Fibrin gel is made of the proteins fibrinogen and thrombin, which are crucial in the blood clotting cascade. Fibrin gels are easy to produce, can have growth factors incorporated into their three-dimensional matrix, and have been shown to promote healing in several different wound types including skeletal muscle (Ye, 2000). Fibrin gels are often used within biomaterials to promote wound healing because the polymerization mechanism of fibrin allows controlled gelation times. Fibrin gels are characterized by their nonlinear elasticity, soft compliance at small strains, and their ability to stiffen to resist deformation (Janmey, 2009). The pros and cons of fibrin gel are outlined in Table 16.

*Table 16: Pros and cons for fibrin gel to promote cellular survival*

<b>Pros</b>	<b>Cons</b>
1. Easy to produce	1. Cells are unable to adhere and move through the fibrin gel
2. The fibrin gel drug delivery system maintains the biological activity of FGF-2	2. Mechanical properties are weak for functional replacement of load-bearing skeletal muscle tissue
3. Parameters such as crosslinking density and fibrin concentration can be controlled in a gel to control the release of FGF-2	3. Degrades rapidly in vivo

### ***Fibrin Film***

Fibrin film is similar to the first mean as it is easy to produce and acts as a natural reservoir for the binding and release of growth factors (Ye, 2000). The dehydration of a fibrin gel into a film makes the network of fibrin tighter and increases the degradation time(Ye, 2000). Fibrin films have been found to enhance cell proliferation and promote an organized cell response to a biomaterial (Campbell, 2005). The mechanical properties of fibrin films make it possible to use patterned arrays of growth factors on its surface, which can be used to seed cells (Campbell, 2005). Table 17 outlines the pros and cons of using fibrin film.

Table 17: Pros and cons for fibrin film to promote cellular survival

<b>Pros</b>	<b>Cons</b>
1. Easy to produce	1. Fragile and brittle
2. Cells are able to move through the fibrin film	2. Limited information about long-term success when used solely
3. Fibrin acts as a natural reservoir for the binding and release of certain GFs including FGF-2	3. Stiffness modulates deeply adhesion, proliferation, and differentiation

### ***Fibrin Microthreads***

Fibrin microthreads have been shown to promote ingrowth of new muscle tissue when implanted in a skeletal muscle deficit (Page, 2011). Fibrin microthreads are 155–165  $\mu\text{m}$  in diameter, which is a proper diameter to promote longitudinal growth and alignment of cells (Page, 2011). It is possible to modify their mechanical strength and degradation rate in order to achieve the optimum functionality for the specific application (Page, 2011). Fibrin microthreads can act as a delivery vehicle for cell implantation by allowing cell seeding and alignment (Page, 2011). On the downside, fibrin microthreads have a time consuming preparation time and can degrade rapidly *in vivo* (Page, 2011). Pros and cons for the use of fibrin microthreads are outlined in

Table 18.

Table 18: pros and cons for fibrin microthreads to promote cellular survival

<b>Pros</b>	<b>Cons</b>
1. Have been shown to direct aligned muscle regeneration	1. Long preparation time
2. Reduce the deposition of collagen in wounds, reducing scar formation	2. Degrade rapidly in vivo if not crosslinked
3. Promote ingrowth of new muscle tissue	3. Lacks user friendliness due to being hard to handle

### ***Composite of Fibrin Gel with Microthreads***

Fibrin gel with microthreads is beneficial because the microthreads can compensate for the weak mechanical properties of the fibrin gel. Fibrin microthreads, when compared to fibrin gel scaffolds (UTS -  $6.5 \pm 2.0$  kPa), have shown significantly more strength with ultimate tensile strengths (UTS) of up to  $4.5 \pm 1.8$  MPa (Cornwell, 2007). Strategically combining fibrin microthreads with a gel provides mechanical properties similar to native tissue (Chroback, 2016). This suggests that using the gel and microthreads together will make the scaffold more robust and conducive to the development of organized and aligned tissue. Although gels with fibrin threads provide a microenvironment that mimics natural physiologic conditions, their strength is usually in the single kilopascal range, which may fall short of that of natural skeletal muscle tissue (Cornwell, 2007). Table 19 shows the pros and cons for using fibrin gel with microthreads.

Table 19: Pros and cons for fibrin gel with microthreads to promote cellular survival

<b>Pros</b>	<b>Cons</b>
1. Microthreads enhance mechanical properties	1. Long preparation time

2. Microthreads make scaffold conducive to tissue regeneration tissue regeneration	
3. Gel acts as reservoir for growth factors	

### ***Composite Fibrin Film with Microthreads***

Fibrin film with microthreads is similar to the fourth mean because the microthreads improve the mechanical properties and increase the rigidity. This concept has not been evaluated before, but has the potential to combine the pros of the fibrin film and the fibrin microthreads, as previously described. While the microthreads enhance the mechanical properties and promote alignment, the film could potentially acts as a reservoir for growth factors and allows the cells to move throughout it (Ye, 2000) The pros and cons are outlined in Table 20.

*Table 20: Pros and cons for fibrin film to promote cellular survival*

<b>Pros</b>	<b>Cons</b>
1. Microthreads enhance mechanical properties	1. Long preparation time
2. Microthreads make scaffold conducive to tissue regeneration	2. Fragile and brittle
3. Better mechanical properties than gel with microthreads	

### **4.2.3 Prolong Degradation Means**

Due to the nature of VML, the natural biochemical cues such as growth factors that signal for cellular processes are absent from the wound site. For a scaffold to be effective in treating VML, the scaffold must remain intact long enough through the repair phase to effectively release growth factors. Additionally, the scaffold should degrade in a timeframe that is both physiologically relevant but additionally promotes regeneration by closely matching the time for

tissue growth (Sung, 2004). In essence, the scaffold ideally should degrade while simultaneously be replaced with new skeletal muscle tissue. Methods to slow down degradation include chemical crosslinking, physical crosslinking, and the incorporation of protease inhibitors (Grasman, 2012; Cornwell, 2007; Thomson, 2013).

### ***Chemical Crosslinking through EDC/NHS***

The chemical crosslinking strategy currently being used in Pins lab is 1-ethyl-3-(3-dimethylaminopropyl) carbodiimide and N-hydroxysulfosuccinimide (NHS) (EDC/NHS) which has been developed for the use with fibrin microthreads (Grasman, 2012). Using these two agents in a neutral buffer has been shown to effectively crosslink fibrin because it tightens the molecular network, and therefore slows down the degradation rate (Grasman, 2012). The pros and cons of EDC/NHS crosslinking are outlined in Table 21.

Table 21: Pros and cons of chemical crosslinking to allow for isomorphous degradation

<b>Pros</b>	<b>Cons</b>
1. Inexpensive	1. Time Consuming
2. Been shown to tether GFs to the surface of scaffolds	2. May not be suitable for all applications needed
3. Fibrin integrity remains intact	3. Changes mechanical properties
4. Possibility for tunable mechanical properties	

### ***Physical Crosslinking through UV Radiation***

The second means is a strategy that involves UV radiation to crosslink the composite, or components of it. The fibrin is subjected to a short burst of UV rays to reinforce the fibrin network and reduce the degradation rate (Cornwell, 2007). UV crosslinking has also been shown to attenuate fibroblast proliferation (Cornwell, 2007). The pros and cons of UV crosslinking is outlined in Table 22.

Table 22: Pros and cons of UV crosslinking to allow for isomorphous degradation

<b>Pros</b>	<b>Cons</b>
1. Faster procedure	1. May damage certain constructs
2. Can assure treatment is the same each time	2. May not be suitable for all applications needed
3. Been shown to tether GFs to the surface of scaffolds	3. Free radical formation
4. Increases mechanical properties	4. Alters cell-matrix interactions

### ***Protease Inhibitors***

The third means is a strategy that plays a role in the natural activity of fibrin. By adding protease inhibitors, such as aprotinin, and incorporating them into the network slowed degradation occurs (Smith, 2007; Thomson, 2013). Aprotinin is a small protein that can diffuse out from the network to allow fibrinolysis to occur (Smith, 2007). By chemically conjugating a protease inhibitors to fibrinogen, it will inhibit the plasmin-mediated fibrin degradation and slow the process (Smith, 2007; Thomson, 2013). Additionally, the concentration of aprotinin can directly tune the degradation rate, which makes it easy to fine tune the scaffold to reach a desired degradation rate (Smith, 2007; Thomson, 2013). Table 23 outlines the pros and cons for the use of protease inhibitors for prolonged degradation.

*Table 23: Pros and cons of protease inhibitors to allow for isomorphous degradation*

<b>Pros</b>	<b>Cons</b>
1. Would be harmless in a fibrin scaffold in small enough doses	1. May not increase mechanical properties
2. Could easily modify to change degradation time	2. Process may be time consuming
3. Best mimics natural processes	

#### **4.2.4 Promote Aligned Myogenesis Means**

For a scaffold to be effective in treating VML, the host cells need to be aligned to form functional muscle tissue. Due to the nature of VML, the natural cues that would promote alignment are absent from the wound site. Specific addition or modification to scaffold surfaces and composition are able to cue cellular alignment (Cezar, 2015). These methods include the use of fibrin microthreads, patterned surfaces, fibrin microthreads with peptide ligands, fibrin

microthreads with patterned surfaces, and patterned surfaces with peptide ligands (Chen, 2015, Cornwell, 2007).

***Fibrin Microthreads***

The first means to promote aligned myogenesis is through the use of fibrin microthreads. The thread-like structure provides an aligned surface for cells to adhere to and fuse together to form functional myofibers (Page, 2011). The fibrin itself also contains biochemical cues, along with the aligned thread structure, promotes tissue regeneration by allowing the cells to form an aligned matrix which mimics native tissue architecture (Cornwell, 2007). Pros and cons for the use of microthreads are outlined in Table 24.

*Table 24: Pros and cons for fibrin microthreads to promote aligned myogenesis*

<b>Pros</b>	<b>Cons</b>
1. Promotes cellular alignment	1. Adds additional fabrication time to the scaffold
2. Fabrication protocol is already established	2. Brittle
3. Easy to make reproducibly	3. Difficult to handle

***Patterned Surface***

For the second means, patterned surfaces with grooves and channels provide indentations on the micro-scale for cells to migrate along as well as align in (Chen, 2015). Cells that have the intrinsic potential for cellular alignment have shown alignment when confined in microarchitectures such as grooves and channels on the surface of scaffolds ranging in groove widths of several nanometers to 100 micrometers (Chen, 2015). The use of these

microarchitectures provides a 3D structure that is favorable for cellular alignment (Aubin, 2010; Chen, 2015). An outline of the pros and cons for using a patterned surface can be found in Table 25.

*Table 25: Pros and cons for patterned surfaces to promote aligned myogenesis*

<b>Pros</b>	<b>Cons</b>
1. Easy to create rigid grid on scaffold	1. Heterogeneous distribution depending on difficult to control and manufacture concentration of patterned grooves
2. Modification beyond conventional patterns allow for more design flexibility	2. Custom wafers for patterns can have a high initial cost
3. Reduced fabrication time	3. Patterns may not work with all scaffold types

### ***Fibrin Microthreads and Peptide Ligands***

The third means to promote cellular alignment are through the use of microthreads and peptide ligands. Fibrin microthreads on their own have already shown potential for cellular alignment by providing a 3D architecture close to that of native tissue (Cornwell, 2010). Peptide ligands have the ability to mimic the adhesive cues of myoblasts (Gribova, 2014). By applying the peptide ligands to the thread, the peptide is able to increase cellular adhesion. The increased cellular adhesion to the aligned fiber promotes cellular fusion into multinucleated myofibrils (Rowley, 1999). Fibronectin is an essential part of the basement membrane of muscle fibers *in vivo* (Sanes, 1982). Therefore by incorporating a fibronectin-derived amino acid sequence, like RGD peptide has been shown to be a potential cue to increase cellular alignment (Sengupta, 2012). The pros and cons of this option are outlined in Table 26.

Table 26: Pros and cons for fibrin microthreads and peptide ligands to promote aligned myogenesis

<b>Pros</b>	<b>Cons</b>
1. Peptides would provide additional cues for alignment	1. Sterilization procedure may need to change from current methods
2. Inexpensive to add to the current microthread fabrication procedure	2. Has the potential to detach/denature and be ineffective
3. Minimizes the risk of immune reactivity or pathogen transfer when compared to xenografts or cadaveric protein sources	3. Increased prep-time required

### ***Fibrin Microthreads and Patterned Surface***

For the fourth means, fibrin microthreads with the addition of patterned surfaces may allow for additional alignment due to an increase in topographical cues along with the chemical cues from the fibrin microthreads. Both the use of fibrin threads and patterned surface individually have shown increased possibility for cellular alignment due to their 3D structures (Cornwell, 20010 Aubin, 2010). Together there may be an increase in cellular alignment due to an increase in topographical and structural cues. The pros and cons of fibrin microthreads and patterned surfaces are outlined in Table 27.

Table 27: Pros and cons for fibrin microthreads and patterned surfaces to promote aligned myogenesis

<b>Pros</b>	<b>Cons</b>
1. Increased alignment possibilities	1. Increased fabrication time
2. Allows for increased design flexibility	2. Pattern may not work with all scaffold types

### ***Patterned Surface and Peptide Ligands***

The fifth means for promoting aligned myogenesis is through the use of patterned surfaces and peptide ligands. Topographically the patterned surface would promote alignment and migration by providing a preferred 3D structure for the cells to align in (Aubin, 2010). With the addition of peptide ligands, the scaffold would be able to provide chemical cues for cellular alignment by mimicking the adhesive cues for myoblasts (Rowley, 1999). Table 28 outlines the pros and cons for the use of patterned surface and peptide ligands.

*Table 28: Pros and cons for patterned surfaces and peptide ligands to promote aligned myogenesis*

<b>Pros</b>	<b>Cons</b>
1. Peptides would provide additional cues for alignment	1. Sterilization procedure may be more difficult
2. Inexpensive to add to patterned surfaces	2. May detach/ denature and be ineffective in the patterns
3. Minimize risk of immune reaction	3. Increase prep-time is required

### **4.2.5 Controlled Release Means**

In order to properly simulate the same niche as natural regeneration, a controlled release of relevant GFs must be developed from the scaffold. The scaffold must be fabricated in such a way that allows for growth factor loading, specifically FGF-2, and to support sustained release of this growth factor throughout the repair phase, about 3-4 weeks (Tatsumi, 2004). In order to accomplish this within a fibrin scaffold, there are a variety of methods previously used, each having their own advantages and disadvantages, such as diffusion, degradation driven, immobilization using heparin, polymer encapsulation, and finally stimuli driven release (Section 2.3.3).

## *Diffusion*

Diffusion driven controlled release utilizes the pores of a specific material in order to control the release of an agent, or growth factor. In the case of the fibrin scaffold developed, a monolithic or matrix device would be used (Fan, 2012). This method of controlled release would be accomplished by soaking the fibrin scaffold in a saturated bath of growth factors and allowing the system to come to equilibrium. This method could also be accomplished by bulk loading of the FGF-2 with the solutions used to create the scaffold. The scaffold could then be placed in the desired environment and the concentration gradient would drive the growth factor out of the scaffold. In order to alter the pores of the scaffold, salts or similar dissolvable materials could be used during the fabrication of the scaffold. A schematic outlining this mechanism can be found in Figure 10 and the pros and cons of using diffusion as a mechanism for controlled release in Table 29.

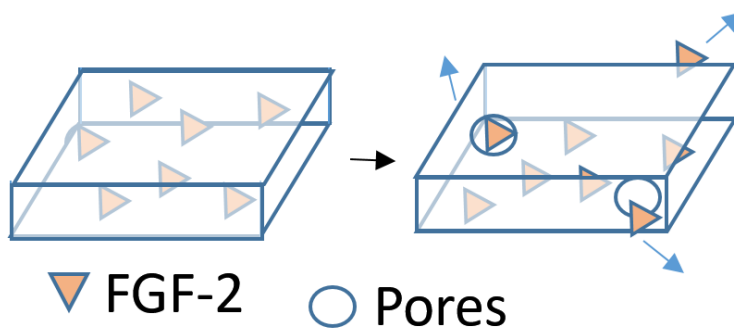


*Figure 10: Diffusion drive release of FGF-2*

Table 29: Pros and cons for diffusion to allow for controlled release

<b>Pros</b>	<b>Cons</b>
1. Allows transport of nutrients and GF within scaffold and with surrounding tissue	1. Heterogeneous distribution depending on difficult to control concentration gradient
2. Pore size can be altered to control what is released using inexpensive salts	

### ***Degradation-driven***

A degradation-driven system utilizes the scaffold degradation to control the release of the active agent, or growth factor. Simplifying the degradation of the scaffold down to only surface degradation will allow for an easier understanding of this method of release. For this method, the growth factor would be fully incorporated within the scaffold. If the scaffold is loaded with the growth factor, similarly to the monolithic method above, the growth factor will be dispersed throughout the entire scaffold. Assuming that the growth factor is too small to diffuse out of the scaffold through the pores, the growth factor will be released as the material of the scaffold erodes. However, bulk degradation as well as surface degradation is frequently observed, making the analytical predictions of this system more complex (Fan, 2000) Figure 11 outlines the mechanism by which degradation driven systems allow for controlled release and Table 30 outlines the pros and cons of this method

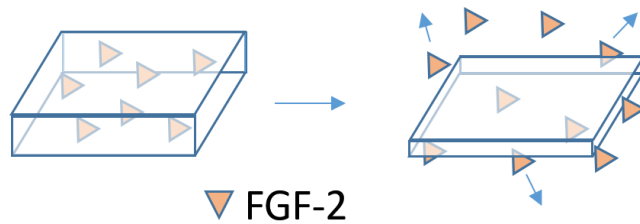


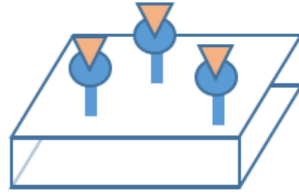
Figure 11: Degradation induced FGF-2 release

Table 30: Pros and cons of a degradation driven system to allow for controlled release

Pros	Cons
1. No additional material needed in scaffold	1. Scaffold may degrade too quickly
	2. Heterogeneous degradation resulting in different release profiles across scaffold

### ***Immobilization using heparin***

Certain growth factors, including FGF-2, have an affinity to the glycosaminoglycan carbohydrate known as heparin. Heparin can ionically bind to the growth factors, temporarily sequestering the factor into the scaffold (Hudalla, 2011). Until disassociation or competitive ionic interaction is able to cleave the heparin-growth factor ionic bond, the growth factor will remain inside the scaffold's matrix. This method would be incorporated by EDC/NHS crosslinking the scaffold with heparin. The growth factor, in solution, would be placed onto the scaffold, allowing the development of the ionic bond between the growth factor and the heparin molecules. The growth factor would remain immobilized until the bond was cleaved, releasing the growth factor into the surroundings. The immobilization of FGF-2 through the use of heparin is characterized in Figure 12 the pros and cons of this method are outlined in Table 31.



▽ FGF-2      ● Heparin

Figure 12: Immobilization of FGF-2 using heparin

Table 31: Pros and cons of immobilization using heparin to allow for controlled release

Pros	Cons
1. Extensive control over release profile	1. Not all GFs have affinity to heparin
2. Can use any GF with affinity to heparin	

### ***Polymer encapsulation***

In this work, polymer encapsulation is referring specifically to the incorporation of polymeric beads, encapsulating the growth factor, into the scaffold to delay the release. Polymer encapsulation controlled release use alternate polymers, such as alginate, to encapsulate the growth factor. The encapsulation of the growth factor inside of these beads will be able to delay the release of the growth factor based on the degradation rate of the polymer in the system. As these polymer beads degrade, the growth factor will be released into the scaffold, which will allow for diffusion out of the scaffold due to the concentration gradient in the system. Before the polymer beads have degraded, the growth factor will be unable to diffuse out of the scaffold due to the additional mass. Altering the compositions of the polymer beads will allow for control of the release rate (Fan, 2012). A schematic depicting the mechanism of encapsulation to allow for

controlled releases is shown in Figure 13 and the pros and cons for this method are outline in Table 32.

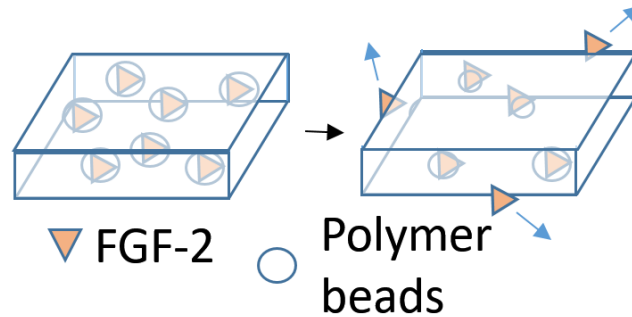


Figure 13: Polymer encapsulation for controlled release

Table 32: Pros and cons of polymer encapsulation to allow for controlled release

Pros	Cons
1. Different polymers have different degradation times	1. Potentially expensive, synthetic polymers can exhibit poor cell adhesion
	2. Possibly complex and time consuming

### 4.3 Means Evaluation

After the pros and cons for each means was thoroughly investigated, the team did a means evaluation through the use of a matrix found in Appendix F: Means Evaluation Matrix. In the matrix, each means was ranked based on how it contributed towards each of our main and sub-objectives. The mean is highlighted in red if it was later determined to not fit within the constraint and it is green if it is top-ranked. Each sub-objective had a 1 to 4 ranking system with a list of ranking quantifiers. A four was considered the highest ranking, while a one was the lowest. If a particular function had no corresponding contribution to a certain sub-function, then

that section was blacked out in the matrix. Only the means that passed the constraints test were scored in this matrix. Each design team member filled out the matrix and then results were discussed until there was a consensus on each ranking. Each means was ranked independent of the other means and was based only upon how well it accomplished the prioritized objectives.

Through this analysis, as seen in Table 33, it was determined that to accomplish function 2, cellular survival, the most efficient means would be **fibrin gel with microthreads** and **fibrin film with microthreads**. For function 3, the degradation of the scaffold, all three means ranked very similarly, so to further determine their performance experimental procedures were needed. For function 4, promoting myogenesis, the highest ranked means were **fibrin microthreads** and a **patterned scaffold with fibrin microthreads**. Finally, for function 5, the controlled release of FGF-2, **degradation**, and **immobilization using heparin** scored the highest. The means for function 1, fabrication success, were not ranked in the same manner due to the need for experimental testing to determine their performance.

*Table 33: Summary of means evaluation*

<b>Function</b>	<b>Means</b>	<b>Overall Score</b>
2	Fibrin film	36
	Fibrin gel	35
	Fibrin microthreads	33
	<b>Fibrin gel with microthreads</b>	38
	<b>Fibrin film with microthreads</b>	39
3	Protease Inhibitors	31
	<b>UV Crosslinking</b>	33
	<b>Chemical Crosslinking*</b>	31
4	<b>Fibrin microthreads</b>	39
	Patterened surface	34
	Microthreads + peptide	34
	<b>Patterned +microthread</b>	39
5	Diffusion	21
	<b>Degradation</b>	26
	<b>Immobilization using heparin*</b>	27
	Polymer encapsulation	20

## 4.4 Feasible designs

After all of the rankings were completed each means' total score was tallied. This helped the group to identify the most promising feasible means for each function. Morphology charts were developed for the means that ranked the highest in each function. The morphology charts for the highest ranking feasible means are shown in Table 34 – 37.

The highest ranked means were combined to create 5 feasible designs. The team developed visual prototypes depicting what the design would look like (Figures 14-18). Each has a top and front view of the composite with green representing the conjugation method of FGF-2 and yellow representing the crosslinking method for the scaffold. Fibrin microthreads are shown in blue, gels are depicted as light gray and films are depicted as dark gray.

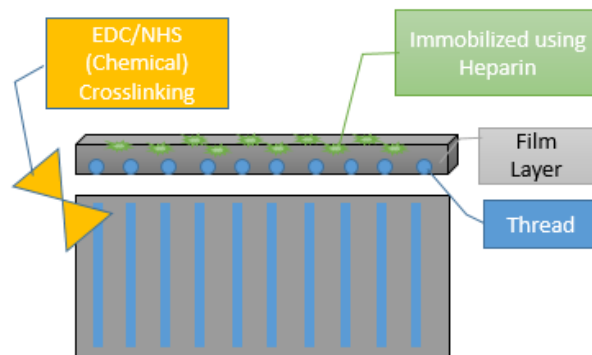


*Figure 14 Film with Microthreads, FGF-2 immobilized using heparin and EDC/NHS crosslinking*

Table 34: Morphology chart 1

Means	1	2	3	4	5
<b>Allows cellular survival through a form factor of a fibrin scaffold</b>	Fibrin Film	Fibrin gel	Fibrin Microthreads	Fibrin gel with Micro threads	Fibrin film with microthreads
<b>Promotes endogenous aligned myogenesis</b>	Fibrin Micro threads	Patterned Surface	Micro threads and peptides	Patterned surface and microthreads	Patterned surface and peptides
<b>Release FGF-2 throughout regeneration phase</b>	Diffusion	Degradation	Polymer Encapsulation	Immobilization using Heparin	-
<b>Spatiotemporal degradation “Isomorphous degradation”</b>	Chemical Crosslinking	UV Crosslinking	Protease Inhibitors	-	-

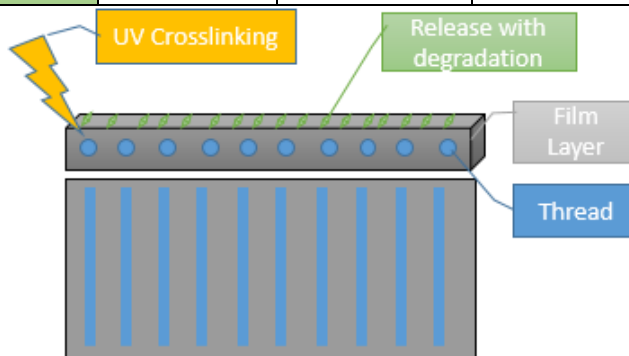


Figure 15: Film with microthreads, FGF-2 incorporated and released with degradation and UV crosslinked

Table 35: Morphology chart 2

Means	1	2	3	4	5
<b>Allows cellular survival through a form factor of a fibrin scaffold</b>	Fibrin Film	Fibrin gel	Fibrin Microthreads	Fibrin gel with Micro threads	Fibrin film with microthreads
<b>Promotes endogenous aligned myogenesis</b>	Fibrin Micro threads	Patterned Surface	Micro threads and peptides	Patterned surface and microthreads	Patterned surface and peptides
<b>Release FGF-2 throughout regeneration phase</b>	Diffusion	Degradation	Polymer Encapsulation	Immobilization using Heparin	-
<b>Spatiotemporal degradation “Isomorphous degradation”</b>	Chemical Crosslinking	UV Crosslinking	Protease Inhibitors	-	-

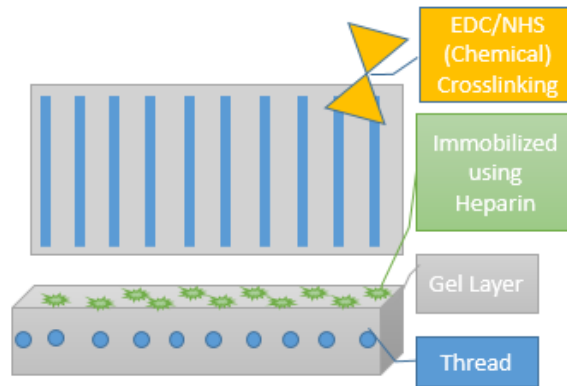


Figure 16: Gel with microthreads, FGF-2 immobilized using heparin and EDC/NHS crosslinked

Table 35: Morphology chart 3

Means	1	2	3	4	5
<b>Allows cellular survival through a form factor of a fibrin scaffold</b>	Fibrin Film	Fibrin gel	Fibrin Microthreads	Fibrin gel with Micro threads	Fibrin film with microthreads
<b>Promotes endogenous aligned myogenesis</b>	Fibrin Micro threads	Patterned Surface	Micro threads and peptides	Patterned surface and microthreads	Patterned surface and peptides
<b>Release FGF-2 throughout regeneration phase</b>	Diffusion	Degradation	Polymer Encapsulation	Immobilization using Heparin	-
<b>Spatiotemporal degradation “Isomorphous degradation”</b>	Chemical Crosslinking	UV Crosslinking	Protease Inhibitors	-	-

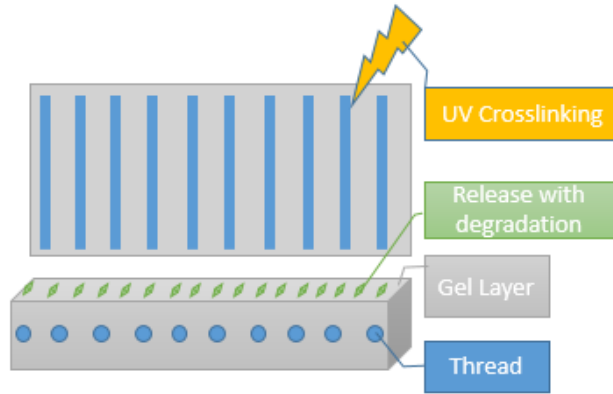


Figure 17: Gel with microthreads, FGF-2 released with degradation and UV crosslinked

Table 36: Morphology chart 4

Means	1	2	3	4	5
<b>Allows cellular survival through a form factor of a fibrin scaffold</b>	Fibrin Film	Fibrin gel	Fibrin Micro threads	Fibrin gel with Micro threads	Fibrin film with microthreads
<b>Promotes endogenous aligned myogenesis</b>	Fibrin Micro threads	Patterned Surface	Micro threads and peptides	Patterned surface and microthreads	Patterned surface and peptides
<b>Release FGF-2 throughout regeneration phase</b>	Diffusion	Degradation	Polymer Encapsulation	Immobilization using Heparin	-
<b>Spatiotemporal degradation "Isomorphous degradation"</b>	Chemical Crosslinking	UV Crosslinking	Protease Inhibitors	-	-

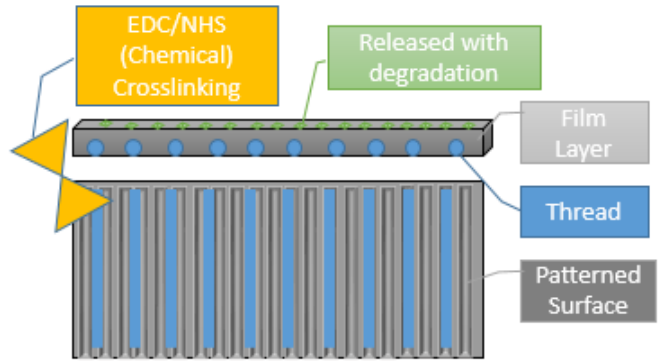


Figure 18: Film with microthreads and patterned surface, FGF-2 released with degradation and EDC/NHS crosslinked

Table 37: Morphology chart 5

Means	1	2	3	4	5
<b>Allows cellular survival through a form factor of a fibrin scaffold</b>	Fibrin Film	Fibrin gel	Fibrin Micro threads	Fibrin gel with Micro threads	Fibrin film with microthreads
<b>Promotes endogenous aligned myogenesis</b>	Fibrin Micro threads	Patterned Surface	Micro threads and peptides	Patterned surface and microthreads	Patterned surface and peptides
<b>Release FGF-2 throughout regeneration phase</b>	Diffusion	Degradation	Polymer Encapsulation	Immobilization using Heparin	-
<b>Spatiotemporal degradation “Isomorphous degradation”</b>	Chemical Crosslinking	UV Crosslinking	Protease Inhibitors	-	-

## 4.5 Final Design

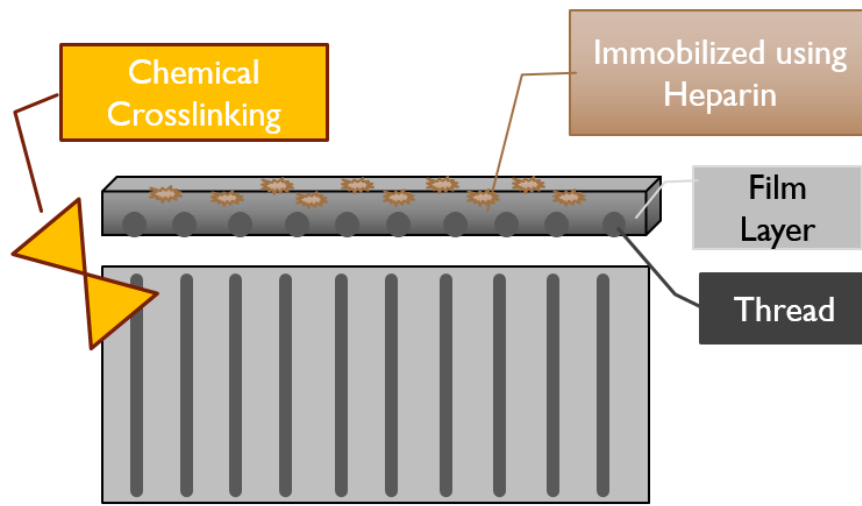


Figure 19: Final Design

The final design is a fibrin film with five uniformly-spaced fibrin microthreads (Figure 19). For the remainder of the report, the final design will be referred to as the composite. The FGF-2 will be incorporated onto the scaffold with the use of heparin. The ionic bond between the FGF-2 and the heparin will temporarily immobilize the FGF-2 until the bond is cleaved, delaying the release rate (Hudalla, 2011). The scaffold will be stabilized with chemical crosslinking via EDC/NHS solution in order to delay degradation throughout the FGF-2 release. The team decided this design is best fit to achieve all of the functions and does so in a way that is user friendly and reproducible.

## 5.0 Design Verification

In order to determine the validity of the design team's theoretical design, a series of characterization tests and experiments were performed to compare potential components of the final design and verify that the PFFT design was the best performing composite. Specifically,

compatibility tests were performed to determine if fibrin scaffold, both gels and films could be incorporated with fibrin microthreads to develop the composite desired for the project.

Ultimately, the team prepared initial experiments to optimize the patterning of the scaffolds, the optimal protocol for the composite and the loading of the FGF-2 growth factor. Once these initial experiments were deemed successful, the team tested the final design for performance in the five project functions. In order to test the capability of the scaffold in fulfilling the functions, the design team designed experiments to characterize the functions. The function that is being tested is stated under each experiment, except for experiment 1, which is not aimed at a specific function but aims rather to ensure reproducibility. Protocols for the following experiments were retrieved from Pins' Lab or created by the team unless otherwise specified and can be found in Appendix H.

## 5.1 Composite Fabrication Optimization

*Function 1: Fabricated with over 90% success and require under 2 hours user labor*

The first experiment performed was to create an optimized protocol for the composite fabrication. This included the creation of the scaffold with threads and the patterning step. The team determined success by adjusting the protocol to find the highest yield of scaffolds possible which quantifies reproducibility. The variables for composite fabrication were coating the casting surface with Pluronic F-127 solution or not, thread attachment with the vacuum alignment device or hand-aligned threads and rinse times for the diH<sub>2</sub>O baths. Batches of composites were made testing the different variable and the yield of each batch was recorded to determine which was most successful. The goal of this experiment was to find a combination of variables that were both high yield and easy to reproduce in a timely manner.

Depending on the casting platform, Pins Lab has traditionally used Pluronic F-127 coating to create a non-stick surface for fibrin polymerization which allows easy removal. Pluronic F-127 is a polymer which can be made into a 1% solution with water for use of baths to coat casting platforms. It is highly lipophilic and prevents the fibrin from adhering to the casting platforms. Previously, acetyl plastic slides have been used for a casting platform but with the new patterned PDMS molds, the team needed to test whether Pluronic F-127 coating was a required step. To test this 2-3 batches (5 composites per batch) were cast on molds that were and were not coated with 1% Pluronic F-127 To be coated, the protocol in Appendix H.

The yield was determined by counting the number of intact, usable films from each 5-film batch. Minor tears that did not impact the overall surface area of the film were considered usable. The results of the experiment are shown in Table 38.

*Table 38: Results from acetyl slide coating experiment*

Batch Number	No Pluronic (Yield)	Pluronic Coating (Yield)
1	3/5	5/5
2	4/5	5/5
3	2/5	4/5
4	3/5	5/5

From this experiment, the yield without coating was 60% versus 95% with the coating. The coating provided a noticeable increase in yield and was determined to be valuable in the fabrication process.

The incorporation of threads into a gel has been previously done using the vacuum alignment device in Pins' Lab developed in a 2015 MQP Project (GXP 1201). However, the team tested the efficiency of hand-aligning the low five-count threads and being able to fixed 12-13 frames per alignment attempt whereas the device only fits three to four frames. This is because

the total length of the 5-thread group with the device is about 3 inches, whereas manually aligning the original length threads yields a group with a total length of about 9-10 inches. To test this, average time to make composites was observed and user preference was recorded for each method.

The second test was to determine the best method for aligning the threads either using a the vacuum device or hand aligning longer threads. The time each method took for the aligning and gluing steps is shown in Table 39. The batch sizes vary based on the number of composites needed for a particular experiment and it is important to note that with both methods, the threads were drawn using Lacey and wet-stretched.

*Table 39: Results for alignment method experiment*

<b>Vacuum Device</b>	<b>Hand Alignment</b>
12 composites/ 45 min	13 composites/ 25 min
9 composites/30 min	6 composites/ 15 min
18 composites/ 60 min	24 composites/ 35
Average Time = 3.5 min/composite	Average Time = 0.54 min (35 seconds) / composite

The results shown that the hand alignment method is more efficient. It is on average, seven times faster for producing large batch sizes. All members of the team preferred this method and it is the final method used in the fabrication protocol.

Finally, incorporation of the threads into the film was a new step in which a protocol had not yet been developed for Pins Lab. For film fabrication, each sample was rinsed to remove calcium salts by submerging it in three dH<sub>2</sub>O baths for five minutes each with each bath being 15 mL. This method was tested with the threads, along with longer times and higher volumes of water to ensure that the calcium ions sufficiently diffused from both the film and threads. It was predicted by the team that a longer time would be necessary since the threads are embedded in the film, providing a potential barrier to diffusion. The success of each method was determined

by the presence of, or lack thereof, a salt ring in the center of the composite which makes it brittle and crack easily. The goal was to find a method that eliminated the presence of this ring.

The initial test performed was to see if pluronics was necessary for coating the acetyl slides on which the films are cast and dried. The yield was determined by counting the number of in-tact, usable films from each 5-film batch. Minor tares that did not impact the overall surface area of the film were considered usable. The results of the experiment are shown in Table 40.

*Table 40: Results from acetyl slide coating experiment*

Batch Number	No Pluronic (Yield)	Pluronic Coating (Yield)
1	3/5	5/5
2	4/5	5/5
3	2/5	4/5
4	3/5	5/5

From this experiment, the yield without coating was 60% versus 95% with the coating. The coating provided a noticeable increase in yield and was determined to be valuable in the fabrication process.

The second test was to determine the best method for aligning the threads: the vacuum device or hand aligning longer threads. The time each method took for the aligning and gluing steps is shown in Table 41. The batch sizes vary based on the number of composites needed for a

particular experiment and it is important to note that with both methods, the threads were drawn using Lacey and wet-stretched.

*Table 41: Results for alignment method experiment*

<b>Vacuum Device</b>	<b>Hand Alignment</b>
12 composites/ 45 min	13 composites/ 25 min
9 composites/30 min	6 composites/ 15 min
18 composites/ 60 min	24 composites/ 35
Average Time = 3.5 min/composite	Average Time = 0.54 min (35 seconds) / composite

The results shown that the hand alignment method is more efficient. It is on average, seven times faster for producing large batch sizes. All members of the team preferred this method and it is the final method used in the PFFT fabrication protocol. The third test completed to optimize the composite fabrication process was the rinse volume and time per sample. As previously mentioned, the standard for films was 15 mL per sample for five minutes each of the three times. To adjust this, longer times and greater volumes were tested. The yield of each variable batch tested was determined by the number of scaffolds which did not contain a salt ring after drying. To characterize the best method, any presence of a salt ring noticeable was determined to be unusable. The results are shown in Table 42.

*Table 42: Results from rinse time and volume experiment*

Time/rinse and Volume/scaffold	Yield
5 min and 15 mL	1/5
10 min and 15 mL	3/5
5 min and 25 mL	3/5
10 min and 25 mL	5/5

From the results, it was determined that the best method is 10 min per rinse and 25 mL per scaffold. For ease of use purposes, a large water bath with the same volume to scaffold ratio was used for a whole 5-composite batch. In other words, 125 mL was used per bath for 5 scaffolds

for 10 minutes. The yield remained 100% and it also saved time so it was determined to be the optimal rinse procedure for the protocol.

## 5.2 Cellular Viability

### *Function 2: Promotes cellular viability*

While fibrin is known to be a biocompatible material, it needed to be shown that the patterned fibrin film with threads design remains biocompatible and promotes cellular proliferation equally to a positive control for cell growth. In order to test the cellular viability of the composite scaffold, resazurin was used *in vitro* to measure cell viability. Resazurin is a molecule that is metabolized by living cells and produces a fluorescence change that can be quantified with a fluorescent plate reader where the fluorescent intensity directly correlates to the number of living cells. When added to the cells, an oxidized form of the resazurin enters the cell membrane and through enzymatic activity in the mitochondria it is converted to the reduced form (Al-Nasiry, 2007). The redox reaction occurs through electron transfer from NADPH, FADH, FMNH and NADH and this corresponds to the color change which goes from indigo to a pink hue (Al-Nasiry, 2007). To perform the assay the resazurin and media solution, which is made at a concentration shown in Appendix H, was added to 12-well tissue culture plates containing (1) composite scaffold, (2) fibrin films and (3) scaffolds with fibrin threads, as well as tissue culture plate (TCP) control (Figure 20). The film provides a group to compare the composite design to without threads, and the threads in a scaffold group provides a group to ensure that adding fibrin threads to the design does not produce any leachable materials that affect cell viability. The TCP wells provide a positive control to compare and ensure cell growth is equivalent for the composite. At t=0 days a low-volume cell solution containing 60,500 cells was added to a

dehydrated composite and allowed to adhere for two hours before adding 2 mL of media to each well.

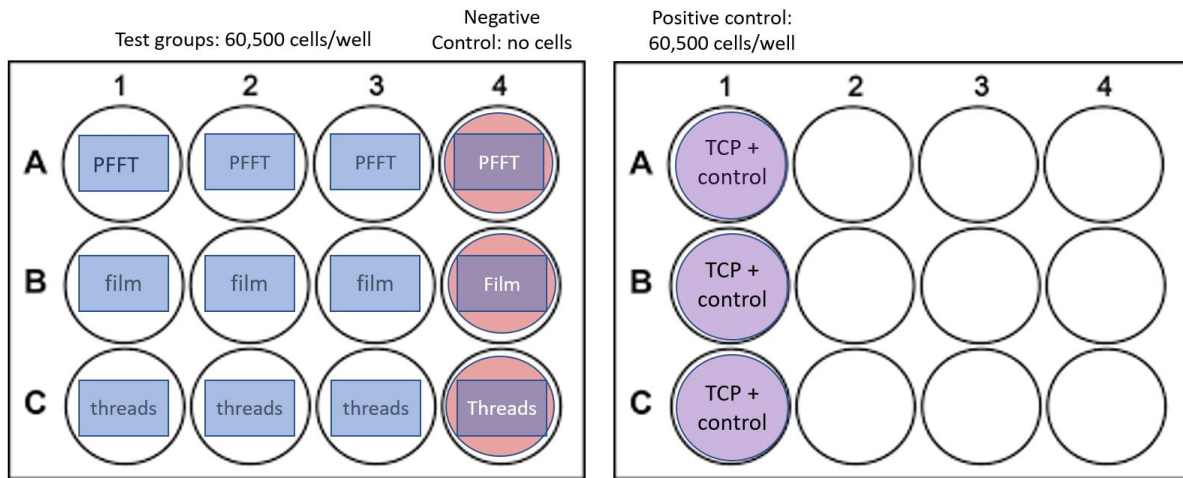


Figure 20: Experimental design of cell viability assay

For each trial, the solution was tested after 1 day and 4 days. The media was aspirated and replaced with 0.5 mL of the resazurin and media solution and incubated two hours. For each well sample, 100  $\mu$ L was pipetted in triplicate to a 96-well plate to be read with the fluorescent plate reader. The protocol for the plate reader was developed by Coburn lab and reads at a wavelength of 580-610 nm emission while using a 540-570 nm excitation wavelength. The full protocol for the resazurin cell viability assay can be found in Appendix H.

The data retrieved from the fluorescent plate was used in combination with a standard curve obtained using a serial dilution of cell totals. The standard curve allowed us to convert the fluorescent intensity to total cell numbers at a 100  $\mu$ l volume for that time point. For the purpose of our study, cell totals based on a consistent concentration were useful when discussing the data but absolute cell total calculations were not necessary as we only need to ensure there is no statistical difference between our sample and the TCP or other groups. A total of four trials were completed and analyzed for results. An ANOVA statistical test was used to compare all groups

for each time point. A p-value of  $<0.05$  was considered significant. All analysis was completed using GraphPad software.

The first step in this experiment was to create a standard curve that could be used to convert fluorescent intensity from the resazurin cell viability assay to a cell count. The results of the standard curve are shown in Appendix G. The  $R^2$  value of 0.9465 indicates that the trend line was a good linear fit for the standard curve data.

In order to show that the cells were surviving and proliferating on the composite scaffold, the resazurin assay fluorescent intensity was recorded for each sample of the composite, film, threads, and TCP. Each sample was loaded into the plate in triplicate, and an average reading was used, which was inserted into the equation shown on the standard curve graph in Appendix G in order to get a cell count based on the fluorescent intensity. For each trial, the data was graphed for the two time points, T1 which was sampled after 24 hours and T4 which was sampled after 4 days, as shown in Figure 21.

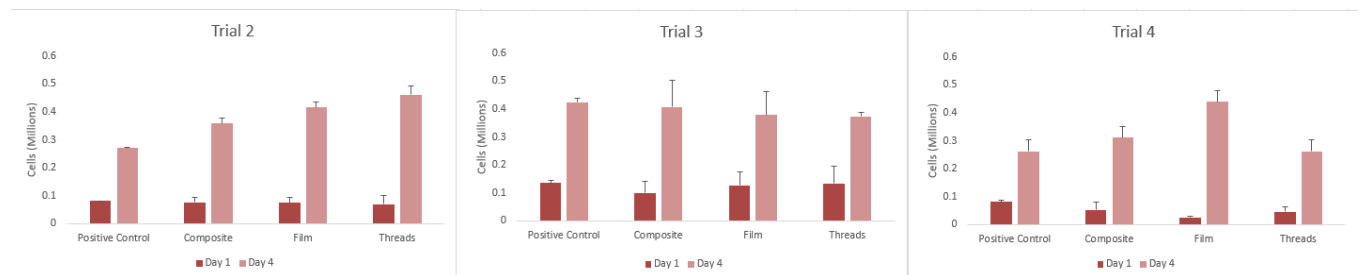


Figure 21: Results from cell viability assay from all 3 trials

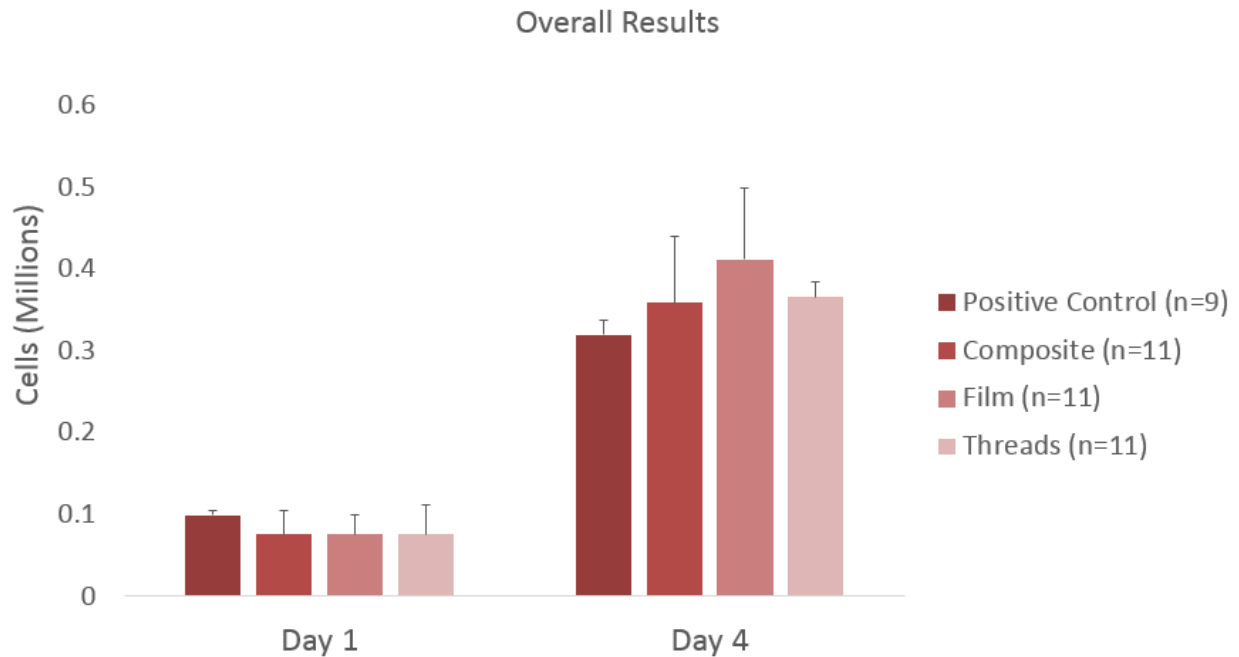


Figure 22: Overall results from cell viability assay

The results from all trials were then averaged in order to obtain the overall results. Visually, it can be seen from Figure 22 that the cell counts between the composite and the other groups are relatively even. In order to determine whether there was a statistical difference between the groups, an ANOVA was performed using the data from the three trials using GraphPad. The negative control shown represents the wells in the test that had only resazurin and no cells. The composite, film, and threads had a sample size of  $n=16$ , the negative control had a sample size of  $n=6$ , and the TCP had a sample size of  $n=12$ . The D'Agostino & Pearson omnibus normality test with a confidence interval of 95% was used to determine if the samples from each group come from a normally distributed population. The positive control and the threads passed this normality test, but the composite and the film did not. It is expected that if more trials were performed, all groups would pass the normality test as the sample size would be higher, but time

restrictions on the project did not allow this. Since all of the data from Trials 2, 3 and 4 did not all pass the normality test, a Kruskal-Wallis non-parametric test was used.

Table 43 shows the p-values for the comparison between each of the groups. The only comparisons that were considered significant according to the parameters stated in section 5.4 were each group vs. the negative control. This means that there is no significant difference in cell viability between the composite, film, and threads, indicating that our design, promotes cell viability as well as a film, threads, and TCP.

*Table 43: t-test p-values*

<b>Groups Tested</b>	<b>Significant? P&lt;0.05</b>	<b>P-value</b>
Composite vs. Film	No	>0.9999
Composite vs. Threads	No	>0.9999
Composite vs. TCP	No	>0.9999
Film vs. Threads	No	>0.9999
Film vs. TCP	No	>0.9999
Threads vs. TCP	No	>0.9999

### 5.3 Degradation Study

*Function 3: Prolongs degradation to preserve partial structural integrity for two weeks*

The design should be structurally intact for the entire period of growth factor release and the team incorporated chemically crosslinking as a way to slow down degradation. In order to characterize the effect of EDC/NHS crosslinking on the film degradation time, originally, the tensile strength of samples was tested at various time points over seven days. Using the Instron,

the scaffolds were mechanically broken by tensile forces for both an uncrosslinked and crosslinked group at zero, three, five and seven day time points. The protocol for measuring the tensile strength can be found in Appendix H.

After initial testing it was decided that this experimental protocol was too cumbersome and would not fit within time frame to continue. The experiment required too many samples. Therefore, after careful consideration, the team and the clients decided to image scaffolds over the span of two weeks and use ImageJ to measure the area loss due to degradation. An example of what was expected for crosslinked for uncrosslinked samples is shown in

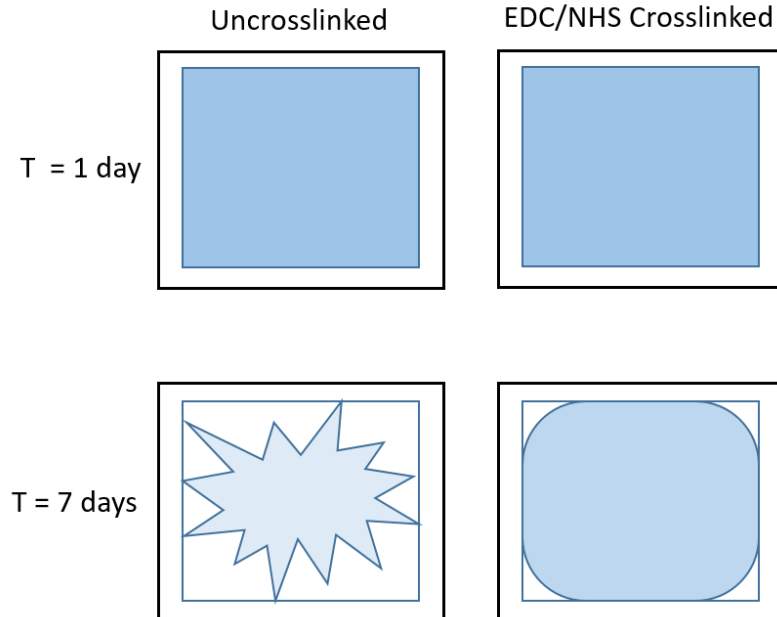


Figure 23: An example showing potential differences in degradation based on time for the composites that are crosslinked vs uncrosslinked

The two conditions for the scaffold, crosslinked and uncrosslinked were sterilized in an 70% ethanol bath and then placed into a sterile six-well plate. A schematic showing the expected difference in degradation is shown in Figure 23 and the experimental design set up is shown in Figure 24.

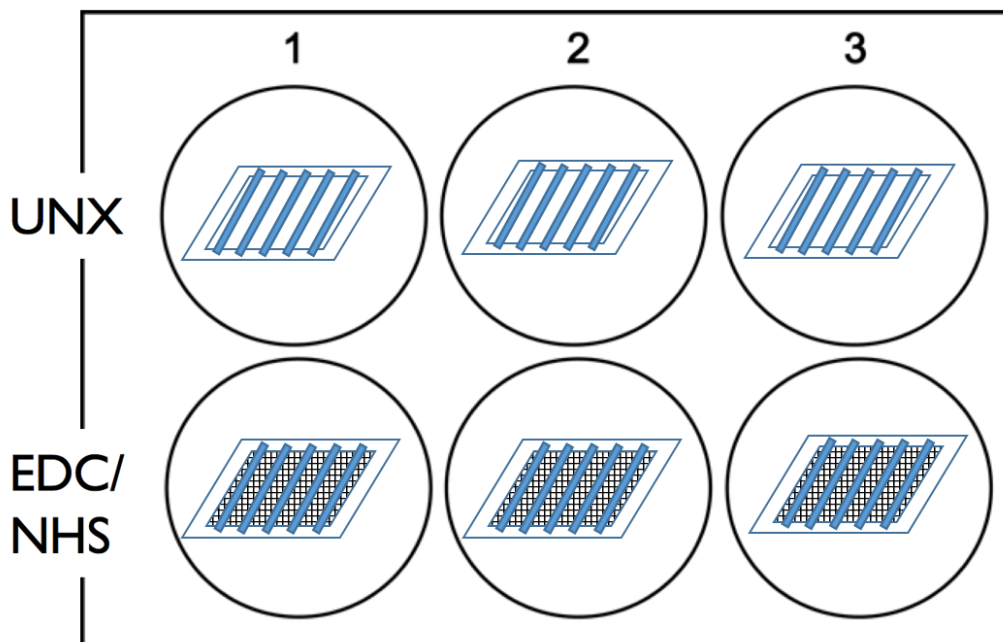


Figure 24: Experimental layout for degradation study where UNX = uncrosslinked composite and EDC/NHS = crosslinked composite using EDC/NHS solution

Both conditions had 50,000 C2C12 cells seeded onto their surface and 2 mL of complete media was added to each well. The six-well plate was then placed into an incubator at 37°C for two weeks. The media was changed every two days to ensure cell survival over two weeks. At specified time points, the scaffolds were imaged using the Zeiss Camera in Page’s lab. Then the images were analyzed using ImageJ to measure the loss due to degradation caused by cells. The protocol for the degradation experiment can be found in Appendix H.

Three separate trials were performed for the degradation experiment giving a sample size of nine for each condition. The results were compiled and is shown in Figure 25. At the end of the trials, it was determined that the crosslinked composites preserved 94% of its physical structure meanwhile uncrosslinked composites preserved 75% of its area. A t-test was performed, specifically a Kolmogorov-Smirnov (KS) t-test was performed since the unpaired groups were compared and the distribution for each group was not normally distributed

(nonparametric) after testing normality. Based on the KS test, only days 10 and 14 were determined to be statistically significant ( $p < 0.05$ ).

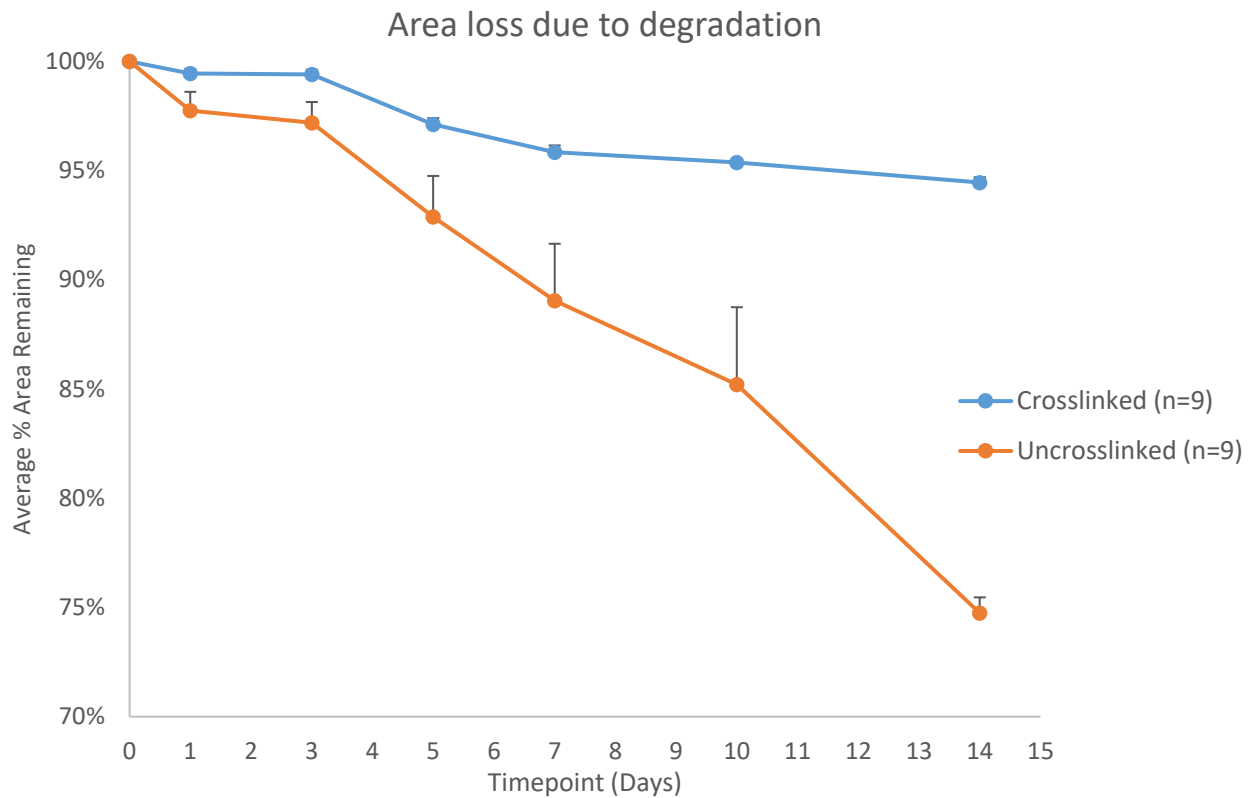


Figure 25: Average area remaining over the course of 14 days for crosslinked and uncrosslinked samples

## 5.4 Alignment analysis

*Function 2: Promotes nuclear alignment along fibrin threads at angles <10 degrees relative to the thread*

To ensure that our composite promotes alignment along the threads, a cell solution containing 60,500 C2C12 mouse myoblasts was delivered to fibrin composite samples and film samples. The cells were allowed to adhere for a two hour incubation period before adding media. All groups were tested with  $n=3$  for each trial. After four days of incubation a nuclear stain was used after fixing the cells to the surface of the sample. To stain for cell alignment Hoechst 33342

(Thermofisher), which is a DNA stain for nuclei of live or fixed cells that is imaged using fluorescent microscopy, was used. The dye is excited by ultraviolet lights and emits blue fluorescence at 460 to 490 nm. This allowed the team to analyze cellular alignment along the thread. The samples were fixed using at 1 mL solution of 4% paraformaldehyde for 30 minutes, dried, and then incubated on a shaker plate in 1 mL of 1:6,000 dilution Hoechst solution for 10 minutes and rinsed. The samples were then imaged with 10x magnification at five regions for each sample near a thread to allow for analysis around the thread. The regions were 7.42 x 5.40 mm for each image and the five regions that were generally imaged for each sample are shown in Figure 26.

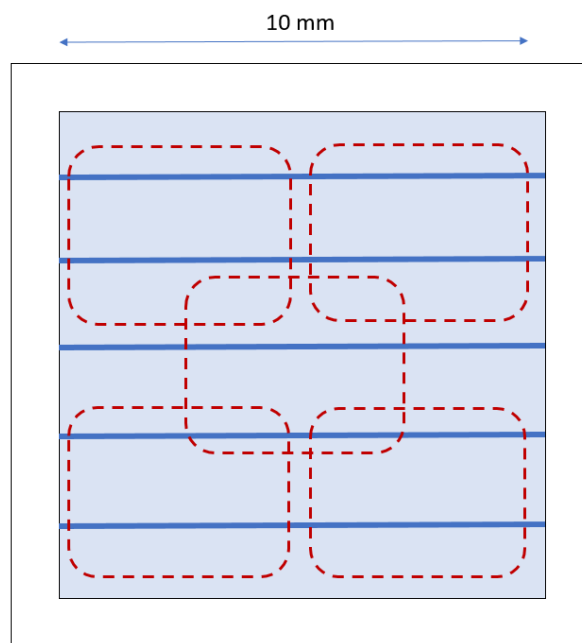


*Figure 26: Cartoon depiction of the composite scaffold and the regions (outlined in red) that were imaged for each sample*

The imaging software used for the analysis was ImageJ. ImageJ is a Java-base image processing program that was developed by the National Institute of Health. The protocol for processing the raw images in ImageJ can be found in Appendix H.

The analysis included defining nuclei as an oblong shape which allowed their angular position to be determined relative to a 0 degree thread in the image. An example of what the ideal nuclear alignment would look like is shown in Figure 27.

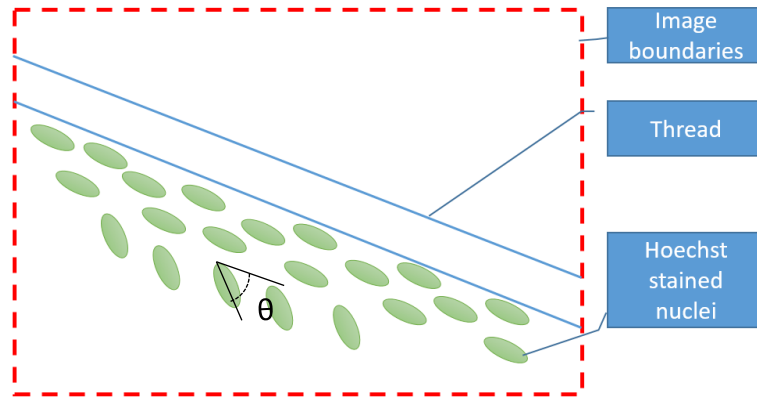


*Figure 27: A depiction of ideal nuclear alignment along the thread for an imaged region. The nuclei closest to the thread would be quantified at 0 degrees and the angle increase as they move farther away from the thread*

The images were used to analyze cellular alignment. The images were analyzed using ImageJ software to determine the cellular alignment of the cells in the samples. After the images were analyzed the data was sorted and normalized. To adjust the data to represent the absolute angle relative to the thread,  $180^\circ$  was added to angles  $-91^\circ$  or less and  $180^\circ$  was subtracted from angle  $91^\circ$  or greater. The absolute value of each angle was then determined, which normalized the range to  $0^\circ$  to  $90^\circ$ .

The data was then grouped and sorted into bins to determine the frequency of alignment in both the Composite and Film only samples, by portraying them in a histogram. A higher percentage of cells close to  $0^\circ$  showed preference toward thread alignment, while a higher percentage of cells close to  $90^\circ$  showed insufficient preference toward alignment. If the samples were successful in showing preference for alignment then they would be normally distributed around  $0^\circ$  with lower bin frequencies toward  $90^\circ$ . This was compared to a film which is expected

to not have a no preferential orientation towards any angle. The data for the cells that had angles 0-10 degrees from the thread angle were then analyzed and a t-test was performed on both sets of data. Three alignment assays were performed and the data is shown in Figure 28 for the composite and Figure 29 for the film. The raw data can be found in Appendix I: Raw Data Table for Alignment Analysis

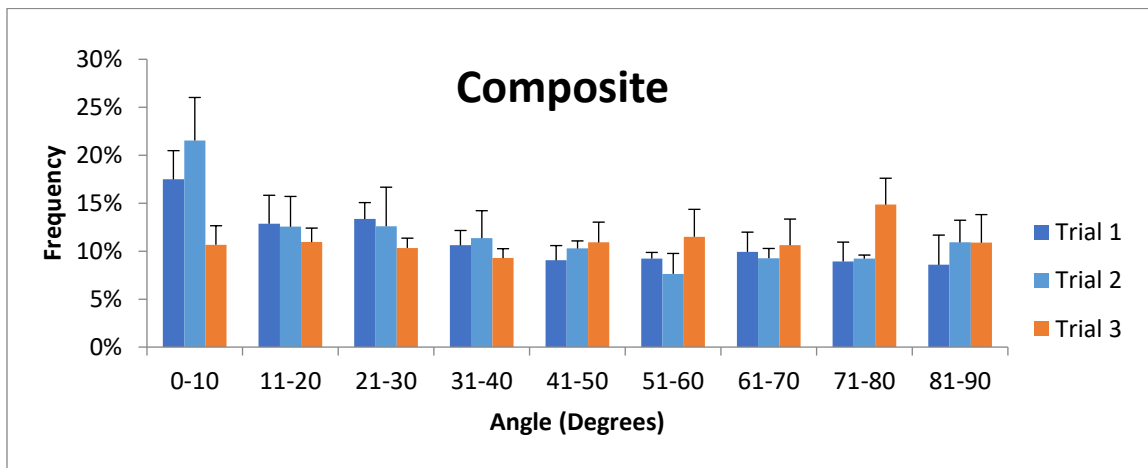


Figure 28: Angle frequency for composite samples

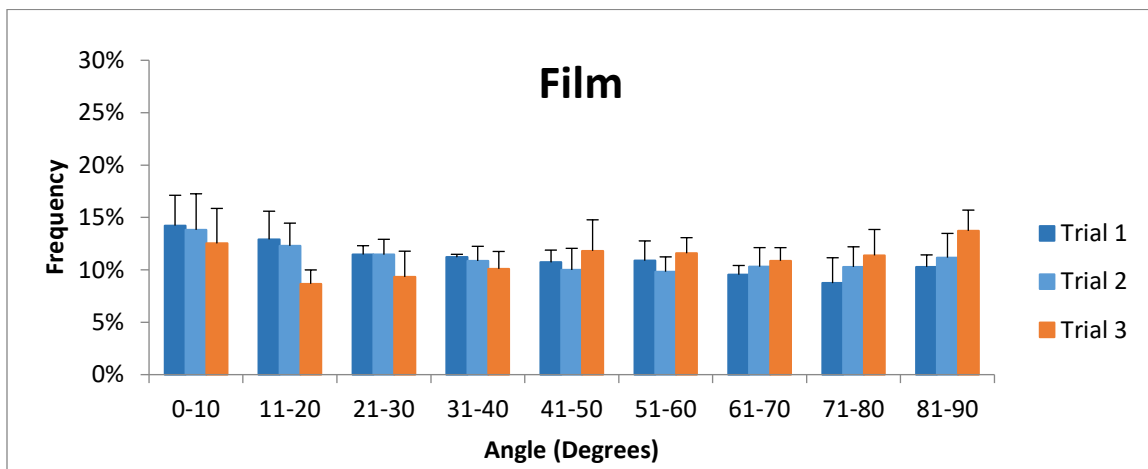


Figure 29: Angle frequency for film samples

For the composite samples, trial 1 and trial 2 showed preferential orientation towards increased alignment to the fibrin film. This is indicated by the higher frequency of cells located

at 0-10 degree angles relative to the thread. Overall for all three film trials, there was no obvious preferential orientation observed in the data.

## 5.5 Release Characterization

*Function 3: Release of FGF-2 throughout the regeneration phase.*

In order to characterize the release of FGF-2, a sandwich ELISA assay (Human FGF-2 Standard ABTS ELISA Development Kit; Peprotech; USA) was performed on the samples collected from the various test groups, with and without. This allowed the team to determine if the release concentrations are at levels high enough to be deemed effective by the literature, and more importantly matches relevant release kinetic models. The scaffolds were placed in a PBS bath for a series of 1-2 weeks and placed on a plate rocker at 37°C. At specified time points, the PBS was completely removed from the vessel and frozen in a microcentrifuge tube with 1% Bovine Serum Albumin (BSA), while new PBS was replaced. The FGF-2 released in the sampled PBS was then evaluated using the ELISA, which indicated a certain optical density which can be then correlated to a concentration of FGF-2 using a standard curve. The protocol for the ELISA kit can be found in Appendix H. By monitoring the scaffold's release over the 1-2 week period, the release profile can be created, and the scaffold properties can be adjusted to either retain or release more of the FGF-2 throughout its use. This was a good initial test to ensure that the target release was being achieved before measuring cellular response to the growth factor.

This experiment utilized two different loading methods of FGF-2 to the scaffold, as seen in Figure 28. One was considered “ON” while the other was considered “IN”. The “ON” scaffold consisted of a fibrin film, crosslinked with heparin on the surface, the FGF-2 was then placed

over the scaffold for 24 hours to allow for binding. This method would utilize immobilization of the FGF-2 by the heparin bound to the scaffold. Alternatively, the “IN” scaffolds were prepared by casting the FGF-2 directly inside of the scaffold with the fibrinogen, thrombin and added heparin. This method of loading would utilize primarily diffusion and degradation driven release of the growth factor out from the scaffold. These scaffolds were then placed into PBS at 37°C and were sampled daily for the remainder of the study.

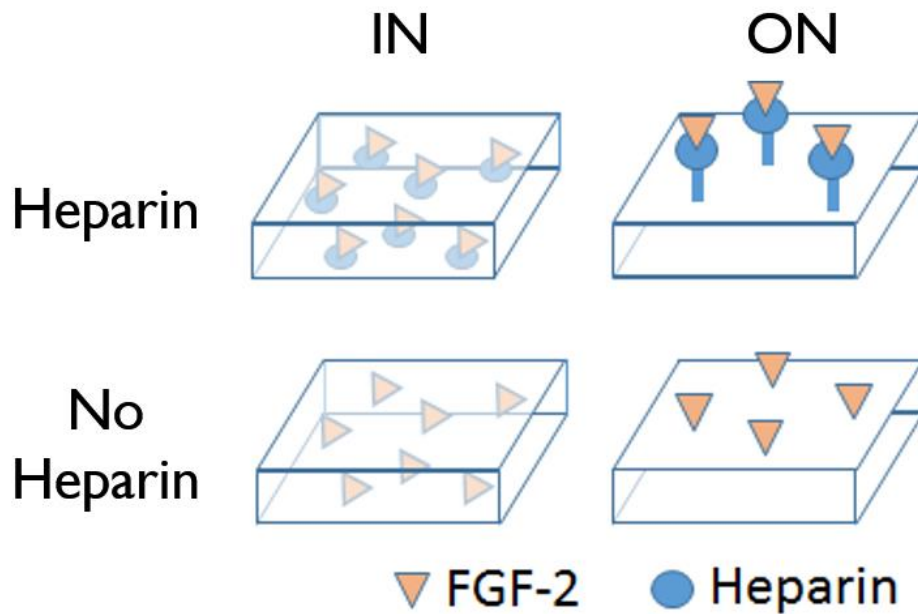


Figure 30: FGF-2 loading methods

In order to correctly characterize the release of the growth factor from the scaffolds, a standard curve with known concentration vs optical densities was created. The standard values collected were fit to a 4-parameter curve to allow for the most accurate fit. Using the standard curve fit, the concentrations of all the samples was determined. Release profiles for both the burst release period, and extended release period were created as shown in Figure 29 and Figure

30 respectively.

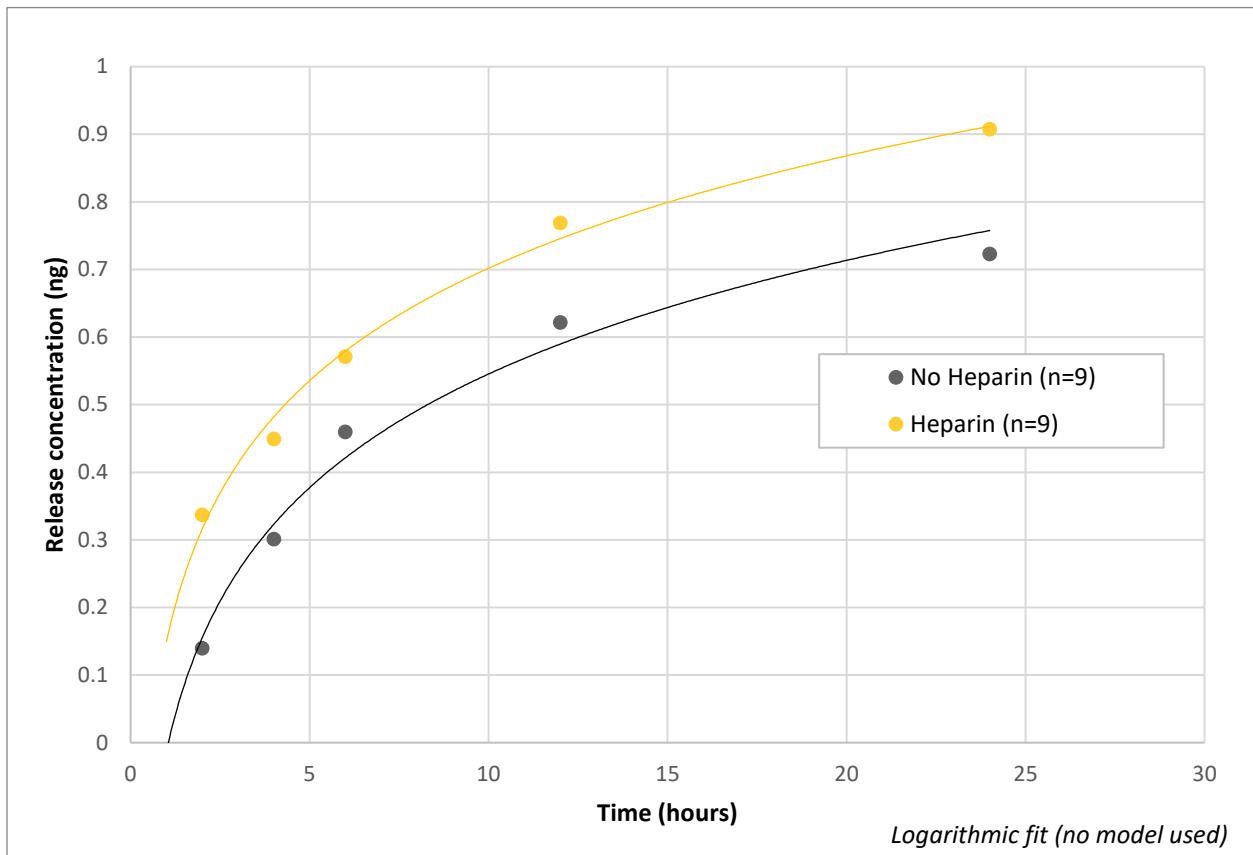


Figure 31: Burst release profile from scaffold

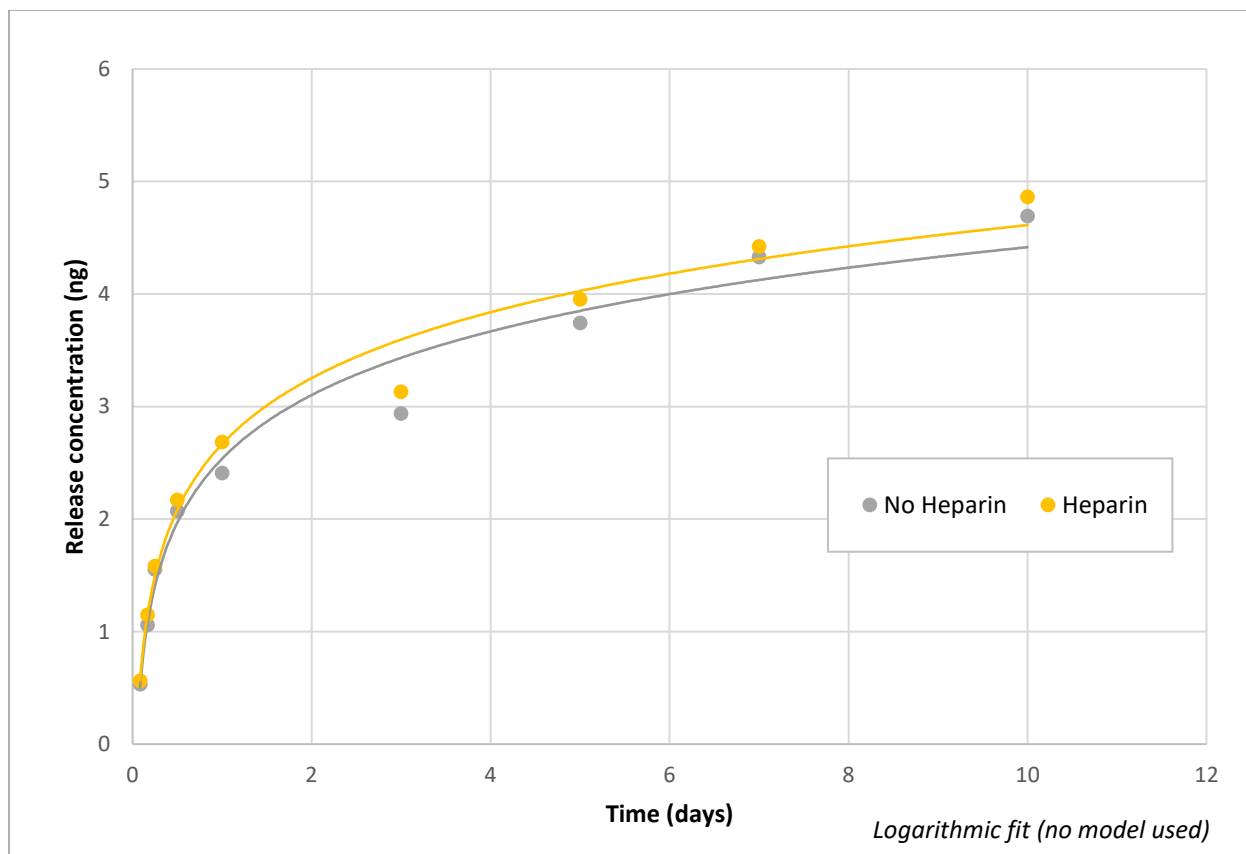


Figure 32: Extended release profile from scaffold

It was observed that both scaffold constructs, the composite with heparin and the scaffold without heparin, were able to sustain the release of the growth factor over the 2 week period. The release profiles created were then matched to zeroth, first, and second order kinetic models, which did not accurately match.

## 5.6 FGF-2 Functional Assay

### *Functions 2 and 5*

Once the individual components of our scaffold were characterized, the scaffold as a whole was tested for the functionality of the FGF-2 incorporated. This test incorporated previous experiments including cellular viability and alignment analysis.

For this experiment, the release kinetics were not measured, but instead, the cellular response to the scaffold and release of FGF-2 was characterized similar to the viability in Section 5.4. The scaffolds with the incorporated growth factor were incubated with C2C12 cells for four days. After the four day trial, the media was aspirated and replaced with 100  $\mu$ L 10x rezaurin and incubated two hours. For each well sample, 100  $\mu$ L was pipetted in triplicate to a 96-well plate to be read with the fluorescent plate reader, which is all consistent with the manufacturer's protocol (Thermofisher). The full protocol for the resazurin cell viability assay can be found in Appendix H. The absorbance measurements in the composites would be compared to the negative control and to the controls without the growth factor to determine if the FGF-2 increased proliferation.

The first trial of this experiment provided unusable results, as the negative controls provided an identical reading to the samples being tested. Due to time constraints, additional experiments were not possible.

## 6.0 Final Design and Validation

### 6.1 Overview of Composite Fabrication

The following section will outline the production of composite scaffold. This information may be used in order to replicate the previous research. All in-depth protocols outlined in this section can be found in Appendix H: Composite Scaffold Fabrication.

The first component necessary to be made is the fibrin microthreads. The fibrin microthreads were extruded by using the automated biopolymer printer for fibrin microthreads called LACEY. Before the machine can be used, stock solutions and aliquots must be made.

Fibrinogen and thrombin aliquots must be made. For stock solutions, HEPES buffered saline (HBS) and calcium chloride must be made.

First, fibrinogen aliquots are made by weighing 1.00g of fibrinogen and poured into a 50mL conical tube, then 13.6 mL must be added to creating an effective protein percentage of 72% and a concentration of 73.5 mg/mL. The conical tube was placed on a rocker plate and adjusted every 30-40 minutes to allow fibrinogen to go into the solution. It was imperative to never shake or vortex the fibrinogen solution, as it may cause fibrinogen to bind to itself and fall out of solution. To allow for the fibrinogen to completely dissolve, the conical tube was incubated at 37°C overnight. The next morning, the fibrinogen solution was separated into 1 mL aliquots in Eppendorf tubes bringing the concentration to 70 U/mL and stored at -20°C.

Thrombin aliquots were made by adding 25 mL of HBS to the bottle of 1 KU thrombin and thoroughly mixed. Afterwards, the thrombin solution was separated into 200  $\mu$ L aliquots in Eppendorf tubes bringing the concentration to 40 U/mL and stored at -20°C.

For the HBS stock solution, 23.83 g of HEPES was weighed out and added to 900 mL of diH<sub>2</sub>O to make 10X of 10 mM HBS (100mM). Afterwards, HBS was brought to a pH of 7.4 using sodium hydroxide and hydrochloric acid. Then the final volume was brought to 1000 mL and stored at room temperature. To make the calcium chloride stock solution, 0.1776 g of it was weighed and 40 mL of diH<sub>2</sub>O was added bringing the final concentration to 40 mM. The 40 mM calcium chloride was then stored at 4°C.

Once all of the solutions have been made and stored in their appropriate places, the preparation for extrusion was started. First, one fibrinogen and thrombin aliquot were thawed at room temperature. Once completely thawed, 150  $\mu$ L of the thrombin and 850  $\mu$ L of calcium chloride was added to a 2mL Eppendorf tube and thoroughly mixed. Then using two 1 mL

syringes, the thrombin and fibrinogen were collected into the two separate syringes. The thrombin and fibrinogen solutions were carefully and slowly collected to avoid air bubbles. The syringes were then inverted and the air bubbles were removed by saturating the tips and tapping the syringes. Then the syringes were adjusted to ensure equal volumes. Next, the 10X HBS stock solution was diluted with 450 mL of diH<sub>2</sub>O to bring the final concentration to 1X and had its pH adjusted to 7.4.

Next came the preparation of the machine which involved the syringe pump system which was its settings configured as explained in Appendix H. Then the blending applicator was set up as shown in Figure 33. The details of the individual components are explained in Appendix H.

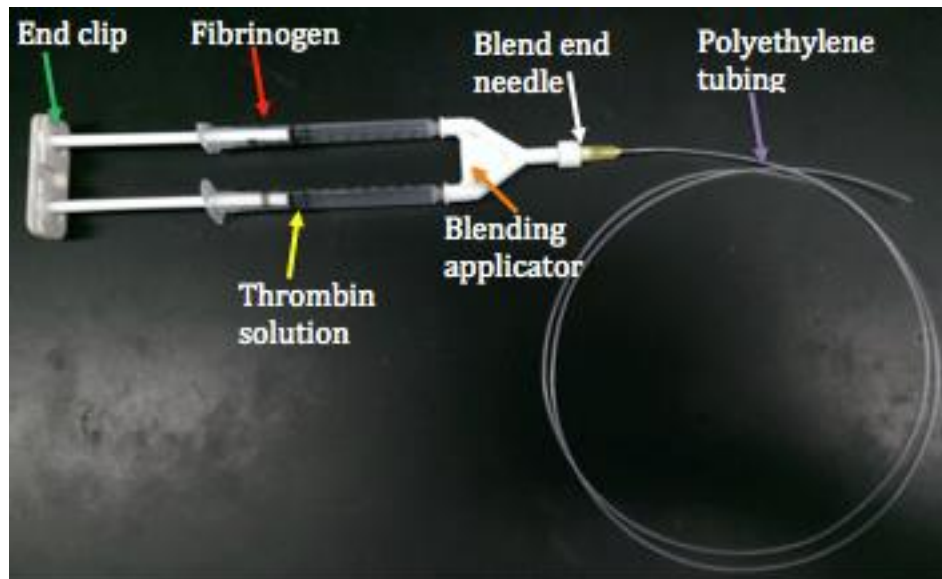


*Figure 33: Blending applicator set up as described in steps 2 - 4.*

Afterwards, the syringe pump was set up as shown in Figure 34. After the syringe pump was set up, the next focus was on the extrusion tip, which was set up as shown in Figure 353 and according to Appendix H.



*Figure 34: Syringe pump set up*

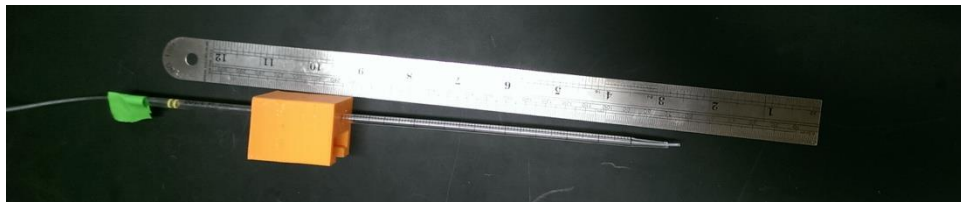


*Figure 35: Extrusion head with pipette tip and polyethylene tubing set up*

The next part involved preparing the LACEY system which involved the shoes and bath set up based on Appendix H and Figure 36.



*Figure 36: Teflon pan inserted into frame on corner notches indicated by red arrows.*

Then the 1X HBS solution was poured into the Teflon pan. Next involved setting up the shoe frame so that it looked like Figure 37 according to Appendix H.



*Figure 37: Shoe frame placed into machine over Teflon pan.*

The shoes were adjusted to ensure that the HBS covered both shoes. The software set up which involved using a laptop and MatLab. The configuration is explained in great detail in Appendix H. After all the set up was complete, extrusion operation guidelines were followed in Appendix H and approximately 10 microthreads were extruded. After polymerization was completed (10 minutes), the threads were stretched in the HBS bath and then placed on the cardboard box as shown in Figure 38 to allow for proper drying. Typically, the fibrin microthreads could be stretched and placed onto the box forming two to three fully stretched microthreads.



*Figure 38: Fibrin microthreads stretched and being dried*

After the microthreads have dried and the frames cut, the threads are aligned and glued to the frame. Five microthreads were removed from the drying box with forceps and placed onto a clear acetyl sheet. A 1 cm width was marked out on either side of the acetyl sheet. Tape was then used to pick up both sides of a microthread and it was aligned between the two 1cm marks. This was then repeated with the other four threads, and the ends of the threads were taped down at each end. About 12 vellum frames were then placed under the aligned bundle of threads. Medical adhesive glue and a blunt needles tip were used to place glue on the edges of the frames and then to push the microthreads and the glue together. This was repeated for all of the frames and then they were left to allow the glue to dry for approximately 6 hours.

To create the fibrin scaffold from the frames with threads, 5 prepared frames are placed on PDMS after coating the PDMS in 1% Pluronic solution to prevent sticking. Fibrin gel solution is prepared use 670  $\mu\text{L}$  fibrinogen aliquot, 150  $\mu\text{L}$  PBS, 80  $\mu\text{L}$   $\text{CaCl}_2$  and 100  $\mu\text{L}$  thrombin aliquot. From the 1 mL solution, 200  $\mu\text{L}$  is pipetted directly on the center of the prepared frames and using a pipette tip, the frame is pushed to be completely surrounded by the gel.

After creating the scaffolds, the constructs then were cross-linked to both prolong the degradation and to chemically sequester the growth factor to the scaffold as well. In order to do this, a solution of EDC/NHS was used. Before crosslinking, the scaffolds were hydrated in  $\text{NaH}_2\text{PO}_4$  Buffer for at least 30 minutes. This  $\text{NaH}_2\text{PO}_4$  Buffer was created by mixing 0.827 g  $\text{NaH}_2\text{PO}_4$  in 60 mL  $\text{dH}_2\text{O}$ . The EDC/NHS solution, 20 mL, was created with 0.0368 g of NHS and 0.1073 g of EDC and 0.002 g of heparin in 20 mL of  $\text{NaH}_2\text{PO}_4$  Buffer. Once properly hydrated using the  $\text{NaH}_2\text{PO}_4$  Buffer, each scaffold was placed in 2 mL of EDC/NHS solution and

left at room temperature for 2 hours. When removed from the EDC/NHS solution, the scaffold was washed 3 times in dH<sub>2</sub>O for 5 mins each wash. After the scaffold was cross-linked with heparin, the scaffold was quenched using a 0.25 % solution of glycine to allow for growth factor binding to the heparin. In order to accomplish this, the scaffold was placed in 2 mL of 0.25% glycine solution for 1 hour. When removed, the scaffold was rinsed 3 times in PBS, for 5 minutes each.

Once the scaffold was prepared with the proper crosslinking and binding agents, the growth factor, FGF-2, was loaded onto the scaffold. In order to accomplish this loading, the scaffold was submerged in 1 mL of a 10 ng/mL solution of FGF-2 for at least 24 hours. If necessary, a greater volume may be used. During this period, the scaffold and solution was placed on a plate rocker. Once loaded with the growth factor, the scaffold may be used in any desired application.

## 6.2 Impact Analysis of Device

The purpose of the following sections is to discuss the impacts of the device in areas such as economics, environment, health and safety, society, politics, ethics, manufacturing, and sustainability. Although this design is a prototype and in its first iteration, it still has the potential to affect the world.

### 6.2.1 Economic Impact

By designing and developing a fibrin composite scaffold, the team helped advance the development of a VML solution in Pins Lab towards reaching clinical viability. The scaffold must be scaled up before it can be viable and actually fill a muscle wound. So far, this represents a significant step in the right direction for future MQP teams to continue optimizing and

characterizing. Major challenges that need to be met before becoming clinically available include the further development and characterization of the design, scaling the design, FDA regulatory approval with animal testing and clinical trials, and final the marketing and distribution of the device.

If approved by the Food and Drug Administration (FDA), it is a possible treatment that could become the industry gold standard, as it may overcome many limitations of current treatments. Another possible advantage is that this device could be more widely used and thus increase the number of treated patients while increasing their standard of living. The treatment could increase the cost of fibrinogen and thrombin since there would be a greater demand for the scaffold. If optimized and allowed for implantation, the device would have some economic impact as a controlled of producing fibrin in mass quantities effectively would need to be established. In addition, the cost of hospital resources, including the implantation procedure and post-operational costs would need to be considered if this device were to be perfected and administered to patients. In theory, the device would promote the create of competitive companies that would try to provide a treatment similar to this. These are just some of the impacts on the economy caused by the scaffold.

### 6.2.2 Environmental Impact

Since the components designed during the project are still limited in research, it will not be advance to the clinical trial phase for some time, there are currently no environmental impacts directly associated with the results of the project. If the design of the fibrin composite scaffold was perfected and potential *in vivo* implantation in patients is possible, then the scaffold could have some potential of impacting the environment. If effective in treating VML, the scaffold would increase the demand of the fibrinogen and thrombin, which polymerize to form fibrin.

Both fibrinogen and thrombin are currently derived from bovine sources, the increase in demand of these two proteins may lead to an increased population of bovines. In turn, the demand may increase the demand for a number of resources needed to house cattle such as land, housing facilities, food, waste management, and increased labor force to maintain the source population. Any increase in energy required to maintain cattle as well as waste produced may significantly impact the environment. For example, sufficient land and water must be set aside for the increased number of bovine sources. This additional need for space may involve clearing trees which can severely impact the area's natural environment. Obtaining enough food to feed the cattle also require additional land allocation which may further contribute to the overall environmental impact. The facilities needed to house the bovine sources will require electricity, which may require an increased use of limited natural fuel resources. Additionally, the increased cattle population could lead to an increase in methane production, one of the most potent contributors to climate change.

Purifying and obtaining the proteins from the source population may also present an impact on the environment. The chemicals used, are the facilities needed to extract the proteins may contribute to affecting the environment as well. Through the proper management, the impact of the source population can have minimized effects if properly regulated. Proper regulation such as using renewable energy sources or converting waste into fertilizer are potential ways to minimize the environmental impact.

### 6.2.3 Health and Safety Impact

The results obtained from the project have the potential to greatly improve the health of patients suffering from VML, in the future. By providing other treatment options for patients, the patients may be able to bypass limitations of current treatments, and therefore have a better

standard of living. Currently continuation of extensive research is mandatory before it is safe enough to implant into patients. Research includes improving reliability, reproducibility, and further design verification. Once these tests are completed and the product is approved by the FDA, it will be considered safe for the majority of the population. Some possible dangers associated with the use of fibrin in clinical trials may surface after further understanding. Fibrin naturally exists *in vivo* as a clotting agent, the presence of fibrin in the body can pose as a risk by forming unexpected clots. Another issue would be tumor formation due to the use of growth factors, if not controlled properly.

#### 6.2.4 Societal Impact

Currently, it is infeasible in the near future for the project to become applicable *in vivo*, but in the future it may pose a substantial impact on society. For instance, if the fibrin composite scaffold was deemed effective in treating VML, the quality of life of patients affected by VML may be improved. The scaffold could have the potential to help patients, such as soldiers dealing with post-traumatic stress disorder, since patients could be fully functional. If the results of this project were to be optimized in the future, the use of fibrin as a scaffold material could likely extend to other tissue engineering applications, calling for an increase in productivity and efficiency of laboratory research.

#### 6.2.5 Political Impact

The project's results currently have minimal political ramifications. The production of fibrin composite scaffold is still in its infancy in terms of research and initial developmental stages. The results produced during the project have little to no effect on the commercial or industrial industries. Until the scaffold becomes commercialized or the results of the project are

adapted and developed to further enhance the research of current tissue engineering scaffolds, there would be little effect on the international market, therefore major political impacts are not foreseeable.

### 6.2.6 Ethical Impact

There are minimal ethical concerns associated with the results of the project. Since the goal of the fibrin composite scaffold is to treat patients dealing with VML, there are no direct ethical concerns associated with it. The only ethical concern that could be raised is the materials used to form fibrin. Fibrinogen and thrombin as mentioned are derived from bovine sources and some potential users may feel uncomfortable using materials from an animal source, even if the manner in which the materials were obtained was ethical.

### 6.2.7 Manufacturing Impact

The fabrication of the fibrin composite scaffold was designed to be straightforward, easy to use, and reproducible. Everything is made in a lab setting and takes less than two hours to fabricate. Manufacturability was taken into account early on in the design process since it was a demanded objective. The fabrication of one of the components of the scaffold, the fibrin microthreads is automated. In the future, if the demand is great enough, the fabrication process could become completely automated therefore minimizing the manufacturing impact.

### 6.2.8 Sustainability

The fibrin composite scaffold is composed entirely of fibrin which demands energy to produce, often from a bovine source. Although the materials used in the device are relatively sustainable, the steps and materials utilized to obtain them may not be as sustainable as it can be.

If the scaffold is deemed commercial viable and successful, the demand for the materials required may in turn allow for the processing of such materials to become more efficient. The demand will spark further interest and funds necessary in maximizing efficiency in becoming more sustainable.

## 7.0 Discussion

Through the series of tests performed to optimize the protocol, the composite was able to be produced at over a 90% success rate and in a user friendly manner. This protocol can possibly be further optimized, but for the scope of the project, the accomplished protocol was sufficient. Using a composite provided an improvement on the original bundle of threads in terms of how easy it is to manage and load them with growth factor.

The results from the cell viability experiments allowed showed that the composite scaffold allows cellular viability with no significant difference compared to the positive control (TCP), films, and threads. This means that if implanted in a volumetric muscle deficit, cells would be able to survive and proliferate on the composite. In terms of how successful this would be in vivo, the cellular viability assay allows the team to ensure that the composite was not only biocompatible but also promoted cellular growth.

The goal of the degradation experiment was to characterize the effect of using EDC/NHS crosslinking on the composite. The results from the degradation experiments suggest that chemical crosslinking the composite enhanced scaffold integrity starting after ten days. Based on the KS test, the t-test determined that there was indeed a significant difference between uncrosslinked and crosslinked composites at days 10 and 14. The statistical analysis validates the notion that the the EDC/NHS crosslinking reduced degradation. The experiments were only

carried out for 14 days but ideally it should have been to six weeks since that is how long the repair phase typically lasts for. Also a sample size of only 9 was used, ideally a larger sample size may have been more beneficial.

The results also confirmed with literature that EDC/NHS crosslinking is an effective means in delaying degradation. Furthermore, the results validate the use of EDC/NHS crosslinking since this crosslinking method incorporates the use heparin to allow for the immobilization of FGF-2. Although the the EDC/NHS crosslinking enhanced scaffold degradation, it may have affected the mechanical properties of the scaffold, which was never addressed. Additionally, it has been shown that EDC/NHS crosslinking may have an adverse effect on cellular adhesion to the scaffold, but this was not analyzed in our project (Grasman, 2012).

The first two trials for the alignment experiment showed very clear preference for cellular alignment in the composite sample group. The third trial, however, closely resembled the control film data. Before staining and imaging occurred for the third trial, a large number of dead cells and cloudy media was observed. This may have had an effect on the alignment of the cells. Another factor that could have prevented the cells from aligning is the thickness of the fibrin film. We assume that all the samples are similar because they were created by the same individual and the same protocol was used, but there is a chance that some films may be thicker than others. This would mean that the threads are encased in a thicker layer of film, preventing the cells from sensing the threads. Further trials would need to be performed to further characterize the alignment capabilities of the composite scaffold.

The results from the release experiments performed imply that both models with and without heparin are able to sustain the release of the FGF-2 over two weeks to match the repair phase of muscle regeneration. With the limited data collected, the release kinetics of this release

mechanism could not be properly modeled using the simple zero, first, and second order models. This is likely due to a lack of data and an over-simplified approach to the model. The system involving the composite includes multiple factors such as degradation, burst release, and different solute diffusion coefficients, which increases the complexity (Fu, 2011). In order to accurately represent the GF release from the composite, a model of the release profile will need to be developed, with these factors full taken into account.

In addition to testing the release profile of the FGF-2 from the scaffold, the functionality of the growth factor was also tested, similar to the viability assay. Unfortunately, the negative controls for the experiment performed were invalid, and therefore no conclusions were able to be drawn from the initial experiment. This invalid data observed was likely due to the contamination of the experiment in the negative control wells. In order to further determine the effect of the growth factor on the cells, this experiment will need to be adjusted and performed again.

## 8.0 Conclusions and Recommendations

The challenge proposed to the team was to design, develop, and characterize a composite fibrin scaffold. Based on the revised client statement, the composite must be able to provide topographical cues for cellular alignment, be easily reproducible, be user friendly, control the release of FGF-2 and prolong scaffold degradation. The team was able to design, create, and test a platform of a composite scaffold for VML. Overall the main objectives of having robust scaffold properties, being user friendly, promoting myogenesis, and having reproducible scaffold properties were achieved through the specified test methods. This was determined through the development of an optimized protocol, and the use of viability assays, degradation studies,

alignment assays, and release studies of FGF-2. From the data we were able to conclude that our conceptual design is a viable option as a preliminary functional layer for the development of a full thickness treatment method for VML.

Future work will require further characterization and optimization of the composite scaffold and increasing the binding capacity of FGF-2 to the scaffold. The platform scaffold we created was 10 x 10 mm, and will need to be scaled up to the size of a volumetric muscle defect. This can be done by layering composites and rolling them in order to increase the volume to fill the void in muscle. Further testing for the understanding the effect of chemical crosslinking is required. The degradation experiments should be carried out until the end of the repair phase which is six weeks. Mechanical characterization needs to be performed to determine how the crosslinking affected the mechanical properties of the composite. Further cell viability testing is required to determine the effects of crosslinking on cellular interactions. The binding capacity of the FGF-2 to the heparin will need to be further researched. This can be accomplished by testing different growth factor concentrations and performing a mass balance on the system. Additionally, staining of the heparin using Jaques' toluidine blue will indicate if the heparin is actually binding to the scaffold. In addition to binding capacity, the functionality of the growth factor in regards to cellular response will also need to be researched. The experiment which was previously developed in Section 5.6 can be used to determine if the FGF-2 increased proliferation.

Further cell alignment studies would also need to be performed to allow for an increased sample number. This is because currently trial 3 does not line up with both trials 1 and 2. A longer sample time can also be used to see if the formation of myotubes can be characterized. Additionally, in-vivo testing in mice should be performed to determine if functional muscle can be restored with the composite. This can be done by using a biopsy punch to create a volumetric

muscle loss defect, then implanting the scaffold (Li, 2014). Ideally, the composite will promote better functional regeneration than what has been seen in previous clinical trials. If clinical trials are successful in mice, they will move on to humans. The ultimate goal of this project is to restore muscle functions in soldiers with debilitating VML injuries, allowing them to return to combat.

## References

Äärimaa, V., Rantanen, J., Heikkilä, J., Helttula, I., & Orava, S. (2004). Rupture of the pectoralis major muscle. *The American journal of sports medicine*, 32(5), 1256-1262.

Ahmed, T. A., Dare, E. V., & Hincke, M. (2008). Fibrin: a versatile scaffold for tissue engineering applications. *Tissue Engineering Part B: Reviews*, 14(2), 199-215.

Al-Nasiry, S., Geusens, N., Hanssens, M., Luyten, C., & Pijnenborg, R. (2007). The use of Alamar Blue assay for quantitative analysis of viability, migration and invasion of choriocarcinoma cells. *Human reproduction*, 22(5), 1304-1309.

American Society of Plastic Surgeons (ASPS). (2015) Report of the 2015 Statistics of Plastic Surgery Statistics

Annabi, N., Nichol, J. W., Zhong, X., Ji, C., Koshy, S., Khademhosseini, A., & Dehghani, F. (2010). Controlling the porosity and microarchitecture of hydrogels for tissue engineering. *Tissue Engineering Part B: Reviews*, 16(4), 371-383.

Aubin, H., Nichol, J. W., Hutson, C. B., Bae, H., Sieminski, A. L., Cropek, D. M., & Khademhosseini, A. (2010). Directed 3D cell alignment and elongation in microengineered hydrogels. *Biomaterials*, 31(27), 6941-6951.

Badylak, S. F., Dziki, J. L., Sicari, B. M., Ambrosio, F., & Boninger, M. L. (2016). Mechanisms by which acellular biologic scaffolds promote functional skeletal muscle restoration. *Biomaterials*, 103, 128-136.

Bae, H., Puranik, A. S., Gauvin, R., Edalat, F., Carrillo-Conde, B., Peppas, N. A., & Khademhosseini, A. (2012). Building vascular networks. *Science translational medicine*, 4(160), 160ps23-160ps23.

Bettadapur, A., Suh, G. C., Geisse, N. A., Wang, E. R., Hua, C., Huber, H. A., ... & McCain, M. L. (2016). Prolonged culture of aligned skeletal myotubes on micromolded gelatin hydrogels. *Scientific Reports*, 6.

Bian, W., & Bursac, N. (2008). Tissue engineering of functional skeletal muscle: challenges and recent advances. *IEEE engineering in medicine and biology magazine: the quarterly magazine of the Engineering in Medicine & Biology Society*, 27(5), 109.

Boontheekul, T., Kong, H. J., Hsiong, S. X., Huang, Y. C., Mahadevan, L., Vandenburgh, H., & Mooney, D. J. (2008). Quantifying the relation between bond number and myoblast proliferation. *Faraday discussions*, 139, 53-70.

Borselli, C., Storrie, H., Benesch-Lee, F., Shvartsman, D., Cezar, C., Lichtman, J. W., & Mooney, D. J. (2010). Functional muscle regeneration with combined delivery of angiogenesis and myogenesis factors. *Proceedings of the National Academy of Sciences*, 107(8), 3287-3292.

- Burattini, S., Ferri, P., Battistelli, M., Curci, R., Luchetti, F., & Falcieri, E. (2004). C2C12 murine myoblasts as a model of skeletal muscle development: morpho-functional characterization. *European journal of histochemistry: EJH*, 48(3), 223.
- Burg, K. J., Porter, S., & Kellam, J. F. (2000). Biomaterial developments for bone tissue engineering. *Biomaterials*, 21(23), 2347-2359.
- Caiozzo, V. J. (2002). Plasticity of skeletal muscle phenotype: mechanical consequences. *Muscle & nerve*, 26(6), 740-768.
- Campbell, P. G., Miller, E. D., Fisher, G. W., Walker, L. M., & Weiss, L. E. (2005). Engineered spatial patterns of FGF-2 immobilized on fibrin direct cell organization. *Biomaterials*, 26(33), 6762-6770.
- Cezar, C. A., & Mooney, D. J. (2015). Biomaterial-based delivery for skeletal muscle repair. *Advanced drug delivery reviews*, 84, 188-197.
- Chakravarthy, M. V., Davis, B. S., & Booth, F. W. (2000). IGF-I restores satellite cell proliferative potential in immobilized old skeletal muscle. *Journal of Applied Physiology*, 89(4), 1365-1379.
- Charge, S. B., & Rudnicki, M. A. (2004). Cellular and molecular regulation of muscle regeneration. *Physiological reviews*, 84(1), 209-238.
- Chen, S., Nakamoto, T., Kawazoe, N., & Chen, G. (2015). Engineering multi-layered skeletal muscle tissue by using 3D microgrooved collagen scaffolds. *Biomaterials*, 73, 23-31.
- Choi, J. S., Lee, S. J., Christ, G. J., Atala, A., & Yoo, J. J. (2008). The influence of electrospun aligned poly (epsilon-caprolactone)/collagen nanofiber meshes on the formation of self-aligned skeletal muscle myotubes. *Biomaterials*, 29(19), 2899-2906.
- Christov, C., Chrétien, F., Abou-Khalil, R., Bassez, G., Vallet, G., Authier, F. J., ... & Gherardi, R. K. (2007). Muscle satellite cells and endothelial cells: close neighbors and privileged partners. *Molecular biology of the cell*, 18(4), 1397-1409.
- Chrobak, M. O. B., Hansen, K. J., Gershlak, J. R., Vratsanos, M., Kanellias, M., Gaudette, G., R., & Pins, G. D. (2016). Design of a Fibrin Microthread Based Composite Layer for Use in a Cardiac Patch. *ACS Biomaterials Science & Engineering*
- Ciciliot, S., & Schiaffino, S. (2010). Regeneration of mammalian skeletal muscle: basic mechanisms and clinical implications. *Current pharmaceutical design*, 16(8), 906-914.
- Clark, R. A. (2001). Fibrin and wound healing. *Annals of the New York Academy of Sciences*, 936(1), 355-367.

- Collins, C. A., Olsen, I., Zammit, P. S., Heslop, L., Petrie, A., Partridge, T. A., & Morgan, J. E. (2005). Stem cell function, self-renewal, and behavioral heterogeneity of cells from the adult muscle satellite cell niche. *Cell*, 122(2), 289-301.
- Cooper, R. N., Tajbakhsh, S., Mouly, V., Cossu, G., Buckingham, M., & Butler-Browne, G. S. (1999). In vivo satellite cell activation via Myf5 and MyoD in regenerating mouse skeletal muscle. *J Cell Sci*, 112(17), 2895-2901.
- Corona, B. T., & Greising, S. M. (2016). Challenges to acellular biological scaffold mediated skeletal muscle tissue regeneration. *Biomaterials*, 104, 238-246.
- Corona, B. T., Wu, X., Ward, C. L., McDaniel, J. S., Rathbone, C. R., & Walters, T. J. (2013). The promotion of a functional fibrosis in skeletal muscle with volumetric muscle loss injury following the transplantation of muscle-ECM. *Biomaterials*, 34(13), 3324-3335.
- Cornelison, D. D. W., & Wold, B. J. (1997). Single-cell analysis of regulatory gene expression in quiescent and activated mouse skeletal muscle satellite cells. *Developmental biology*, 191(2), 270-283.
- Cornwell, K. G., & Pins, G. D. (2007). Discrete crosslinked fibrin microthread scaffolds for tissue regeneration. *Journal of Biomedical Materials Research Part A*, 82(1), 104-112.
- Cornwell, K. G., & Pins, G. D. (2010). Enhanced proliferation and migration of fibroblasts on the surface of fibroblast growth factor-2-loaded fibrin microthreads. *Tissue Engineering Part A*, 16(12), 3669-3677.
- Crapo, P. M., Gilbert, T. W., & Badylak, S. F. (2011). An overview of tissue and whole organ decellularization processes. *Biomaterials*, 32(12), 3233-3243.
- de la Puente, P., Ludeña, D., Fernández, A., Aranda, J. L., Varela, G., & Iglesias, J. (2011). Autologous fibrin scaffolds cultured dermal fibroblasts and enriched with encapsulated bFGF for tissue engineering. *Journal of Biomedical Materials Research Part A*, 99(4), 648-654.
- de la Puente, P., & Ludeña, D. (2014). Cell culture in autologous fibrin scaffolds for applications in tissue engineering. *Experimental cell research*, 322(1), 1-11.
- Deng, B., Wehling-Henricks, M., Villalta, S. A., Wang, Y., & Tidball, J. G. (2012). IL-10 triggers changes in macrophage phenotype that promote muscle growth and regeneration. *The Journal of Immunology*, 189(7), 3669-3680.
- Devore, D. I., Walters, T. J., Christy, R. J., Rathbone, C. R., Hsu, J. R., Baer, D. G., & Wenke, J. C. (2011). For combat wounded: extremity trauma therapies from the USAISR. *Military medicine*, 176(6), 660-663.
- Drury, J. L., & Mooney, D. J. (2003). Hydrogels for tissue engineering: scaffold design variables and applications. *Biomaterials*, 24(24), 4337-4351.

D'Souza, S. E., Ginsberg, M. H., & Plow, E. F. (1991). Arginyl-glycyl-aspartic acid (RGD): a cell adhesion motif. *Trends in biochemical sciences*,*16*, 246-250.

D'Souza, S. (2014). A review of in vitro drug release test methods for nano-sized dosage forms. *Advances in Pharmaceutics*, 2014.

Dym, C. L., & Little, P. (2000). Engineering design: A project-based introduction. New York: John Wiley.

Dziki, J., Badylak, S., Yabroudi, M., Sicari, B., Ambrosio, F., Stearns, K., ... & Rubin, J. P. (2016). An acellular biologic scaffold treatment for volumetric muscle loss: results of a 13-patient cohort study. *npj Regenerative Medicine*, *1*, 16008.

Eckardt, A., & Fokas, K. (2003). Microsurgical reconstruction in the head and neck region: an 18-year experience with 500 consecutive cases. *Journal of Cranio-Maxillofacial Surgery*, *31*(4), 197-201.

Engineer, C., Parikh, J., & Raval, A. (2011). Review on hydrolytic degradation behavior of biodegradable polymers from controlled drug delivery system. *Trends Biomater Artif Organs*,*25*(2), 79-85.

Engler, A. J., Sen, S., Sweeney, H. L., & Discher, D. E. (2006). Matrix elasticity directs stem cell lineage specification. *Cell*, *126*(4), 677-689.

Fan, L. T., & Singh, S. K. (2012). Controlled release: A quantitative treatment (Vol. 13). Springer Science & Business Media.

Fox, S. I. (1996). Human Physiology 9<sup>th</sup> Edition.

Fu, Y., & Kao, W. J. (2010). Drug Release Kinetics and Transport Mechanisms of Non-degradable and Degradable Polymeric Delivery Systems. *Expert Opinion on Drug Delivery*, *7*(4), 429-444.

Garg, K., Ward, C. L., Hurtgen, B. J., Wilken, J. M., Stinner, D. J., Wenke, J. C., ... & Corona, B. T. (2015). Volumetric muscle loss: persistent functional deficits beyond frank loss of tissue. *Journal of Orthopaedic Research*, *33*(1), 40-46.

Gentile, N. E., Stearns, K. M., Brown, E. H., Rubin, J. P., Boninger, M. L., Dearth, C. L., ... & Badylak, S. F. (2014). Targeted rehabilitation after extracellular matrix scaffold transplantation for the treatment of volumetric muscle loss. *American Journal of Physical Medicine & Rehabilitation*,*93*(11), S79-S87.

Gilbert, P. M., Havenstrite, K. L., Magnusson, K. E., Sacco, A., Leonardi, N. A., Kraft, P., & Blau, H. M. (2010). Substrate elasticity regulates skeletal muscle stem cell self-renewal in culture. *Science*,*329*(5995), 1078-1081.

- Gómez-Guillén, M. C., Giménez, B., López-Caballero, M. A., & Montero, M. P. (2011). Functional and bioactive properties of collagen and gelatin from alternative sources: A review. *Food Hydrocolloids*, 25(8), 1813-1827.
- Grasman, J. M., Zayas, M. J., Page, R. L., & Pins, G. D. (2015). Biomimetic scaffolds for regeneration of volumetric muscle loss in skeletal muscle injuries. *Acta biomaterialia*, 25, 2-15.
- Grasman, J. M., Page, R. L., Dominko, T., & Pins, G. D. (2012). Crosslinking strategies facilitate tunable structural properties of fibrin microthreads. *Acta biomaterialia*, 8(11), 4020-4030.
- Gribova, V., Gauthier-Rouvière, C., Albigès-Rizo, C., Auzely-Velty, R., & Picart, C. (2013). Effect of RGD-functionalization and stiffness modulation of polyelectrolyte multilayer films on muscle cell differentiation. *Acta Biomaterialia*, 9(5), 6468–6480.
- Gu, F., Amsden, B., & Neufeld, R. (2004). Sustained delivery of vascular endothelial growth factor with alginate beads. *Journal of Controlled Release*, 96(3), 463-472.
- Huang, Y. C., Dennis, R. G., Larkin, L., & Baar, K. (2005). Rapid formation of functional muscle in vitro using fibrin gels. *Journal of Applied Physiology*, 98(2), 706-713.
- Hudalla, G. A., Koepsel, J. T., & Murphy, W. L. (2011). Surfaces That Sequester Serum-Borne Heparin Amplify Growth Factor Activity. *Advanced Materials (Deerfield Beach, Fla.)*, 23(45), 5415–5418. <http://doi.org/10.1002/adma.201103046>
- Huh, J., Stinner, D. J., Burns, T. C., Hsu, J. R., & Late Amputation Study Team. (2011). Infectious complications and soft tissue injury contribute to late amputation after severe lower extremity trauma. *Journal of Trauma and Acute Care Surgery*, 71(1), S47-S51.
- Horsley, V., & Pavlath, G. K. (2004). Forming a multinucleated cell: molecules that regulate myoblast fusion. *Cells Tissues Organs*, 176(1-3), 67-78.
- Janmey, P. A., Winer, J. P., & Weisel, J. W. (2009). Fibrin gels and their clinical and bioengineering applications. *Journal of the Royal Society Interface*, 6(30), 1-10.
- Janson, I. A., & Putnam, A. J. (2015). Extracellular matrix elasticity and topography: Material-based cues that affect cell function via conserved mechanisms. *Journal of Biomedical Materials Research Part A*, 103(3), 1246-1258.
- Järvinen, T. A., Järvinen, T. L., Kääriäinen, M., Kalimo, H., & Järvinen, M. (2005). Muscle injuries biology and treatment. *The American journal of sports medicine*, 33(5), 745-764.
- Jeon, O., Ryu, S. H., Chung, J. H., & Kim, B. S. (2005). Control of basic fibroblast growth factor release from fibrin gel with heparin and concentrations of fibrinogen and thrombin. *Journal of controlled release*, 105(3), 249-259.

- Kim, M. S., Bhang, S. H., Yang, H. S., Rim, N. G., Jun, I., Kim, S. I., ... & Shin, H. (2010). Development of functional fibrous matrices for the controlled release of basic fibroblast growth factor to improve therapeutic angiogenesis. *Tissue Engineering Part A*, 16(10), 2999-3010.
- Kroehne, V., Heschel, I., Schügner, F., Lasrich, D., Bartsch, J. W., & Jockusch, H. (2008). Use of a novel collagen matrix with oriented pore structure for muscle cell differentiation in cell culture and in grafts. *Journal of cellular and molecular medicine*, 12(5a), 1640-1648.
- Lazarous, D. F., Scheinowitz, M., Shou, M., Hodge, E., Rajanayagam, M. S., Hunsberger, S., ... & Unger, E. F. (1995). Effects of chronic systemic administration of basic fibroblast growth factor on collateral development in the canine heart. *Circulation*, 91(1), 145-153.
- Li, M. T. A., Willett, N. J., Uhrig, B. A., Guldberg, R. E., & Warren, G. L. (2014). Functional analysis of limb recovery following autograft treatment of volumetric muscle loss in the quadriceps femoris. *Journal of biomechanics*, 47(9), 2013-2021.
- Lee, K. Y., & Mooney, D. J. (2012). Alginate: properties and biomedical applications. *Progress in polymer science*, 37(1), 106-126.
- Lee, K. Y., Silva, E. A., & Mooney, D. J. (2011). Growth factor delivery-based tissue engineering: general approaches and a review of recent developments. *Journal of the Royal Society Interface*, 8(55), 153-170.
- Lefaucheur, J. P., & Sébille, A. (1995). Muscle regeneration following injury can be modified in vivo by immune neutralization of basic fibroblast growth factor, transforming growth factor  $\beta$ 1 or insulin-like growth factor I. *Journal of neuroimmunology*, 57(1), 85-91.
- Loh, Q. L., & Choong, C. (2013). Three-dimensional scaffolds for tissue engineering applications: role of porosity and pore size. *Tissue Engineering Part B: Reviews*, 19(6), 485-502.
- Makridakis, J. L. (2010). Braided Collagen Microthreads as a Cell Delivery System in Bioengineered Muscle Regeneration (Doctoral dissertation, Worcester Polytechnic Institute).
- Masini, B. D., Waterman, S. M., Wenke, J. C., Owens, B. D., Hsu, J. R., & Ficke, J. R. (2009). Resource utilization and disability outcome assessment of combat casualties from Operation Iraqi Freedom and Operation Enduring Freedom. *Journal of orthopaedic trauma*, 23(4), 261-266.
- Menetrey, J., Kasemkijwattana, C., Day, C. S., Bosch, P., Vogt, M., Fu, F. H., ... & Huard, J. (2000). Growth factors improve muscle healing in vivo. *Bone & Joint Journal*, 82(1), 131-137.
- Nemani, K. V., Moodie, K. L., Brennick, J. B., Su, A., & Gimi, B. (2013). In vitro and in vivo evaluation of SU-8 biocompatibility. *Materials Science and Engineering: C*, 33(7), 4453-4459.
- Nguyen, H. X., Lusic, A. J., & Tidball, J. G. (2005). Null mutation of myeloperoxidase in mice prevents mechanical activation of neutrophil lysis of muscle cell membranes in vitro and in vivo. *The Journal of physiology*, 565(2), 403-413.

- Owens, B. D., Kragh Jr, J. F., Wenke, J. C., Macaitis, J., Wade, C. E., & Holcomb, J. B. (2008). Combat wounds in operation Iraqi Freedom and operation Enduring Freedom. *Journal of Trauma and Acute Care Surgery*, 64(2), 295-299.
- O'reilly, C., McKay, B., Phillips, S., Tarnopolsky, M., & Parise, G. (2008). Hepatocyte growth factor (HGF) and the satellite cell response following muscle lengthening contractions in humans. *Muscle & nerve*, 38(5), 1434-1442.
- Page, R. L., Malcuit, C., Vilner, L., Vojtic, I., Shaw, S., Hedblom, E., ... & Dominko, T. (2011). Restoration of skeletal muscle defects with adult human cells delivered on fibrin microthreads. *Tissue Engineering Part A*, 17(21-22), 2629-2640.
- Proulx, Megan K., et al. "Fibrin microthreads support mesenchymal stem cell growth while maintaining differentiation potential." *Journal of Biomedical Materials Research Part A* 96.2 (2011): 301-312.
- Rowley, J. A., Madlambayan, G., & Mooney, D. J. (1999). Alginate hydrogels as synthetic extracellular matrix materials. *Biomaterials*, 20(1), 45-53.
- Rowley, J. A., & Mooney, D. J. (2002). Alginate type and RGD density control myoblast phenotype. *Journal of biomedical materials research*, 60(2), 217-223.
- Sahni, A., & Francis, C. W. (2000). Vascular endothelial growth factor binds to fibrinogen and fibrin and stimulates endothelial cell proliferation. *Blood*, 96(12), 3772-3778.
- Sakiyama-Elbert, S. E., & Hubbell, J. A. (2000). Controlled release of nerve growth factor from a heparin-containing fibrin-based cell ingrowth matrix. *Journal of Controlled Release*, 69(1), 149-158.
- Sanes, J. R. (1982). Laminin, fibronectin, and collagen in synaptic and extrasynaptic portions of muscle fiber basement membrane. *The Journal of cell biology*, 93(2), 442-451.
- Sanes, J. R. (2003). The basement membrane/basal lamina of skeletal muscle. *Journal of Biological Chemistry*, 278(15), 12601-12604.
- Sarrazin, S., Lamanna, W. C., & Esko, J. D. (2011). Heparan sulfate proteoglycans. *Cold Spring Harbor perspectives in biology*, 3(7), a004952.
- Sengupta, D., Gilbert, P. M., Johnson, K. J., Blau, H. M., & Heilshorn, S. C. (2012). Protein-Engineered Biomaterials to Generate Human Skeletal Muscle Mimics. *Advanced healthcare materials*, 1(6), 785-789.
- Sicari, B. M., Rubin, J. P., Dearth, C. L., Wolf, M. T., Ambrosio, F., Boninger, M., ... & Brown, E. H. (2014). An acellular biologic scaffold promotes skeletal muscle formation in mice and humans with volumetric muscle loss. *Science translational medicine*, 6(234), 234ra58-234ra58.

- Smith, C. W., Klaasmeyer, J. G., Woods, T. L., & Jones, S. J. (1999). Effects of IGF-I, IGF-II, bFGF and PDGF on the initiation of mRNA translation in C2C12 myoblasts and differentiating myoblasts. *Tissue and Cell*, 31(4), 403-412.
- Smith, J. D., Chen, A., Ernst, L. A., Waggoner, A. S., & Campbell, P. G. (2007). Immobilization of aprotinin to fibrinogen as a novel method for controlling degradation of fibrin gels. *Bioconjugate chemistry*, 18(3), 695-701.
- Stilhano, R. S., Madrigal, J. L., Wong, K., Williams, P. A., Martin, P. K., Yamaguchi, F. S., ... & Silva, E. A. (2016). Injectable alginate hydrogel for enhanced spatiotemporal control of lentivector delivery in murine skeletal muscle. *Journal of Controlled Release*, 237, 42-49.
- Sung, H. J., Meredith, C., Johnson, C., & Galis, Z. S. (2004). The effect of scaffold degradation rate on three-dimensional cell growth and angiogenesis. *Biomaterials*, 25(26), 5735-5742.
- Tatsumi, R., & Allen, R. E. (2004). Active hepatocyte growth factor is present in skeletal muscle extracellular matrix. *Muscle & nerve*, 30(5), 654-658.
- Thomson, K. S., Korte, F. S., Giachelli, C. M., Ratner, B. D., Regnier, M., & Scatena, M. (2013). Prevascularized Microtemplated Fibrin Scaffolds for Cardiac Tissue Engineering Applications. *Tissue Engineering. Part A*, 19(7-8), 967-977.
- Turner, N. J., & Badylak, S. F. (2012). Regeneration of skeletal muscle. *Cell and tissue research*, 347(3), 759-774.
- Uhrich, K. E., Cannizzaro, S. M., Langer, R. S., & Shakesheff, K. M. (1999). Polymeric systems for controlled drug release. *Chemical reviews*, 99(11), 3181-3198.
- Ulery, B. D., Nair, L. S., & Laurencin, C. T. (2011). Biomedical Applications of Biodegradable Polymers. *Journal of Polymer Science. Part B, Polymer Physics*, 49(12), 832-864.
- Velleman, S. G., Li, X., Coy, C. S., & McFarland, D. C. (2008). The effect of fibroblast growth factor 2 on the in vitro expression of syndecan-4 and glypican-1 in turkey satellite cells. *Poultry science*, 87(9), 1834-1840.
- Wang, L., Shansky, J., Borselli, C., Mooney, D., & Vandenberg, H. (2012). Design and fabrication of a biodegradable, covalently crosslinked shape-memory alginate scaffold for cell and growth factor delivery. *Tissue Engineering Part A*, 18(19-20), 2000-2007.
- Whitaker, M. J., Quirk, R. A., Howdle, S. M., & Shakesheff, K. M. (2001). Growth factor release from tissue engineering scaffolds. *Journal of Pharmacy and Pharmacology*, 53(11), 1427-1437.
- Wolf, M. T., Daly, K. A., Reing, J. E., & Badylak, S. F. (2012). Biologic scaffold composed of skeletal muscle extracellular matrix. *Biomaterials*, 33(10), 2916-2925.

Wolf, M. T., Dearth, C. L., Sonnenberg, S. B., Lobo, E. G., & Badylak, S. F. (2015). Naturally derived and synthetic scaffolds for skeletal muscle reconstruction. *Advanced drug delivery reviews*, 84, 208-221.

Yablonka-Reuveni, Zipora, and Anthony J. Rivera. "Proliferative Dynamics and the Role of FGF2 During Myogenesis of Rat Satellite Cells on Isolated Fibers." *Basic and applied myology : BAM 7.3-amp4* (1997): 189–202. Print.

Yamamoto, M., Ikada, Y., & Tabata, Y. (2001). Controlled release of growth factors based on biodegradation of gelatin hydrogel. *Journal of Biomaterials Science, Polymer Edition*, 12(1), 77-88.

Yannas, I. V. (2005). Facts and theories of induced organ regeneration. In *Regenerative Medicine I*(pp. 1-38). Springer Berlin Heidelberg.

Ye, Q., Zünd, G., Benedikt, P., Jockenhoevel, S., Hoerstrup, S. P., Sakyama, S., ... & Turina, M. (2000). Fibrin gel as a three dimensional matrix in cardiovascular tissue engineering. *European Journal of Cardio-Thoracic Surgery*, 17(5), 587-591.

Yin, H., Price, F., & Rudnicki, M. A. (2013). Satellite cells and the muscle stem cell niche. *Physiological reviews*, 93(1), 23-67.

Yock, P. G. (2015). *Biodesign: The process of innovating medical technologies*. Cambridge: Cambridge University Press.

Yoseph, B., & Soker, S. (2015). Redefining the satellite cell as the motor of skeletal muscle regeneration. *J. Sci. Appl.: Biomed*, 3, 76-82.

# Appendices

## Appendix A: Gantt Charts

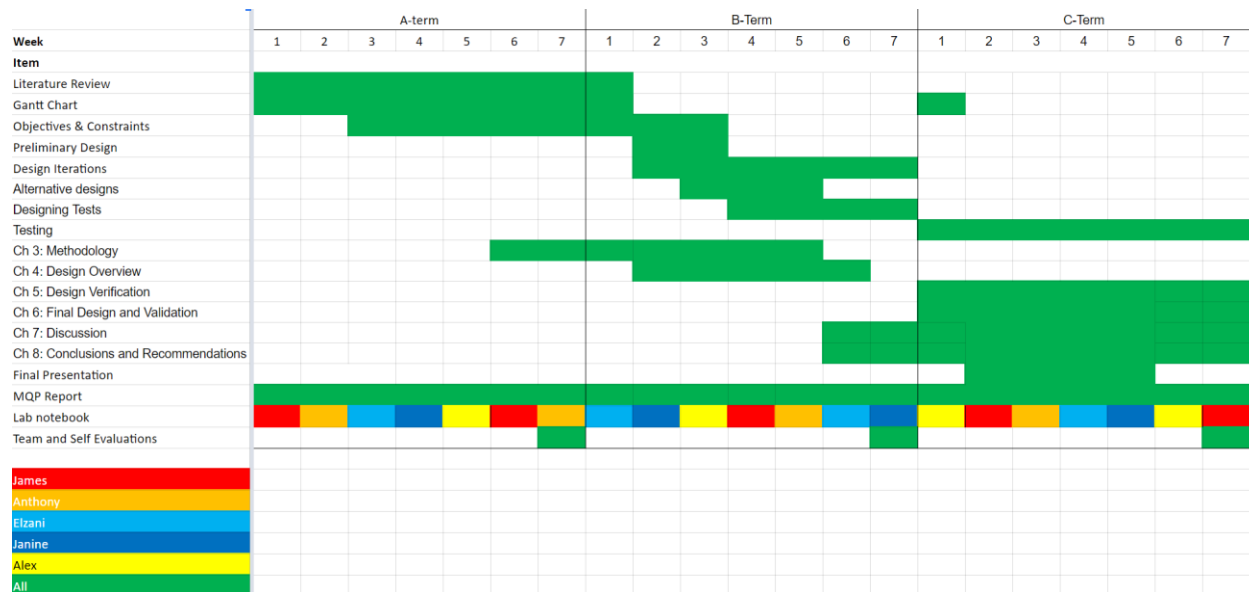


Figure 39: Full year Gantt chart



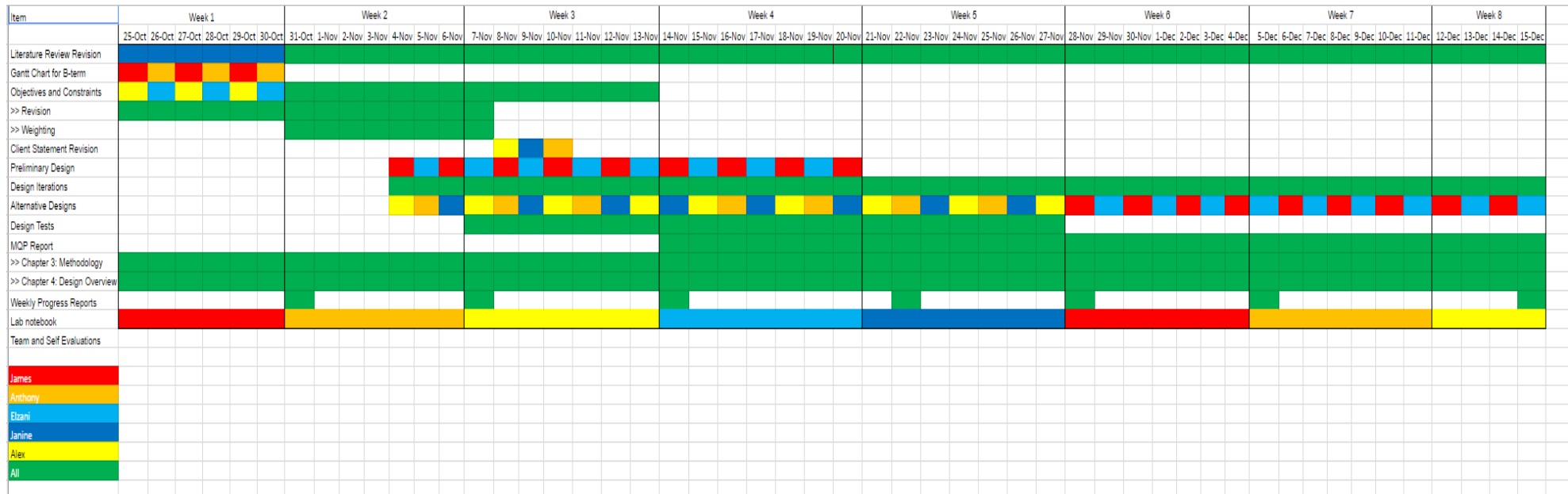


Figure 41: B-Term detailed Gantt chart



Figure 42: C-term detailed Gantt Chart

## Appendix B: Constraints Test for Developed Means

### Constraints Test For Developed Means

Function	Means	Constraints				
		Money	Time	Availability	Materials	Sterility
		Passes (Y) / Fails (N)				
1	Fibrin film	Y	Y	Y	Y	Y
	Fibrin gel	Y	Y	Y	Y	Y
	Fibrin microthreads	Y	Y	Y	Y	Y
	Fibrin gel with microthreads	Y	Y	Y	Y	Y
	Fibrin film with microthreads	Y	Y	Y	Y	Y
	Fibrin gel with ECM proteins	N	Y	Y	Y	Y
2	Fibrin microthreads	Y	Y	Y	Y	Y
	Patterened surface	Y	Y	Y	Y	Y
	Microthreads + peptide	Y	Y	Y	Y	Y
	Microthreads + ECM proteins	N	Y	Y	Y	Y
	Patterened + ECM proteins	N	Y	Y	Y	Y
	Patterned +microthread	Y	Y	Y	Y	Y
	Patterned + Peptide	Y	Y	Y	Y	Y
3	Diffusion	Y	Y	Y	Y	Y
	Degradation	Y	Y	Y	Y	Y
	Immobilizaition using heparin*	Y	Y	Y	Y	Y
	Polymer encapsulation	Y	Y	Y	Y	Y
4	UV Crosslinking	Y	Y	Y	Y	Y
	Protease Inhibitors	Y	Y	Y	Y	Y
	Chemical Crosslinking*	Y	Y	Y	Y	Y

## Appendix C: Pairwise Comparison Charts of clients, users, and design team

Client 1: Professor George Pins

	User friendly	Reproducible composite fabrication	Robust scaffold properties	Promote myogenesis	Promote angiogenesis	Promote innervation	Cost efficient	Minimize environmental impact	Sum
User friendly		0	0	0	1	1	0.5	1	3.5
Reproducible composite fabrication	1		0.5	0.5	1	1	0.5	1	5.5
Robust scaffold properties	1	0.5		0.5	1	1	0.5	1	5.5
Promote myogenesis	1	0.5	0.5		1	1	0.5	1	5.5
Promote angiogenesis	0	0	0	0		1	0	0	1

Promote innervation	0	0	0	0	0		0	0	0
Cost efficient	0.5	0.5	0.5	0.5	1	1		1	5
Minimize environmental impact	0	0	0	0	1	1	0		2

Sub-Objective User Friendly

	Minimal Preparation Time	“Off the shelf” design	Modular Capabilities
Minimal Preparation Time		0.5	0
“Off the shelf” design	0.5		1
Modular Capabilities	0	1	

Sub-objective Reproducible Composite Fabrication

	Consistent Scaffold Properties	Can achieve consistent functionality
Consistent Scaffold Properties		0.5
Can achieve consistent functionality	0.5	

Sub-Objective Robust Scaffold Properties

	Promotes Cell Alignment	Physiologically Relevant Degradation	Physiologically relevant stiffness and strength
Promotes Cell Alignment		0.5	0.5
Physiologically Relevant Degradation	0.5		0.5
Physiologically relevant stiffness and strength	0.5	0.5	

Sub-objective Promote Myogenesis

	Cell Migration	Cell Proliferation	Cell Differentiation
Cell Migration		0.5	1
Cell Proliferation	0.5		1
Cell Differentiation	0	0	

Sub-objective Promote Angiogenesis

	Sprouting of Existing Blood Vessels	Splitting angiogenesis	Maturation of Blood Vessels
Sprouting of Existing Blood Vessels		1	1
Splitting angiogenesis	0		1
Maturation of Blood Vessels	0	0	

Sub-objective Promote Innervation

	Differentiation of new nerve cells	Infiltration of existing nerve cells	Formation of motor units	Adjusting innervation ratio
Differentiation of new nerve cells		0.5	1	1
Infiltration of existing nerve cells	0.5		1	1
Formation of motor units	0	0		1
Adjusting innervation ratio	0	0	0	

Sub-objective Cost Efficient

	Can be purchased sustainably	Fabrication equipment is inexpensive
Can be purchased sustainably		1
Fabrication equipment is inexpensive	0	

Sub-objective Minimize Environmental Impact

	Minimize Organize Solvent Use	Minimize waste Production

Minimize organic solvent use		0
Minimize waste production	1	

Client 2: Professor Jeannine Coburn

	User friendly	Reproducible composite fabrication	Robust scaffold properties	Promote myogenesis	Promote angiogenesis	Promote innervation	Cost efficient	Minimize environmental impact	Sum
User friendly	x	0	0	0	0	1	1	0.5	2.5
Reproducible composite fabrication	1	x	0.5	1	1	1	1	1	6.5
Robust scaffold properties	1	0.5	x	1	1	1	1	1	6.5
Promote myogenesis	1	0	0	x	0.5	1	1	1	4.5
Promote angiogenesis	1	0	0	0.5	x	1	1	1	4.5
Promote innervation	0	0	0	0	0	x	0	1	1
Cost efficient	0	0	0	0	0	1	x	0.5	1.5
Minimize environmental impact	0.5	0	0	0	0	0	0	x	0.5

Sub-Objective User Friendly

	Minimal Preparation Time	“Off the shelf” design	Modular Capabilities
Minimal Preparation Time	x	0	0
“Off the shelf” design	1	x	1
Modular Capabilities	1	0	x

Sub-objective Reproducible Composite Fabrication

	Consistent Scaffold Properties	Can achieve consistent functionality
Consistent Scaffold Properties	x	1
Can achieve consistent functionality	0	x

Sub-Objective Robust Scaffold Properties

	Promotes Cell Alignment	Physiologically Relevant Degradation	Physiologically relevant stiffness and strength
Promotes Cell Alignment	x	1	0.5
Physiologically Relevant Degradation	0	x	0.5
Physiologically relevant stiffness and strength	0.5	0.5	x

Sub-objective Promote Myogenesis

	Cell Migration	Cell Proliferation	Cell Differentiation
Cell Migration	x	1	1
Cell Proliferation	0	x	1
Cell Differentiation	0	0	x

Sub-objective Promote Angiogenesis

	Sprouting of Existing Blood Vessels	Splitting Angiogenesis	Maturation of Blood Vessels
Sprouting of Existing Blood Vessels	x	1	0.5
Splitting Angiogenesis	0	x	0
Maturation of Blood Vessels	0.5	1	x

Sub-objective Promote Innervation

	Differentiation of new nerve cells	Infiltration of existing nerve cells	Formation of motor units	Adjusting innervation ratio
Differentiation of new nerve cells		0	1	1
Infiltration of existing nerve cells	1		1	1
Formation of motor units	0	0		1
Adjusting innervation ratio	0	0	0	

Sub-objective Cost Efficient

	Can be purchased sustainably	Fabrication equipment is inexpensive
Can be purchased sustainably	x	1
Fabrication equipment is inexpensive	0	x

Sub-objective Minimize Environmental Impact

	Minimize Organic Solvent Use	Minimize waste Production
Minimize organic solvent use	x	1
Minimize waste production	0	x

User 1: Meagan Carnes

	User friendly	Reproducible composite fabrication	Robust scaffold properties	Promote myogenesis	Promote angiogenesis	Promote innervation	Cost efficient	Minimize environmental impact	summary
User friendly		0	0	0	0.5	1	1	1	3.5
Reproducible composite fabrication	1		1	0.5	1	1	1	1	6.5
Robust scaffold properties	1	0		0.5	0.5	1	1	1	5
Promote myogenesis	1	0.5	0.5		1	1	1	1	6
Promote angiogenesis	0.5	0	0.5	0		1	1	1	4
Promote innervation	0	0	0	0	0		1	1	2
Cost efficient	0	0	0	0	0	0		1	1

Minimize environmental impact	0	0	0	0	0	0	0	0
-------------------------------	---	---	---	---	---	---	---	---

Sub-Objective User Friendly

	Minimal Preparation Time	“Off the shelf” design	Modular Capabilities
Minimal Preparation Time		1	0.5
“Off the shelf” design	0		0.5
Modular Capabilities	0.5	0.5	

Sub-objective Reproducible Composite Fabrication

	Consistent Scaffold Properties	Can achieve consistent functionality
Consistent Scaffold Properties		0.5
Can achieve consistent functionality	0.5	

Sub-Objective Robust Scaffold Properties

	Promotes Cell Alignment	Physiologically Relevant Degradation	Physiologically relevant stiffness and strength
--	-------------------------	--------------------------------------	---

Promotes Cell Alignment		1	0.5
Physiologically Relevant Degradation	0		
Physiologically relevant stiffness and strength	0.5	1	

Sub-objective Promote Myogenesis

	Cell Migration	Cell Proliferation	Cell Differentiation
Cell Migration		0.5	1
Cell Proliferation	0.5		1
Cell Differentiation	0	0	

Sub-objective Promote Angiogenesis

	Sprouting of Existing Blood Vessels	Splitting angiogenesis	Maturation of Blood Vessels
Sprouting of Existing Blood Vessels		0.5	0.5
Splitting angiogenesis	0.5		0.5
Maturation of Blood Vessels	0.5	0.5	

Sub-objective Promote Innervation

	Differentiation of new nerve cells	Infiltration of existing nerve cells	Formation of motor units	Adjusting innervation ratio
Differentiation of new nerve cells		0	0	1
Infiltration of existing nerve cells	1		0.5	1

Formation of motor units	1	0.5		1
Adjusting innervation ratio	0	0	0	

Sub-objective Cost Efficient

	Can be purchased sustainably	Fabrication equipment is inexpensive
Can be purchased sustainably		1
Fabrication equipment is inexpensive	0	

Sub-objective Minimize Environmental Impact

	Minimize Organize Solvent Use	Minimize waste Production
Minimize organic solvent use		0.5
Minimize waste production	0.5	

User 2: Johanna Santos

	User friendly	Reproducibl e composite fabricatio n	Robust scaffold properti es	Promote myogene sis	Promote angiogene sis	Promote innervati on	Cost efficie nt	Minimize environme ntal impact
User friendly		0	0	0.5	0.5	1	1	1
Reproducibl e composite fabrication	1		0.5	0.5	0.5	1	1	1
Robust scaffold properties	1	0.5		1	1	1	1	1
Promote myogenesis	0.5	0	0		0.5	1	1	1

Promote angiogenesis	0.5	0	0	0.5		1	1	1
Promote innervation	0	0	0	0	0		1	1
Cost efficient	0	0	0	0	0	0		0.5
Minimize environmental impact	0	0	0	0	0	0	0.5	

Sub-Objective User Friendly

	Minimal Preparation Time	“Off the shelf” design	Modular Capabilities
Minimal Preparation Time		1	1
“Off the shelf” design	0		0.5
Modular Capabilities	0	0.5	

Sub-objective Reproducible Composite Fabrication

	Consistent Scaffold Properties	Can achieve consistent functionality
Consistent Scaffold Properties		0.5
Can achieve consistent functionality	0.5	

Sub-Objective Robust Scaffold Properties

	Promotes Cell Alignment	Physiologically Relevant Degradation	Physiologically relevant stiffness and strength
Promotes Cell Alignment		0.5	0.5
Physiologically Relevant Degradation	0.5		0
Physiologically relevant stiffness and strength	0.5	1	

Sub-objective Promote Myogenesis

	Cell Migration	Cell Proliferation	Cell Differentiation
Cell Migration		0.5	1
Cell Proliferation	0.5		1
Cell Differentiation	0	0	

Sub-objective Promote Angiogenesis

	Sprouting of Existing Blood Vessels	Splitting angiogenesis	Maturation of Blood Vessels
Sprouting of Existing Blood Vessels		0.5	0.5
Splitting angiogenesis	0.5		0.5

Maturation of Blood Vessels	0.5	0.5	
--------------------------------	-----	-----	--

Sub-objective Promote Innervation

	Differentiation of new nerve cells	Infiltration of existing nerve cells	Formation of motor units	Adjusting innervation ratio
Differentiation of new nerve cells		0.5	0	1
Infiltration of existing nerve cells	0.5		0.5	1
Formation of motor units	1	0.5		1
Adjusting innervation ratio	0	0	0	

Sub-objective Cost Efficient

	Can be purchased sustainably	Fabrication equipment is inexpensive
Can be purchased sustainably		1
Fabrication equipment is inexpensive	0	

Sub-objective Minimize Environmental Impact

	Minimize Organic Solvent Use	Minimize waste Production
Minimize organic solvent use		0
Minimize waste production	1	

Design Team

	User friendly	Reproducible composite fabrication	Robust scaffold properties	Promote myogenesis	Promote angiogenesis	Promote innervation	Cost efficient	Minimize environmental impact	Sum
User friendly		0	0	0	0	1	1	0.5	2.5
Reproducible composite fabrication	1		0.5	1	1	1	1	1	6.5
Robust scaffold properties	1	0.5		1	1	1	1	1	6.5
Promote myogenesis	1	0	0		0.5	1	1	1	4.5
Promote e	1	0	0	0.5		1	1	1	4.5

angiogenesis									
Promote innervation	0	0	0	0	0		0	1	1
Cost efficient	0	0	0	0	0	1		0.5	1.5
Minimize environmental impact	0.5	0	0	0	0	0	0		0.5

Sub-Objective User Friendly

	Minimal Preparation Time	“Off the shelf” design	Modular Capabilities
Minimal Preparation Time		0	0
“Off the shelf” design	1		1
Modular Capabilities	1	0	

Sub-objective Reproducible Composite Fabrication

	Consistent Scaffold Properties	Can achieve consistent functionality
Consistent Scaffold Properties		1
Can achieve consistent functionality	0	

Sub-Objective Robust Scaffold Properties

	Promotes Cell Alignment	Physiologically Relevant Degradation	Physiologically relevant stiffness and strength
Promotes Cell Alignment		1	0.5
Physiologically Relevant Degradation	0		0.5

Physiologically relevant stiffness and strength	0.5	0.5	
---	-----	-----	--

Sub-objective Promote Myogenesis

	Cell Migration	Cell Proliferation	Cell Differentiation
Cell Migration		1	1
Cell Proliferation	0		1
Cell Differentiation	0	0	

Sub-objective Promote Angiogenesis

	Sprouting of Existing Blood Vessels	Splitting Angiogenesis	Maturation of Blood Vessels
Sprouting of Existing Blood Vessels		1	0.5
Splitting Angiogenesis	0		0
Maturation of Blood Vessels	0.5	1	

Sub-objective Promote Innervation

	Differentiation of new nerve cells	Infiltration of existing nerve cells	Formation of motor units	Adjusting innervation ratio
Differentiation of new nerve cells		0	1	1
Infiltration of existing nerve cells	1		1	1
Formation of motor units	0	0		1
Adjusting innervation ratio	0	0	0	

Sub-objective Cost Efficient

	Can be purchased sustainably	Fabrication equipment is inexpensive
Can be purchased sustainably		1
Fabrication equipment is inexpensive	0	

Sub-objective Minimize Environmental Impact

	Minimize Organize Solvent Use	Minimize waste Production
Minimize organic solvent use		1
Minimize waste production	0	

Appendix D: Summary of Pairwise Comparison Charts

Main Objectives

	Clients			Users			Team
	Pins	Coburn	Average	Santos	Carnes	Average	
User Friendly	3.5	4	3.75	4	3.5	3.75	2.5

Reproducible Composite Fabrication	5.5	5	5.25	5.5	6.5	6	6.5
Robust Scaffold Properties	5.5	4.5	5	6.5	5	5.75	6.5
Promote Myogenesis	5.5	3.5	9	4	6	5	4.5
Promote Angiogenesis	1	3.5	2.25	4	4	4	4.5
Promote Innervation	0	2.5	1.25	2	2	2	1
Cost Efficient	5	3.5	4.25	0.5	1	0.75	1.5
Minimize Environmental Impact	2	1	1.5	0.5	0	0.25	0.5

#### Main Objectives: Summary

	Clients	Users	Design Team	Total
User Friendly	3.75	3.75	2.5	10
Reproducible Composite Fabrication	5.25	6	6.5	17.75
Robust Scaffold Properties	5	5.75	6.5	17.25

Promote Myogenesis	9	5	4.5	18.5
Promote Angiogenesis	2.25	4	4.5	10.75
Promote Innervation	1.25	2	1	4.25
Cost Efficient	4.25	0.75	1.5	6.5
Minimize Environmental Impact	1.5	0.25	0.5	2.25

Sub-Objective User Friendly

	Clients			Users			Team
	Pins	Coburn	Average	Santos	Carnes	Average	
Minimal preparation time	0.5	1	0.75	2	1.5	1.75	0
“off the shelf” design	1.5	1.5	1.5	0.5	0.5	0.5	2
Modular capabilities	1	0.5	0.75	0.5	1	0.75	1

Sub-Objective User Friendly: Summary

	Clients	Users	Design Team	Total
Minimal preparation time	0.75	1.75	0	2.5
“off the shelf” design	1.5	0.5	2	4
Modular capabilities	0.75	0.75	1	2.5

Sub-objective Reproducible Composite Fabrication

	Clients			Users			Team
	Pins	Coburn	Average	Santos	Carnes	Average	

Consistent Scaffold Properties	0.5	0.5	0.5	0.5	0.5	0.5	1
Can achieve consistent functionality	0.5	0.5	0.5	0.5	0.5	0.5	0

Sub-objective Reproducible Composite Fabrication: Summary

	Clients	Users	Design Team	Total
Consistent Scaffold Properties	0.5	0.5	1	2
Can achieve consistent functionality	0.5	0.5	0	1

Sub-Objective Robust Scaffold Properties

	Clients			Users			Team
	Pins	Coburn	Average	Santos	Carnes	Average	
Promotes Cell Alignment	1	2	1.5	1	1.5	1.25	1.5
Physiologically Relevant Degradation	1	0.5	0.75	0.5	0	0.25	0.5
Physiologically relevant stiffness and strength	1	0.5	0.75	1.5	1.5	0.5	1

Sub-Objective Robust Scaffold Properties: Summary

	Clients	Users	Design Team	Total
Promotes Cell Alignment	1.5	1.25	1.5	4.25
Physiologically Relevant Degradation	0.75	0.25	0.5	1.5
Physiologically relevant stiffness and strength	0.75	0.5	1	2.25

Sub-objective Promote Myogenesis

	Clients			Users			Team
	Pins	Coburn	Average	Santos	Carnes	Average	
Cell Migration	1.5	0.5	1	1.5	1.5	1.5	2
Cell Proliferation	1.5	0.5	1	1.5	1.5	1.5	1

Cell Differentiation	0	0.5	0.25	0	0	0	0
-------------------------	---	-----	------	---	---	---	---

Sub-objective Promote Myogenesis: Summary

	Clients	Users	Design Team	Total
Cell Migration	1	1.5	2	4.5
Cell Proliferation	1	1.5	1	3.5
Cell Differentiation	0.25	0	0	0.25

Sub-objective Promote Angiogenesis

	Clients			Users			Team
	Pins	Coburn	Average	Santos	Carnes	Average	
Sprouting of Existing Blood Vessels	2	1.5	1.75	1	1	1	1.5
Splitting Angiogenesis	1	1.5	1.25	1	1	1	0
Maturation of Blood Vessels	0	0	0	1	1	1	1.5

Sub-objective Promote Angiogenesis: Summary

	Clients	Users	Design Team	Total
Sprouting of Existing Blood Vessels	1.75	1	1.5	4.25
Splitting Angiogenesis	1.25	1	0	2.25
Maturation of Blood Vessels	0	1	1.5	2.5

Sub-objective Promote Innervation

	Clients			Users			Team
	Pins	Coburn	Average	Santos	Carnes	Average	

Differentiation of new nerve cells	2.5	1	1.75	1.5	1	1.25	2
Infiltration of existing nerve cells	2.5	2.5	2.5	2	2.5	2.25	3
Formation of motor units	1	1.5	1.25	2	2.5	2.25	1
Adjusting innervation ratio	0	0.5	0.25	0	0	0	0

Sub-objective Promote Innervation: Summary

	Clients	Users	Design Team	Total
Differentiation of new nerve cells	1.75	1.25	2	5
Infiltration of existing nerve cells	2.5	2.25	3	7.75
Formation of motor units	1.25	2.25	1	4.5
Adjusting innervation ratio	0.25	0	0	0.25

Sub Objective Cost Efficient

	Clients			Users			Team
	Pins	Coburn	Average	Santos	Carnes	Average	

Can be purchased sustainably	1	1	1	1	1	1	1
Fabrication equipment is inexpensive	0	0	0	0	0	0	0

Sub Objective Cost Efficient: Summary

	Clients	Users	Design Team	Total
Can be purchased sustainably	1	1	1	3
Fabrication equipment is inexpensive	0	0	0	0

Sub-objective Minimize Environmental Impact

	Clients			Users			Team
	Pins	Coburn	Average	Santos	Carnes	Average	
Minimize organic solvent use	0	0	0	0	0.5	0.25	1
Minimize waste production	1	1	1	1	0.5	0.75	0

Sub-objective Minimize Environmental Impact: Summary

	Clients	Users	Design Team	Total
Minimize organic solvent use	0	0.25	1	1.25
Minimize waste production	1	0.75	0	1.75

## Appendix E: Weighted Sub-Objectives

Main Objectives	Weight
Promote Myogenesis	6.5
Reproducible Composite Fabrication	5.8
Robust Scaffold Properties	5.6
User Friendly	3.5
Promote Angiogenesis	3.4
Cost Efficient	2.3
Promote Innervation	1.5
Minimize Environmental Impact	0.8

Sub-Objective User Friendly	Weight
“off the shelf” design	1.2
Minimal preparation time	1
Modular capabilities	0.8

Sub-objective Reproducible Composite Fabrication	Weight
Consistent Scaffold Properties	0.6
Can achieve consistent functionality	0.4

Sub-Objective Robust Scaffold Properties	Weight
Promotes Cell Alignment	1.4
Physiologically relevant stiffness and strength	0.7

Physiologically Relevant Degradation	0.5
--------------------------------------	-----

Sub-objective Promote Myogenesis	
Cell Migration	1.4
Cell Proliferation	1.2
Cell Differentiation	0.1

Sub-objective Promote Angiogenesis	Weight
Sprouting of Existing Blood Vessels	1.4
Splitting Angiogenesis	0.9
Maturation of Blood Vessels	0.7

Sub-objective Promote Innervation	Weight
Infiltration of existing nerve cells	2.5
Differentiation of new nerve cells	1.6
Formation of motor units	1.6
Adjusting innervation ratio	0.1

Sub Objective Cost Efficient	Weight
Can be purchased sustainably	1
Fabrication equipment is inexpensive	0

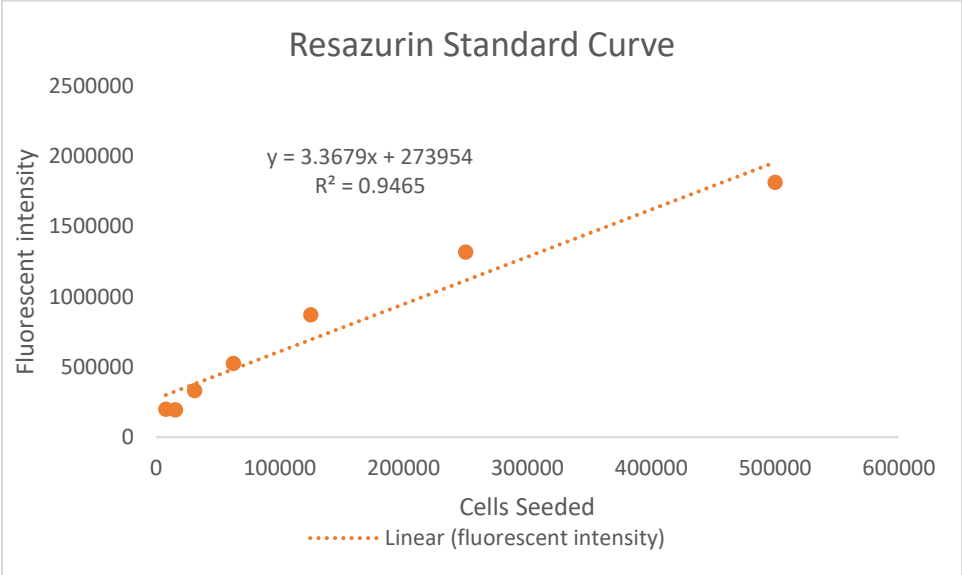
Sub-objective Minimize Environmental Impact	Weight
Minimize waste production	0.7
Minimize organic solvent use	0.3



# Appendix F: Means Evaluation Matrix

Function	Means	Constraints					Objectives											
		Money	Time	Availability	Materials	Sterility	User Friendly			Reproducible Composite		Robust			Promote Myogenesis		Cost Efficient	
		Passes (Y) / Fails (N)					Minimal Prep	"Off the shelf"	Modular Capabilities	Consistent scaffold properties	Achieve consistent functionality	Cellular Alignment	Relevant degradation	Stiffness + Strength	Cell Migration	Cell proliferation	Sustainable purchase	Inexpensive fabrication equipment
							4: 1-2 hrs 3: 2-4 hrs 2: 4-6 hrs 1: 6+ hrs	4: everything storable 3: 50-99% storable 2: 25-50% storable 1: 0-25% storable	4: scalable and stackable 3: scalable or stackable 2: slightly scalable or stackable 1: not scalable or stackable	4: always exact same (within 10%) 3: slight differences (within 25%) 2: a few differences (> 25%) 1: many differences (> 25%)	4: always same success rate in all objectives 3: same success rate in most objectives (90%) 2: same success rate in more than one objective 1: success rate in one objective	4: Desired cellular alignment 3: Moderate cellular alignment 2: little cellular alignment 1: No cellular alignment	4: degrades within 3-4 weeks 3: degrades 2-3 wks 2: degrades 1-2 weeks 1: degrades 0-1 week	4: identical to muscle tissue 3: 50% as strong as muscle 2: strong as muscle tissue 1: no structural support	4: high influx of SCs 3: moderate influx 2: low influx 1: no influx	4: inductive and high proliferation 3: inductive and moderate prolif. 2: moderate prolif 1: little to no prolif	4: \$0-20 per scaffold 3: \$20-50 2: \$50-100 1: \$100+	4: no fabrication equip. 3: inexpensive fabr. equip. (0-\$250) 2: moderate fabr. equip. (\$250-500) 1: expensive fabr. equip (\$500+)
1	Fibrin film	Y	Y	Y	Y	Y	4	4	4	4	3	1	4	3	1	1	4	3
	Fibrin gel	Y	Y	Y	Y	Y	4	4	4	4	3	1	4	2	1	1	4	3
	Fibrin microthreads	Y	Y	Y	Y	Y	3	4	4	4	3	3	4	2	1	2	1	2
	Fibrin gel with microthreads	Y	Y	Y	Y	Y	3	4	4	4	3	4	4	3	1	1	4	3
	Fibrin film with microthreads	Y	Y	Y	Y	Y	3	4	4	4	3	4	4	3	1	1	4	3
	Fibrin gel with ECM proteins	N	Y	Y	Y	Y												
2	Fibrin microthreads	Y	Y	Y	Y	Y	4	4	4	4	3	3	4	3	3	3	4	4
	Patterned surface	Y	Y	Y	Y	Y	4	2	4	4	3	3	2	2	3	3	4	4
	Microthreads + peptide	Y	Y	Y	Y	Y	3	3	4	4	2	1	4	3	4	4	2	4
	Microthreads + ECM proteins	Y	N	Y	Y	Y												
	Patterned + ECM proteins	Y	N	Y	Y	Y												
	Patterned + microthread	Y	Y	Y	Y	Y	3	4	4	4	3	3	4	3	4	3	4	4
3	Patterned + Peptide	Y	Y	Y	Y	Y	3	2	4	4	2	1	2	2	4	3	2	4
	Diffusion	Y	Y	Y	Y	Y	3	2		2	1	1		2	2	4	4	
	Degradation	Y	Y	Y	Y	Y	4	1		3	2	1		4	3	4	4	
	Direct chem. Conjugation	Y	Y	Y	Y	Y	4	1		3	2	1		4	3	4	4	
	Chem. Conjug. to binding factor*	Y	Y	Y	Y	Y	3	2		3	2	1		4	4	4	4	
	Polymer encapsulation	Y	Y	Y	Y	Y	2	1		2	2	1		2	2	4	4	
5	Chemical Crosslinking*	Y	Y	Y	Y	Y	2	4	4	3	3		3	3			4	4
	UV Crosslinking	Y	Y	Y	Y	Y	4	4	4	4	3		3	2			4	4
	Protease Inhibitors	Y	Y	Y	Y	Y	2	3	4	3	3		4	4			3	4

# Appendix G: Standard Curve for Cell Viability Assay



## Appendix H: Experiment Protocols

### Fibrinogen and Thrombin Aliquot Preparation

#### Objective:

Preparing fibrinogen and thrombin stock aliquots, which are used for dilution and fibrin thread creation

#### Materials:

Fibrinogen (82022, MP)

Thrombin (T4648, Sigma)

CaCl<sub>2</sub> (MW = 110.99) - ref. \_\_\_\_\_

NaCl (MW = 58.44)

HPS - ref. \_\_\_\_\_

Micropipette

Conical tubes

Eppendorf tubes

#### Procedure:

**NOTE:** Not all fibrinogen in product is clottable. This needs to be taken into account. Previous optimization of results was done with product from Sigma Aldrich (SA)

SA: *Effective protein = 75% protein \* 96% clottable*

**NOTE:** Current product is from MP Biomedicals

MP: *Effective protein = 72% protein \* 93.6 % clottable*

**NOTE:** To get the % protein and % clottable, review the certificate of analysis, which comes in with the product. It might be different for each batch

Originally, the aliquots are made to concentration of 70 mg/ml, based on SA's procedure. Using that, determine the concentration of the new product needed to have an equivalent concentration of effective protein (EP) as SA's aliquots.

$$\begin{aligned} [SA] * (EP:SA) &= X * (EP:MP) \\ 70mg/ml * (75% * 96\%) &= X * (72% * 93.6\%) \\ X &= 79.2 mg/ml \end{aligned}$$

$$\begin{aligned} \text{To dissolve 1000 mg: } 1000/X mg/ml &= 79.2 mg/ml \\ X &= 12.6 ml \end{aligned}$$

#### Fibrinogen Aliquot (70mg/ml)

1. Weigh 1.00 g of fibrinogen and pour in conical tube.
2. Measure X (specifically calculated for each batch) of Hepes buffered saline (HBS) and add to fibrinogen in conical tube

3. Place conical tube on rocker plate, adjusting position every 30-40 min until fibrinogen is no longer visible on the inside of the tube

**NOTE:** There may be clumps visible in the solution, which is OK

4. Measure 1 ml aliquots in eppendorf tubes and store at -20°C

### **Thrombin Aliquot (40U/ml)**

1. Add 25 ml HBS to bottle of 1 KU thrombin
2. Mix well
3. Aliquot 200 µl into eppendorf tubes and store in -20°C

**NOTE:** Final concentration should be 8 U/ 200 µl

### Fibrinogen and Thrombin Diluted Aliquot Preparation

#### **Objective:**

Preparing diluted fibrinogen and diluted thrombin aliquots for fibrin gel scaffolds

#### **Materials:**

Fibrinogen (82022, MP) Stock Solution - ref. \_\_\_\_\_

Thrombin (T4648, Sigma) Stock Solution - ref. \_\_\_\_\_

HBS - ref. \_\_\_\_\_

40 mM CaCl<sub>2</sub> - ref. \_\_\_\_\_

PBS (can be substituted with cell media if using cells)

PDMS - curing agent & elastomer base

Eppendorf tubes

Centrifuge tubes

#### **Procedure:**

##### **Diluted fibrinogen solution (2X solution) (dFb solution)**

1. Pipette 137.8µL of fibrinogen stock solution into a centrifuge tube
2. Add 862.2µL of HBS into centrifuge tube

- Final concentration = 11mg/mL

**NOTE:** Mix gently! Try to avoid polymerization

**Diluted thrombin solution (2.35 U/mL) (dTh solution)**

1. Pipette 58.75µL of Thrombin stock solution into centrifuge tube
2. Add 941.25µL HBS to the tube
3. Mix (triturate)

Fibrin Films and Gels Protocol

**Objective:** Record current procedure for making fibrin films

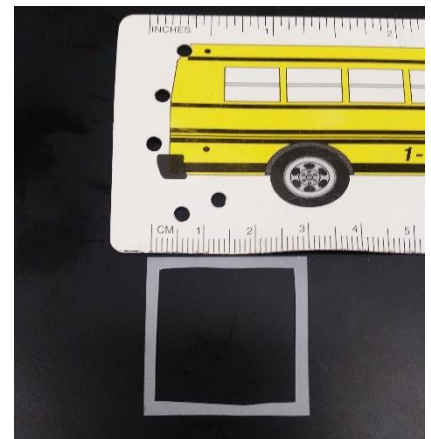
**Materials:**

- Fibrinogen aliquot ((11 mg/mL) Ref #MO1:26
- Thrombin aliquot (2.35 U/mL) Ref #MO1:26
- 40 mM CaCl<sub>2</sub>
- PBS
- Acetyl plastic slide
- di H<sub>2</sub>O
- Vellum paper
- Ruler (with millimeter markings)
- Scissors
- Razor Blade

**Procedures:**

**Prep of Vellum Frame for Film**

1. With vellum paper, measure a strip 30 mm wide and cut strip from sheet
2. Along strip, mark every 30 mm lengthwise and cut along markings, creating 30x30mm squares
3. On a hard surface, use razor blade to cut squares centers from the 30x30 square so that there is a 2mm thick border on all sides
4. The distance from inner edge to inner edge on each frame should be 26mm across horizontally and vertically when finished



**Prep of Fibrin Gel (from Fibrin Gel Basic Protocol – MO)**

1. Prep Acetyl slide (sterilize with ethanol if necessary)
2. Mix the following reagents in a centrifuge tube
  - a. 2680 uL fibrinogen solution (2x solution)
  - b. 320 uL CaCl<sub>2</sub> (40mM)
  - c. 600 uL PBS (or cell media if using cells)
3. Add 400 uL thrombin solution and triturate to gently mix with other reagents in centrifuge tube
4. For standard 26x26mm film frame:
  - a. Pipette 1.32 mL of mixed solution onto acetyl slide with frame
  - b. Use pipette tip to submerge frame edges into solution
5. Allow 30 minutes for polymerization

#### **Prep of Fibrin Film**

1. Use forceps to place frame in diH<sub>2</sub>O bath (room temp) for 10 minutes
2. Switch frame into fresh water bath for 5 minutes
3. Switch frame into final water bath for 5 minutes
4. Remove from water bath and place onto acetyl plastic slide to dry completely for 2-3 hours

REV 12/2015 AB

## User Manual for LACEY

### Biopolymer Printer for Fibrin Microthread Fabrication

#### Terms and Definitions

The following are terms and definitions that will be used throughout this user manual to describe key components of the system.

#### *Shoes*

These are the Lexan U-shaped frames with a steel mesh bottom that sit on the Teflon pan and anchor the ends of the threads as they are extruded and stretched in the bath.

#### *Shoe Sliders*

These are 3D printed parts that are placed on the long sides of the shoe frame and have holes in them that facilitate the insertion of the steel rods of the shoes. They move smoothly along the frame to facilitate controlled stretching.

### *Shoe Frame*

This is the metal frame that is used to facilitate the movement of the shoe slides and the shoes within the bath. After the threads are fabricated they can then be removed by lifting this frame and placing it on the benchtop.

### *Squeegee Pieces*

Pieces of Lexan and PDMS that are sandwiched together and sit on top of the shoes to secure the ends of the threads during stretching and removal from the bath.

### *Extrusion Head*

This is the removable printed piece with a 1mL pipette tip secured that is placed onto the machine, moving in both x and y directions. The polyethylene tubing is placed into the pipette tip.

### *Stretch Percentage*

This is the terminology used for how far the threads are stretched. 100% is when the threads are left unstretched and the other percentages are stretched length based on initial length of the threads. For example, 200% stretch means that 6 cm threads were stretched an additional 6 cm giving a final length of 12 cm threads.

### *Strain Rate*

This is the terminology used for the rate, in mm/s, that the threads are stretched at.

### *Extrusion Rate*

This is the terminology used for the rate at which the extruder head moves lengthwise to extrude the threads

### *Teflon Pan*

This is the actual container that holds the buffer bath and in which the shoes will sit to be stretched. It is made of Teflon and is coated before fabrication with Plurionics to further decrease the adherence of the fibrin to the bottom.

Solution Preparation - Stock Solutions and Aliquots

## 2.1 Fibrinogen Aliquots

Weigh 1.00g of fibrinogen (MP Biomedicals, 08820224) and pour into 50mL conical tube

Calculate the volume of HBS needed to have an effective protein (EP) percentage of 72% in 70 mg/mL  
(This is EP and concentration used from a previous Sigma-Aldrich fibrinogen batch that was used for optimization of microthreads previously)

Determine amount of protein in fibrinogen you will be using from mpbio.com

Navigate to “Certificate for a typical lot” for the Catalog number of the fibrinogen purchased and identify clottable protein percentage (highlighted in Figure 43 below)

Test	Specification	Result
Identity Test	Passes	Passes
Source	Bovine	Passes
Clottable Protein	≥ 90%	95.3%
Form	Lyophilized	Passes
Country of Origin	New Zealand	Passes

Figure 43: MP Biomedical Certificate for Fibrinogen

Calculate the concentration needed of the fibrinogen to have 72% EP in 70 mg/ml

Effective protein of current batch = Amount of Protein \* Clottable Protein

*Example:  $0.72 * 0.953 = 0.686$*

Concentration needed =  $(70 \text{ mg/ml} * .72)/(EP)$

*Example:  $(70 * .72)/(0.686) = 73.5 \text{ mg/ml}$*

The amount of HBS needed for 1000mg of fibrinogen is then calculated by: HBS Volume =

$1000\text{mg}/(\text{Concentration})$

*Example:  $1000\text{mg}/(73.5 \text{ mg/ml}) = 13.6 \text{ ml}$*

Add calculated volume of HBS to conical tube.

Place conical tube on rocker plate, adjusting the positions every 30-40 minutes until fibrinogen goes into solution

Note: Never shake/vortex fibrinogen solution! This will cause fibrinogen to fall out of solution and bind to itself!

Incubate conical tube at 37°C for 24hrs to ensure fibrinogen is completely dissolved.

After fibrinogen is dissolved, measure 1 mL aliquots into Eppendorf tubes and store at -20°C.

## 2.2 Thrombin Aliquots (40 U/mL)

Add 25 mL HBS to bottle of 1KU thrombin, mix well.

Aliquot 200 µL into Eppendorf tubes and store at -20°C (final concentration: 8U / 200 µL).

## 2.3 HEPES Buffered Saline (HBS) 10X Stock Solution

Add 23.83g of HEPES to 900 mL of diH<sub>2</sub>O to make 10X of 10 mM HEPES buffer (100mM).

pH to 7.4 using NaOH/HCl

Bring final volume to 1000 mL

Store at room temperature.

## 2.4 Calcium Chloride (40 mM)

Add 0.1776 g of CaCl<sub>2</sub> to 40 mL of diH<sub>2</sub>O.

Store at 4°C.

## 3. Solution Preparation - Preparation for Extrusion

### 3.1 Pluronic Coating Bath Preparation

Note: This should be performed each time after the pans have been washed to ensure that the threads do not adhere to the pan and can be stretched uniformly.

Create a 350mL, 2% w/v F127 Pluronic solution in diH<sub>2</sub>O

Weigh out 0.07g of F127 Pluronic

Mix in with 350mL of diH<sub>2</sub>O, ensure that all particles are in solution as some larger particles may take longer to dissolve.

Pour onto Teflon pan, let sit for 10 minutes.

Note: Shoes should not in bath at this time.

Remove liquid from tray and allow to air dry before using Teflon pan.

Do not dry with paper towel as this may remove coating.

### 3.2 Fibrinogen and Thrombin

Thaw at room temperature, one aliquot of fibrinogen and of thrombin prepared previously.

Note: Thaw the fibrinogen aliquot for 5 min in a water bath (~37°C) to ensure that the solution is properly thawed and dissolved

Using a 2mL Eppendorf tube, add 150 µL of thawed thrombin to 850 µL of calcium chloride (40mM)

Prime two 1 mL syringes by moving the plunger several times.

Collect all of the thrombin and fibrinogen into two separate syringes.

Collect solutions slowly and carefully, as failure to do so may result in insoluble fibrinogen formulation.

Invert syringe, carefully remove all bubbles and ensure that both syringes have equal volumes.

### 3.3 HEPES Buffered Saline (HBS) 1X Solution

Add 50 mL of 10X HBS stock solution with 450 mL of diH<sub>2</sub>O.

pH to 7.4

## 4. Preparation of Machine

### 4.1 Syringe pump preparation

Turn syringe pump on

Press SELECT.

Toggle to Table, press SELECT.

Toggle to Bec. Dic. Plastic, press SELECT.

Toggle to 1 cc 4.70 mm, press SELECT.

Enter volume: 1.0 mL, press ENTER

Enter extrusion rate: 0.225 mL/min, press ENTER

NOTE: syringe pump will be run later in Step 5 Extrusion Procedure

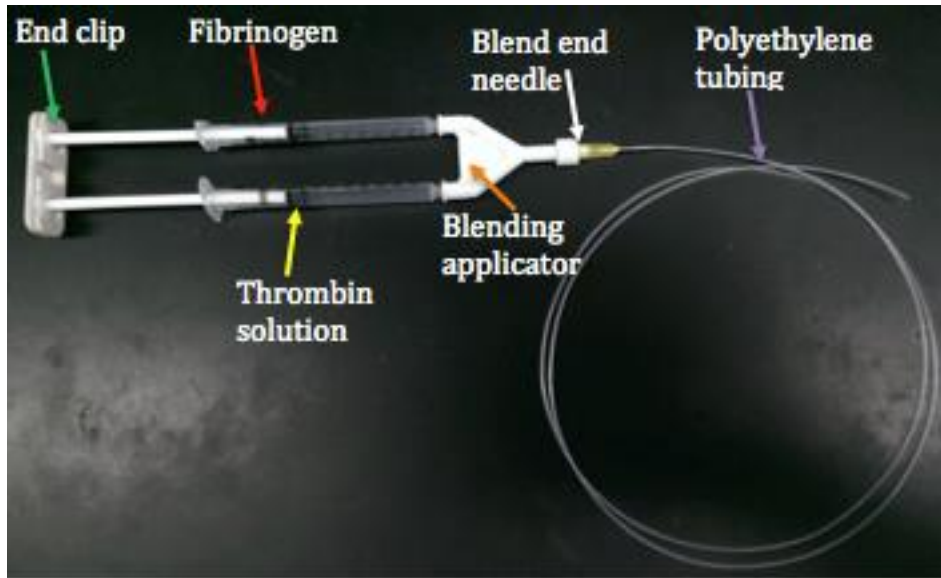


Figure 44: Blending applicator set up as described in steps 2 - 4.

Place blunt end needle (25 gauge, BD)(white arrow) into 0.86 mm ID polyethylene tubing(pink arrow), 97cm in length

Luer lock blunt end needle onto end of the blending connector

Place each 1 mL syringe of fibrinogen (red arrow) and thrombin (yellow arrow) solutions into the back end of the blending applicator (orange arrow).

Place the fibrinogen solution in the blending applicator opening with the circle on it.

Secure syringes into end clip (green arrow).

Secure the ends of the syringes connected to the blending applicator construct into the syringe pump and place syringe pump to the left of the printer on top of small table as shown.



Figure 45: Syringe pump set up

Secure pipette tip into the extrusion head so that (~162) mm of the pipette is below the extrusion head.

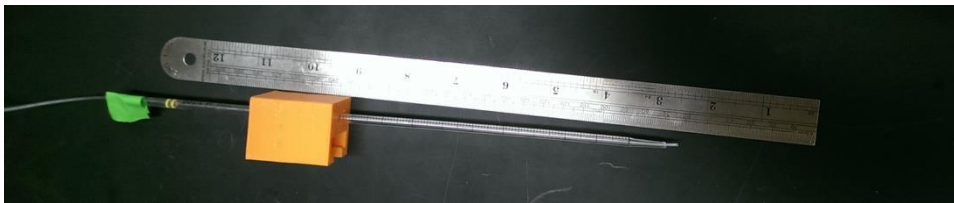


Figure 46: Extrusion head with pipette tip and polyethylene tubing set up

Feed end of polyethylene tubing into pipette tip that is connected to extrusion head so that of the tubing is touching the top of the stationary shoe in the bath, approximately (~15) mm beyond the pipette tip.

Secure the top of the tubing with tape to ensure that the tubing placement is maintained.

Place this extrusion head set up on side until Step 5 Extrusion Procedure.

Shoe and bath preparation

Place Teflon pan into frame, ensuring that it is sitting on the lowest setting of the corner notches. By rotating the corner notches, it will raise and lower the pan's corners.



Figure 47: Teflon pan inserted into frame on corner notches indicated by red arrows.

Combine 50 mL of 10X HBS with 450 mL of diH<sub>2</sub>O and pH to 7.4.

Pour 500 mL of this 1X HBS into the Teflon pan as shown below.

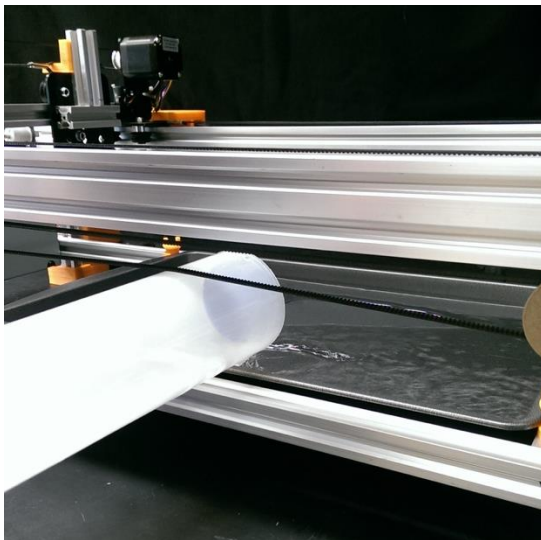


Figure 48: Pouring HBS into Teflon pan

Invert shoe frame on bench top so that the four feet are facing upward and the frame lies flat with shoe sliders positioned parallel on either side, with a slight gap between each pair on the same side.

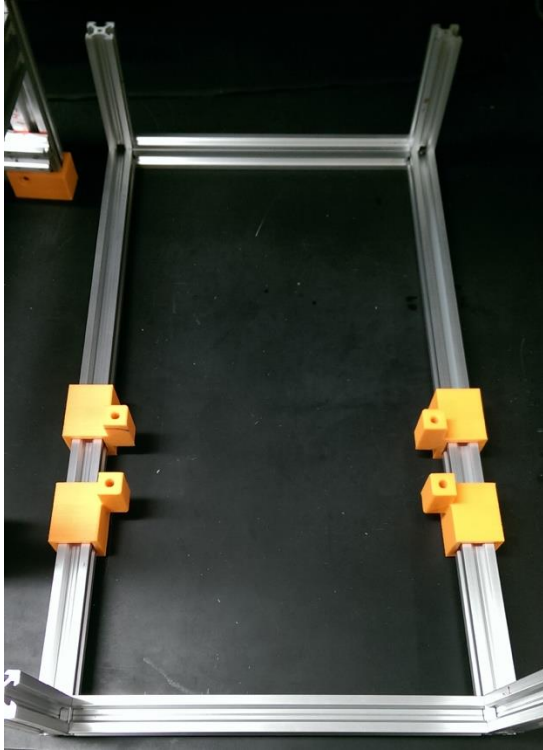


Figure 49: Inverted shoe frame

Place stainless steel rods of the shoes into holes on the shoe sliders. The shoe with the shorter rods (~3") should be placed in shoe sliders closer to user with the gap of the U facing away from the user. The other shoe with longer rods (~4") should be placed in the shoe sliders further away the user with the gap of the U facing toward the user.

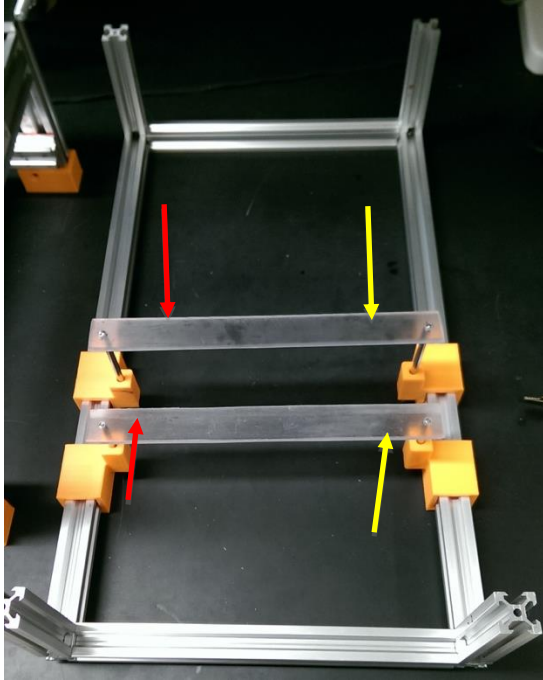


Figure 50: Inverted shoe frame with shoes placed into shoe sliders, yellow arrows indicating sloped edges, red arrows indicating roughened edges.

Secure shoes by placing clips on all four steel rods on sides closest to the bench top.

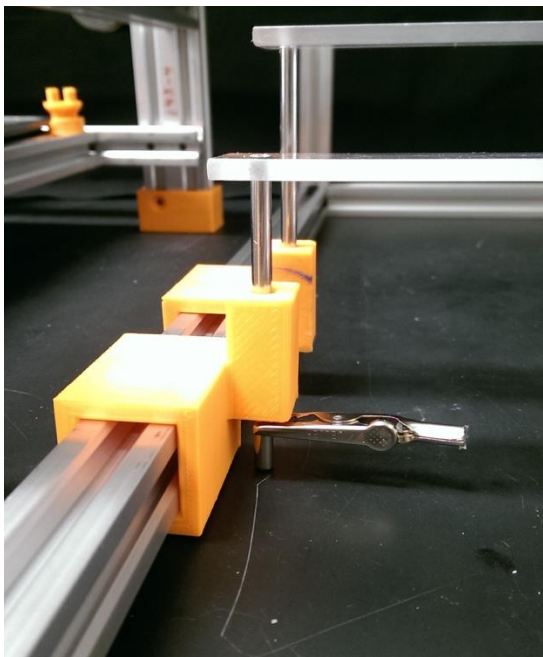


Figure 51: Clip securing shoe in shoe slider.

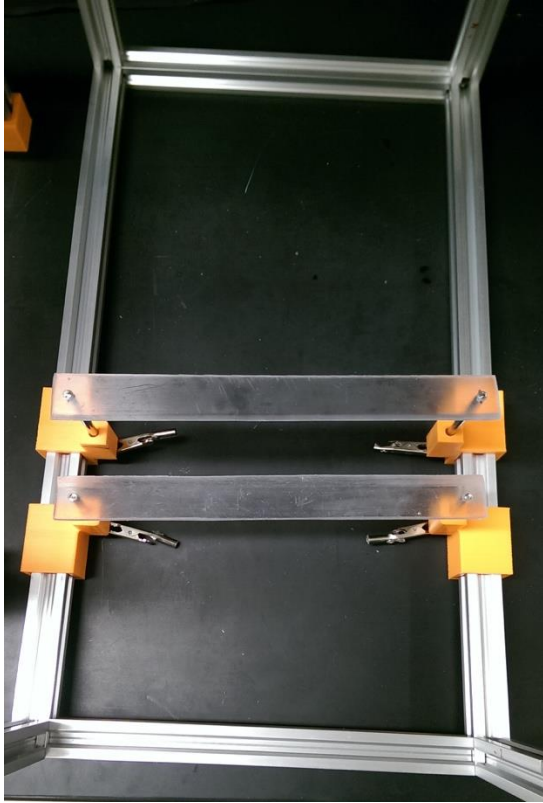


Figure 52: Top view of clips securing shoes into shoe sliders.

Revert shoe frame on bench top.

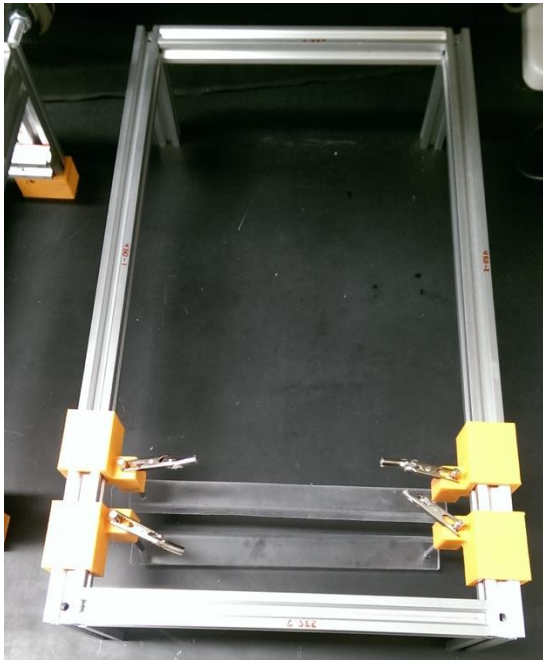


Figure 53: Reverted shoe frame with shoes secured in place.

Place shoe frame into machine over the Teflon pan by sliding four corners into place.

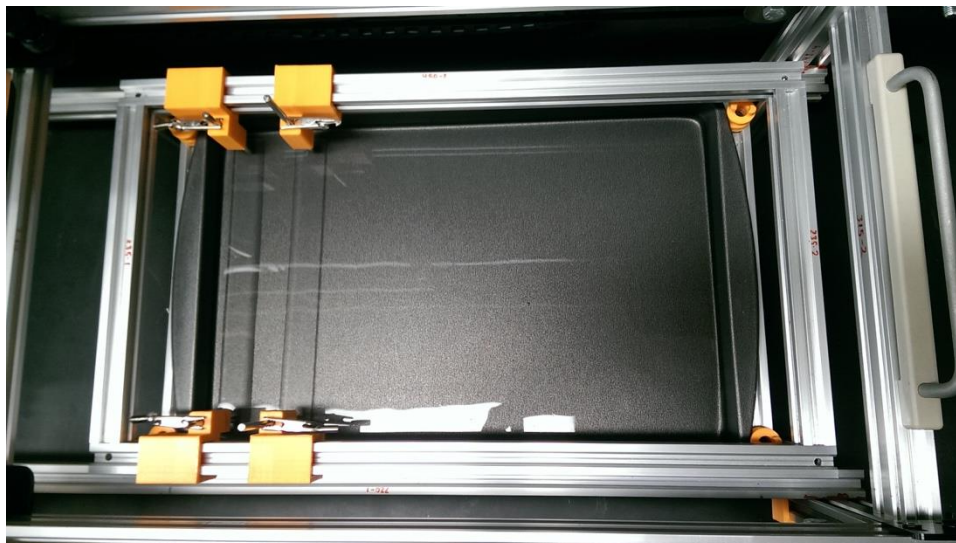


Figure 54: Shoe frame placed into machine over Teflon pan.

Ensure that clips are flush against the shoe sliders to avoid any unwanted interference with the extruder.



Figure 55: Clips flush against shoe sliders.

Move shoe slides back and forth as necessary to ensure that HBS covers the bottom steel mesh layer ~~top~~ of both shoes.

Move shoes to sit in left side of the bath (closest to the syringe pump and emergency stop button).

Secure stationary shoe in place at 20 mm from the edge of the bath to the bottom of the U-shaped ~~rough~~ edge of the stationary shoe. Set screws should maintain this position, so measure this distance to ensure that the shoe is accurately in place.

## Software Set up

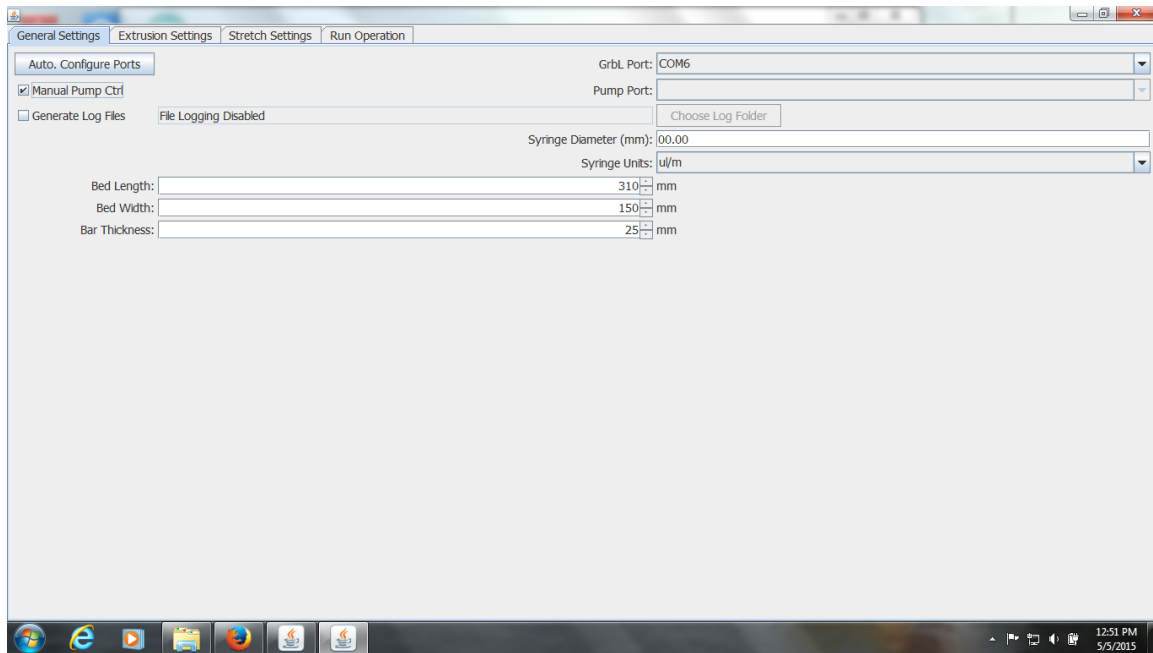
These are now the instructions for setting up the software on the laptop that should be placed next to the machine.

The program for LACEY can be run from any computer available. There are 2 software applications required for the LACEY program to work. The first is Java 8, which can be downloaded from <http://www.oracle.com/technetwork/java/javase/downloads/jre8-downloads-2133155.html>. The code will most likely work with future Java version, but if not, there is a installation program in the "Lacey system" folder. The second program needed is Arduino console, version 1.6.4. It can be downloaded from <http://www.arduino.cc/en/Main/Software>. It is unclear if future version will have the same language commands, so there is version of the current program saved on the "Lacey system" folder, from the time when the system and its software were created.

Plug in the power cord to the machine and then connect the electronics to a USB port on the computer. This must be done before opening the program. The green LED on the power supply should be lit once plugged in. If not, check that the E-stop button has not been pressed.

Open the program by double clicking on the file name. The window shown above should appear. On the lab computer the file is located in "BME - NB04" > "Local Disk(C:) > "FibrinPrinterControllerNullMinMax.jar". That last file is the one you will need. If you plan to use this program regularly it would be best to save this to your desktop. Between consecutive runs, the program should be closed and opened.

## General Settings Tab



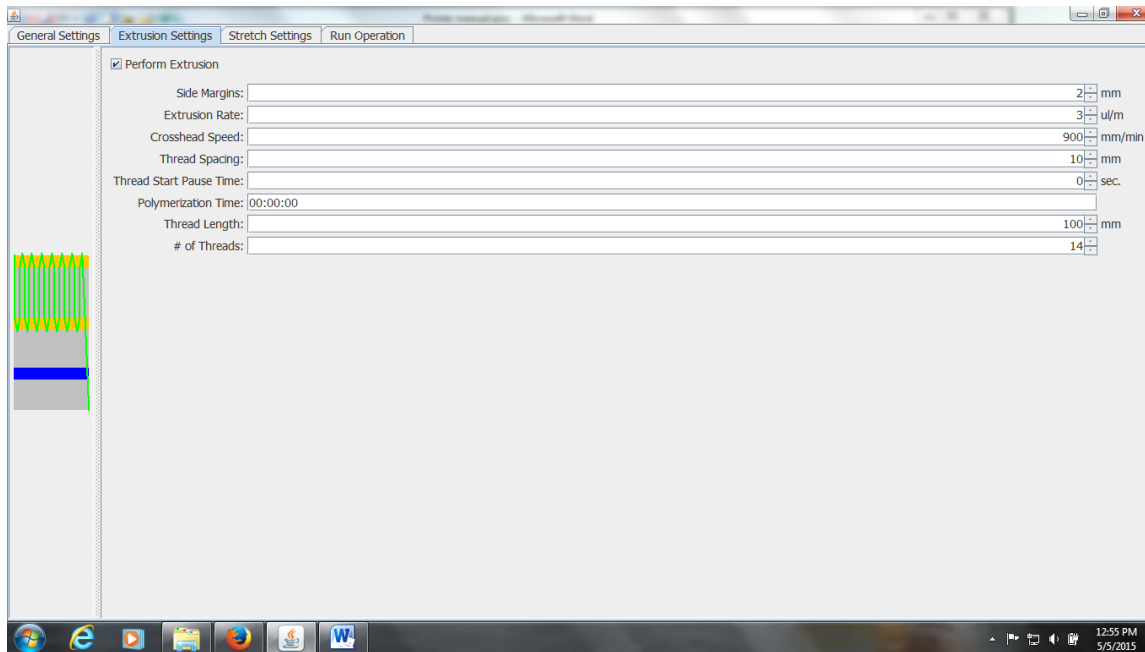
On the opening page of the software, select the COM port (Shown on the right hand side of the window) for the Arduino. In this figure, "COM6" is selected however this can be different on each computer. The "Auto. Configure Ports" button will try to find the Arduino when pressed. If this fails then you may need to find what port it is using the device manager on the computer.

If the syringe pump is not connected to the computer, you must check the "Manual Pump Ctrl" box otherwise there will be an error later in the program. If this error shows up, close the program and restart.

**Change or make sure that the "Bed Length" is set to 310mm and the "Bed Width" to 150mm. This is reversed in the default settings for the first use!**

Move to the next tab to continue.

## Extrusion Settings Tab



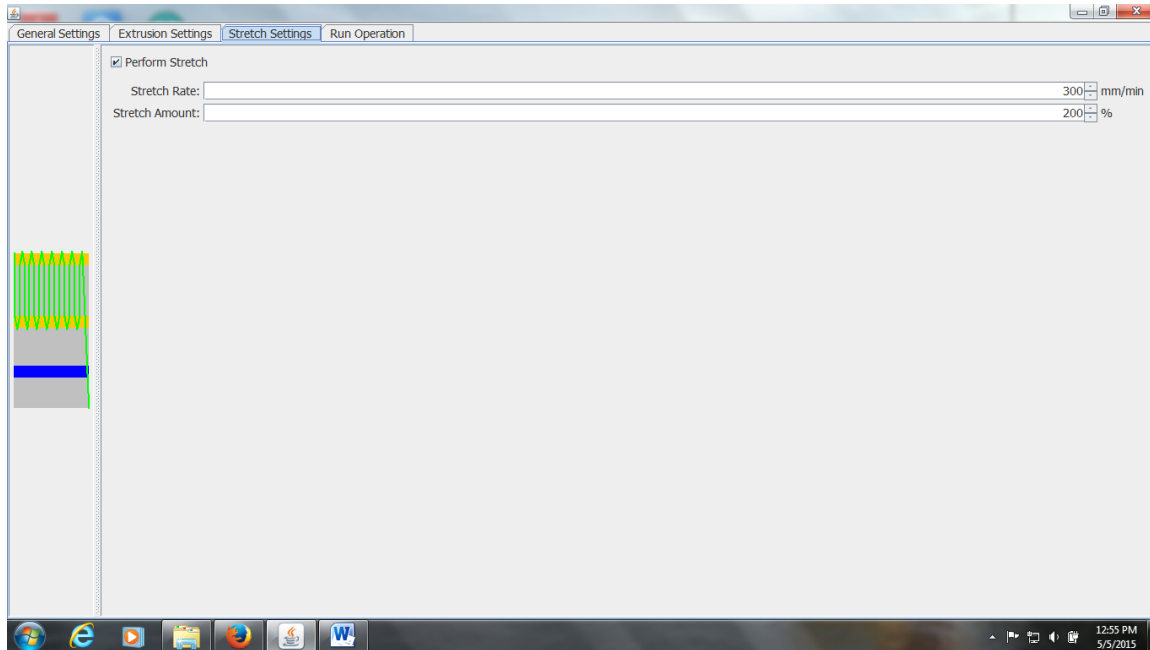
Check the "perform extrusion" first. If you just want to perform a stretching operation then make sure this box is unchecked

Set your desired parameters from the top down. If you have used the program before then many if not all of the parameters will be remembered. It is important to verify each one because some numbers are limited by other entries. If you change a separate field it may cause additional fields to change unexpectedly.

If a thread length of 100mm is wanted, but the program will change that value to a lower number when entered then check the next tab. If the "stretch amount" is set too high for that thread length then the original thread length is limited. In this case percent extension will need to be entered before the desired values can be entered.

Not all parameters will do things if the pump is not connected to the computer. Changing them can be used to notate and manually input values into the pump.

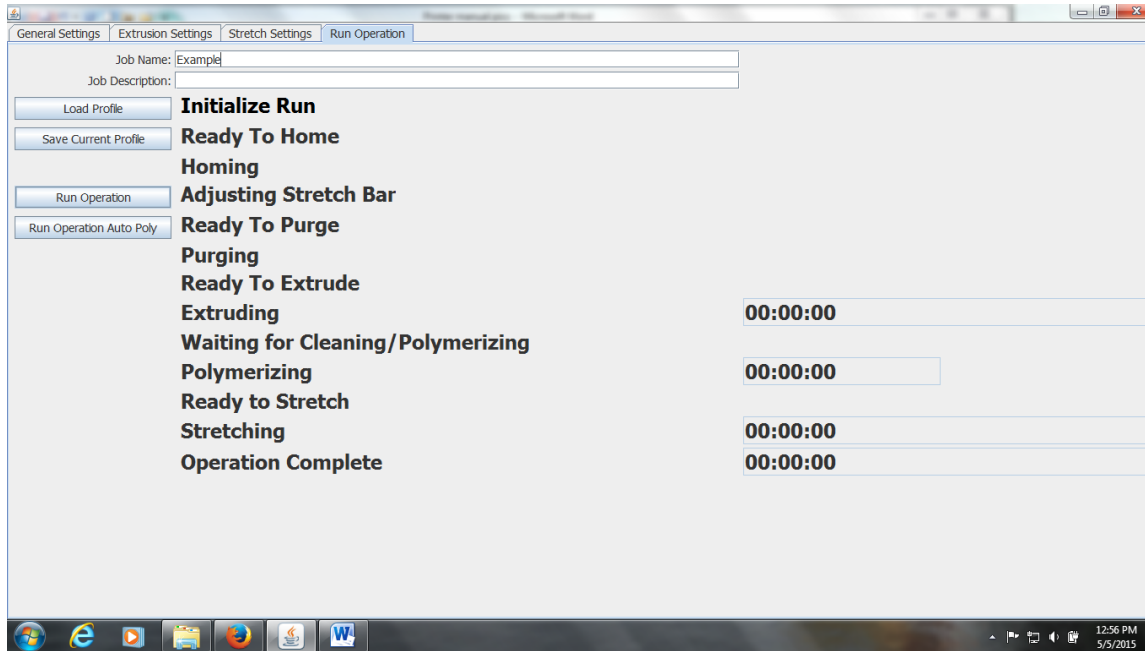
## Stretch Settings Tab



Check the perform stretch box if stretching is wanted. Set or check all parameters before moving to the next tab.

The inputs on this page will cause changes in the previous tab. Use caution, especially if a high "stretch amount" has been entered because this will cause lengths in the previous tab to change. Double check the previous tab to make sure no changes were made to the desired parameters before moving on.

## Run Operation Tab



This tab will allow you to run the set parameters by clicking "Run Operation". Clicking "OK" will move the machine directly to the next step. Follow instructions in 5. Machine Operation that go along with the on screen cues from the software.

After the operation has been run close the program and unplug the machine. If multiple sets of threads are to be made then keep everything plugged in, but close out and restart the program. The program can not be run twice. Settings should be saved from the previous test, however it is good practice to check this.

### 5. Extrusion Operation

After pressing Run Operation, the machine will home the stretching and extrusion bars. Ensure that the extrusion head is not in place at this time.

After hitting the next "OK" cue, the stretch bar will move the moving shoes into place and return to home.

Once stretch bar is in place, you may not place extrusion head with polyethylene tubing in place as previously prepared in Step 4.7.

When directed to, start the syringe pump for extrusion, watching the flow of the fibrin through the tube. Once it reaches the bath it begins extruding into the buffer, press “OK” to start the movement of the extrusion head.

At the end of extrusion, the head will stay in its last location ~~move to the far end of the bath~~. Stop the syringe pump and remove the extrusion head.

Immediately following the completion of extrusion, clean out polyethylene tubing by flushing through with 3-5 washes of water and 3 of air using a 10 mL syringe connected to the blending applicator.

#### 6. Intermediate Dry Step and Stretch

NOTE: Follow these instructions if you would like to add an intermediate dry step to your fabrication process. If you would like to immediately stretch without this step, skip these instructions and follow 7. Stretching Operation.

After the threads have polymerized for 10 minutes following extrusion, place the squeegee pieces on top of the shoes.

Be careful to not move the shoes in the bath as this will damage the threads

Placement of the squeegees on the shoes should be vertically down on top of the shoe.



Figure 56: Squeegee pieces in place on top of extruded threads.

Tilt the Teflon pan by turning two of the corner pieces counter-clockwise on one side of the Teflon pan closest to the extruded threads.

Using either a micropipette or an aspirator, remove the liquid from the Teflon pan being careful to avoid contact with the threads.

Remove the shoe frame from the bath slowly and place on the bench top for 24 hours.

Refill the Teflon with 500mL of diH<sub>2</sub>O at room temperature.

Replace the shoe frame with dried threads into place over the bath, allowing the threads to rehydrate for 1 hour.

Restart the machine and uncheck the box at the top of the Extrusion Settings tab. Ensure that the Stretch Settings are set to the desired stretch percentage.

Following the stretch, follow steps 2-4 to remove liquid from the Teflon pan.

Tilt the Teflon pan by turning two of the corner pieces counter-clockwise on one side of the Teflon pan closest to the extruded threads.

Using either a micropipette or an aspirator, remove the liquid from the Teflon pan being careful to avoid contact with the threads.

Remove the shoe frame from the bath slowly and place on bench top for 24 hours.

## 7. Stretching Operation

After the threads have polymerized for 10 minutes following extrusion, place the squeegee pieces on top of the shoes.

Be careful to not move the shoes in the bath as this will damage the threads

Placement of the squeegees on the shoes should be vertically down on top of the shoe.



Figure 57: Squeegee pieces in place on top of extruded threads.

Press OK on software to initiate stretching after 10 minutes is shown on the timer.

Tilt the Teflon pan by turning two of the corner pieces counter-clockwise on one side of the Teflon pan closest to the extruded threads.

Using either a micropipette or an aspirator, remove the liquid from the Teflon pan being careful to avoid contact with the threads.

Remove the shoe frame from the bath slowly and place on bench top for 24 hours.

#### 8. Cleaning

Ensure that the shoe frame and any remaining fibrin is removed from the bath.

Ensure that polyethylene tubing is flushed as instructed previously following extrusion.

Drain remaining liquid in bath by lifting pan out of machine and disposing of liquid in sink.

Manually wash pan with soap, water and diH<sub>2</sub>O.

Dispose of syringes in sharps container.

Turn off and unplug syringe pump.

After 24 hours and once threads removed from shoe frames, clean squeegee and shoes using soap, water and diH<sub>2</sub>O.

#### 9. Emergency Stop

In the case that the machine is out of control, unable to be stopped with the software, and in danger of causing damage press this button.

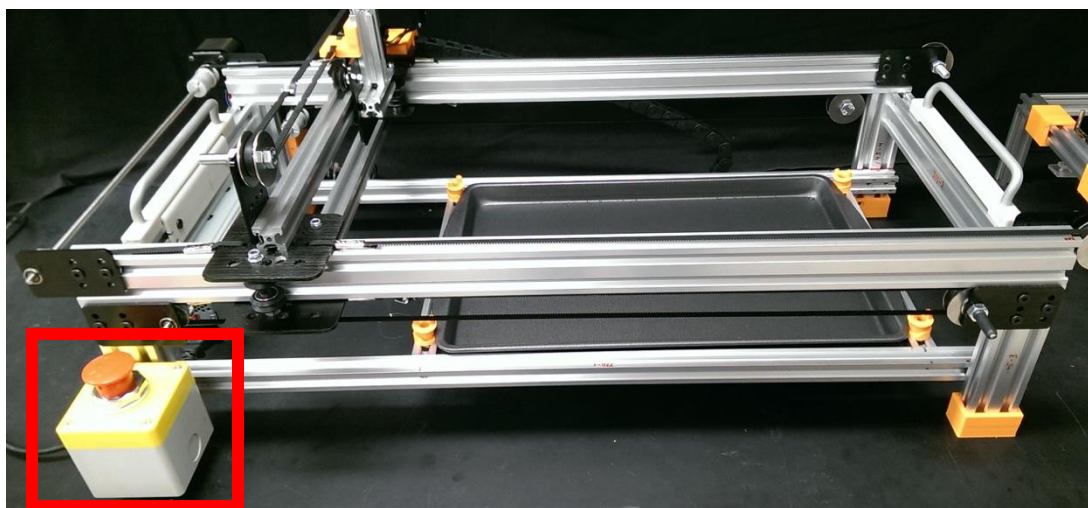


Figure 58: Emergency stop button highlighted by red square.

This will shut down the power supply and stop the machine from moving.

If pressed, wait a full minute and stop the software before releasing the E-stop button. To release, turn in the direction of the arrow and allow to pop up. The Green LED on the power supply should be lit to indicate that the power supply is on.

## 10. Machine Power Supply

The machine has no button to turn on or off. Plugging the machine in will turn it on and the green LED on the power supply should be lit. If the machine is plugged in and nothing is on then check to see that the E-stop has not been pressed down.

Unplug the machine after use to prevent long-term damage.

## 11. Maintenance and Modification

### 11.1 Belt Tightening

As the machine is used, some of the belts may increase in length. Three of the belts are fitted with tensioning springs. These should keep those belts at the proper tension even if they are to stretch. The two long top belts do not have spring tensioners. If they become noticeably loose and cause the position to slip during operation then the two bearings on the opposite side from the power supply can be loosened and slid out to increase tension.

This should not be a problem for many hours of use and only needs to be checked if a problem occurs.



## 11.2 Hardware Adjustments

Nearly all hardware is held in place using M5 machine screws. To adjust or tighten them, a 3mm Allen wrench can be used. Careful not to over tighten these because the screws are much stronger than the aluminum threads.

## 11.3 Printed Parts & CAD Files

All files for the 3D printed parts are included in folder “Microthread ISP CAD Files”. They have been designed to be used with a plastic extrusion based printer and the necessary tolerances of one.

The current parts are made of PLA, but ABS should also work just as well.

## 11.4 Electronics and Control

The machine is powered by a 12 volt computer power supply and controlled through an Arduino UNO with a GRBL shield. The software loaded onto the Arduino is a version of GRBL, an open source software that interprets G-code and is able to be easily downloaded from the internet.

G-code is a universal machine code that instructs the machine to move to coordinates and a speed to do so. The current (first) program on the computer generates the path in G-code and sends segments of it when the user prompts the program to do so.

In the future, a program called "universal G-code sender" or any other similar program could be downloaded to control the machine by inputting custom G-code. Caution should be used because the software limits are only set in the current (first) computer program and not on the Arduino itself.

### 11.5 Addition of a 4th Motor

The current machine is designed for operation with three motors. The addition of a fourth motor (NEMA 17) is possible with the addition of an A4988 Stepper driver on the GRBL shield. This would also require a modification in the GRBL software currently on the board.

## 12. Recommendations for Future Optimization/Troubleshooting

### 12.1 Shape of end of polyethylene tubing

Various tubing shapes were utilized with the aim of optimizing the flow of fibrin out of the tubing to avoid accumulation on the end of the tube and allow for consistent thread volume. By cutting the end of the tube to a 30 or 45 degree angle with a razor blade, this decreased the accumulation by the end of the tube. There was no noticeable difference between 30 and 45 degrees. With the 45 degree cut, the bottom of the tube was also cut to allow for limited accumulation. Even though this decreased the accumulation it did not completely remove it.

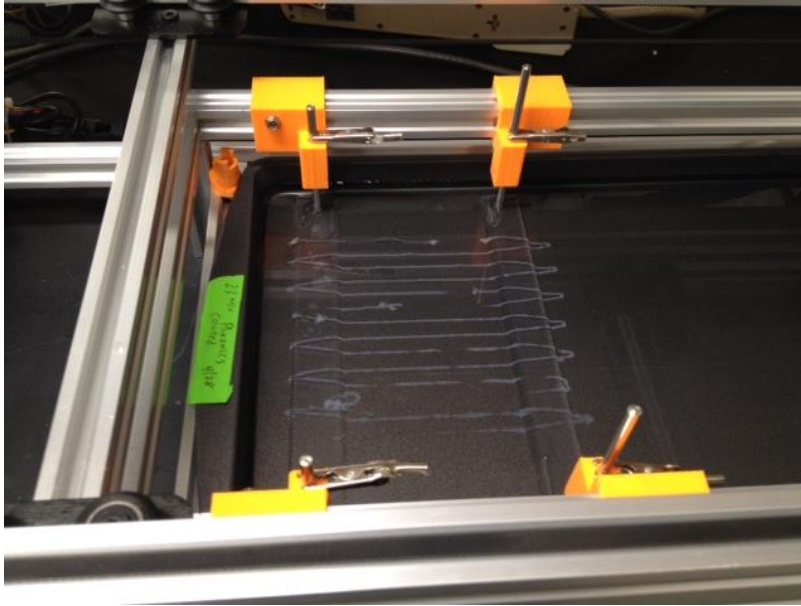


Figure 59: Extruded threads using 45 degree cut in tubing.

### 12.2 Extrusion head speed

By increasing or decreasing the extrusion head speed it will modify the thickness of the threads. By increasing the thickness this could allow threads to be less likely to break during stretching and removal.

### 12.3 Volume of HBS buffer

The team decreased the initial buffer amount from 600ml to 500ml to have less space for the threads to accumulate above the shoes so that they would be able to adhere better to them.

### 12.4 Angle at edge of tubing

The team attempted letting longer amounts of the tubing to be dragged for extrusion of the threads to simulate the angle from manual extrusion. However, this causes inconsistency with thread placement and a jump to occur when moving over the shoes so this would not be recommended for use with this system unless it can be better controlled.

### 12.5 Decreasing residence time of fibrin

By decreasing the amount of time that the fibrin spends within the tubing polymerizing, the team believes that this will allow a more even extrusion into the bath. This can be achieved by either decreasing the

length of the tubing where the fibrinogen and thrombin are mixed by having separate tubes until further down where a blending applicator would be located. Also this could be achieved more easily through increasing the rate of the syringe pump. This should be compensated for with the extrusion speed.

#### 12.6 Priming the tubing

When new tubing is used for the machine, it can cause the fibrin to have inconsistent flow within the tubing, therefore the team suggests priming the tubing with either HBS from the bath or diH<sub>2</sub>O to remove any inconsistencies as possible within the tubing.

#### 12.7 Different blending applicator

Through attempts at consistent extrusion, the team observed that the fibrin had inconsistencies when extruded that caused breakages to the extruded threads. A potential solution to this would be changing the blending applicator to a different model that would allow for more mixture of the two solutions for a more homogenous thread composition when extruded.

#### 12.8 Misaligned primary extrusion head bar

After multiple uses and possible bumps into the system, the primary extrusion head bar, which moves along the length of the bath, could become misaligned. This means that the bar is not perpendicular to the 2 rails on the side. This misalignment causes the bar to wheels on the bar to exert more resistance on the primary extrusion bar, which causes the electromotor to jam. To fix this, first, the belts on both sides of the primary extrusion head need to be released, and the outer wheel needs to be rotated to loosen the bar. This will allow the user to readjust the loose bar, and straighten it, reducing the excess resistance. Once the primary extrusion bar has been realigned, fix and tighten all the loose pieces, and reset the system.

#### 14. Parts List

All Solidworks parts and assemblies are in a folder labeled "LACEY Parts Files". The final 3D printed parts are in a folder within that folder labeled "Printed Parts". Previous versions during development as well as STL files used to print are included as well for reference or for future modification.

## Fibrin Composite Scaffold Fabrication Protocol

**Objective:** Record current procedure for making fibrin films

**Materials:**

- Fibrinogen aliquot ((11 mg/mL) Ref #MO1:26
- Thrombin aliquot (2.35 U/mL) Ref #MO1:26
- 40 mM CaCl<sub>2</sub>
- PBS
- Silicone wafer with gradient pattern
- di H<sub>2</sub>O
- Vellum paper
- Ruler (with millimeter markings)
- Scissors
- Razor Blade

**Procedures:**

**Prep of Vellum Frame for Film**

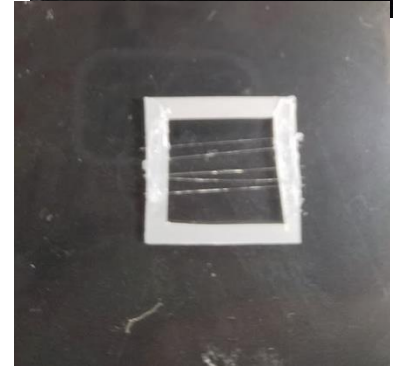
1. With vellum paper, measure a strip 12 mm wide and cut strip from sheet
2. Along strip, mark every 12 mm lengthwise and cut along markings, creating 12x12mm squares
3. On a hard surface, use razor blade to cut squares centers from the 12x12 square so that there is a 2mm thick border on all sides leaving an inner area of 100 mm<sup>2</sup>
4. The distance from inner edge to inner edge on each frame should be 10mm across horizontally and vertically when finished

**Prep of Frame with Threads**

1. Follow protocol to make fibrin threads using Lacey
2. After drying overnight, align 5 threads on clear plastic sheet taped at each end and ensure that the total width is around 9mm
3. Place about 12 vellum frames underneath the bundle and be sure to leave space to cut in between each one
4. Use medical adhesive glue and a blunt needle tip to glue the threads to each side of the frame
5. Allow to dry for 1 hour or until glue is hard
6. Starting at one end, cut frames from bundle and remove excess threads from the side of the frame.

**Prep of Fibrin Gel (from Fibrin Gel Basic Protocol – MO)**

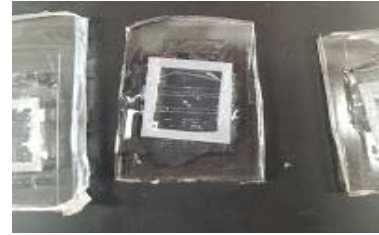
1. Prep Patterned Silicone wafer slide by soaking in 1% Pluronic F-127 in enough volume to cover the wafers for at least 15 min and allow to air dry (sterilize with ethanol if necessary[MO2] )
2. Mix the following reagents in a 1.5 mL centrifuge tube
  - a. 670 uL fibrinogen solution (2x solution)
  - b. 80 uL CaCl<sub>2</sub> (40mM)
  - c. 150 uL PBS (or cell media if using cells)
3. Add 100 uL thrombin solution and titrate (at least 10x) to gently mix with other reagents in centrifuge tube
4. For a standard 10x10mm film frame:



- a. Pipette 200  $\mu$ L of mixed solution onto silicone wafer with frame
  - b. Use pipette tip to submerge frame edges into solution
5. Allow 30 minutes for polymerization

**Prep of Fibrin Film**

1. Use forceps to place composite in diH<sub>2</sub>O bath (room temp) for 10 minutes
  - a. 5 scaffolds in 125 mL bath is ideal volume
2. Switch frame into fresh water bath for 10 minutes
3. Switch frame into final water bath for 10 minutes
4. Remove from water bath and place onto acetyl plastic slide to dry completely for 5-6 hours



REV 04/2017 AB

---

## Resazurin Cell Viability Assay Protocol

**Objective:**

Determining the cellular viability on the composite scaffold.

Total time: 2 hrs 50 min

**Materials:**

1. Resazurin stock
2. 1 black 96 well plate (4 samples X 3 aliquots/sample x 1 timepoint) = 12 wells needed
3. Media
4. Fluorescent plate reader
- 5.

**Procedure:**

1. Make resazurin stock solution and warm for 10 minutes (20 min total)
  1. Add 500  $\mu$ L stock to 2.5 mL complete media (both in fridge)
  2. Mix and place in water bath for 10 min
2. Aspirate media from samples - hold down frames with forceps and keep pasteur pipette away from composites (5 min)
3. Add 600  $\mu$ L resazurin solution to each sample (5 min)
4. Incubate plate in cell culture for 2 hours (2 hours)
5. Transfer 100  $\mu$ L from each well to a black 96 well plate in triplicate (5 min)
6. Read fluorescence with a plate reader (20 min)
7. Record results using fluorescence or absorbance as follows:

**Fluorescence:** Read fluorescence using a fluorescence excitation wavelength of 540–570 nm (peak excitation is 570 nm). Read fluorescence emission at 580–610 nm (peak emission is 585 nm).

**Absorbance:** Monitor the absorbance of resazurin at 570 nm, using 600 nm as a reference wavelength (normalized to the 600 nm value).

**Note:** Fluorescence mode measurements are more sensitive. When fluorescence instrumentation is unavailable, monitor the absorbance of resazurin reagent. Assay plates or tubes can be wrapped in foil, stored at 4°C, and read within 1–3 days without affecting the fluorescence or absorbance values.

## Laser Thickness Measurements

### Objective:

Determining the thickness of gels, films, and composites.

### Materials:

Laser displacement machine

Acetyl Slide

Gel, film, or composite to be measured

### Procedure:

1. Power on and screw in metal plate with four screws to ensure that plate is evenly attached
2. “Zero” the device
3. Place acetyl slide across all four screws to ensure stability
4. Record readout for acetyl voltage by aiming laser where no film or gel is present
5. Move acetyl slide where laser is on gel or film and record voltage value
6. Repeat three times on different locations of gel or film

**NOTE:** Move the gel or film to different locations on the slide, but do not move acetyl slide, or else calibration will not be valid.

7. Use sheet to record measurements called “Laser Displacement Measurements”
8. Calculate thickness using the following equation:

$$\text{Sample thickness } (\mu\text{m}) = \frac{1000 * 1.7 \text{ mm (acetal slide)} * [\text{Avg. (V)} - \text{Acetal (V)}]}{\text{Acetal (V)}}$$

## Human FGF-2 Standard ABTS ELISA Protocol

Phase 1: Coat plate with capture antibody

- Centrifuge vial of capture antibody
- Reconstitute capture antibody in sterile water to concentration of 100 ug/mL. Allow to reconstitute for 10 min minimum
- Centrifuge reconstituted vial for 3 minutes at max speed

- Dilute capture antibody with 1X PBS to conc of 1 ug/mL. Vortex.
- Add 100 uL to ELISA plate wells
- Seal plate
- Incubate at 25 C overnight
- Discard liquid, blot on clean paper towel
- Add 300 ul of wash buffer to each well then aspirate, 4x
- After last wash, invert plate to remove liquid

#### Phase 2: Blocking non-specific binding

- BSA used as blocking buffer, 300 uL blocking buffer to each well
- Seal plate
- Incubate for 1 hr at RT

#### Phase 3: Specific binding of antigen

- Prior to end of previous incubation period, centrifuge vial of FGF-2
- Reconstitute to 1 ug/mL using 1 mL sterile water for 10 min minimum
- Rinse plate with wash buffer 4x, invert plate
- Centrifuge reconstituted vial for 3 min at max speed
- Dilute to conc of 2 ng/mL with diluent, vortex

#### Standard Curve

- Add 100 ul of diluent to each well except 1<sup>st</sup> row
- Add 200 ul of standard (2 ng/mL) to first row
- Dilute 1:2 for each standard
- Include at least 6 blank wells with only diluent
- Each well should have 100 ul

- Add samples, 100 ul to remaining wells
- Seal plate, incubate at least 2 hours at RT

#### Phase 4: Sandwich formation

- Centrifuge and reconstitute detection antibody in 1 mL of sterile water to 100 ug/mL
- Wash plate 4x, invert
- Centrifuge 3 min at max speed and dilute with diluent to 0.25 ug/mL. Vortex.
- Immediately add 100 uL to each well
- Seal plate, incubate at RT for 2 hr

#### Phase 5: Addition of enzyme-linked avidin-hrp to the sandwich

- Let vial of avidin that to RT
- Wash plate 4x, invert
- Dilute 5.5 ul avidin 1:2000 in diluent for volume of 11 mL, mix solution
- Immediately add 100 uL to each well
- Incubate at RT, 30 min

#### Phase 6: Conversion of colorless substrate to colored solution

- Wash after incubation, 4x, invert
  - On last wash remove wash solution from well and add 100 ul of ABTS, watch for color change, if none continue. If color change, continue washing.
- Add 100 ul ABTS to each well
- Incubate at RT for color detection
- Check plate every 5 min up to 60 mins
- Read plate at 405 nm – every 5 minutes for 60 min

## EDC/NHS Crosslinking with Heparin Protocol

### Materials:

Sodium Phosphate Monobasic Monohydrate

N-(3-Dimethylaminopropyl)-N-Ethylcarbodiimide hydrochloride (EDC)

N-Hydro-succinimide (NHS)

Heparin

- Create NaH<sub>2</sub>PO<sub>4</sub> solution and pH to 7.4
- Hydrate scaffolds in NaH<sub>2</sub>PO<sub>4</sub> solution for at least 30 minutes
- Add 0.0368 g of NHS, 0.1073 g EDC, and 0.002 g heparin to 20 mL of similar buffer – for 100 ug/mL solution of heparin
- Submerge scaffolds in EDC/NHS + heparin solution for 2 hours at room temperature
- Remove the scaffolds from the solution
- Rinse 3x 5 minutes each in dH<sub>2</sub>O

## Glycine Quenching Protocol

-Create 0.25% solution of glycine in 1x PBS

-Submerge scaffolds completely in 2mL of glycine per scaffold, 1 hour

-Remove the scaffolds from the glycine solution

-Rinse each scaffold 3 times, 5 min each in PBS

## Loading of FGF-2 Protocol

- Block 12-well plate with 2mL of 1% BSA per well for at least 1 hour
- Reconstitute FGF-2 to a concentration of 10 ng/mL
- Make sure solution is properly mixed by vortexing
- Submerge each scaffold in 1mL of FGF-2 solution

- Place on plate rocker for 24 hours

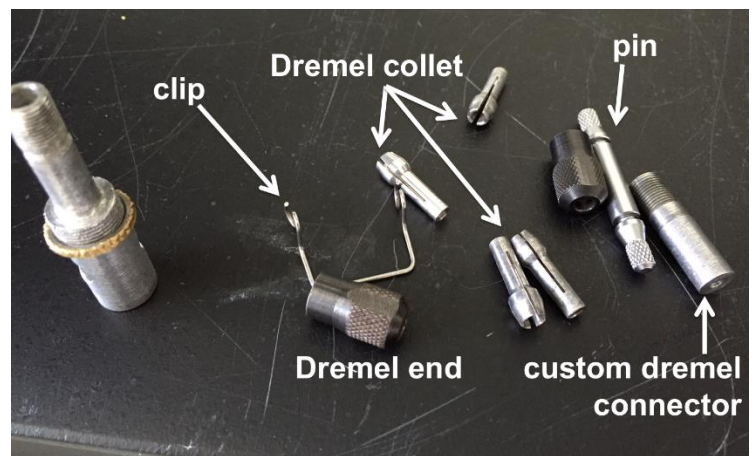
## Instron Testing Protocol

*Prepared by Meagan Carnes*

### **MATERIALS:**

From Pins lab:

- From Instron room (in baggie on top of shelving):



## INSTRUCTIONS – SETUP:

Make sure the INSTRON is oriented on its side, where the actuator is parallel to the table.

Place the short spacer ring and 6-hole base plate on the bottom base of the instron (opposite from the the actuating side). The “T” on the base plate should be oriented to the top. Secure this in place with two M8 bolts. (use a hex wrench to secure these on)

On the base plate, attach the transducer-base spacer. This is attached with a 1’ 6M bolt. NOTE – in this picture the “T” on the base plate is located on the side, rather than being oriented on top. Always orient the T to be facing on top.

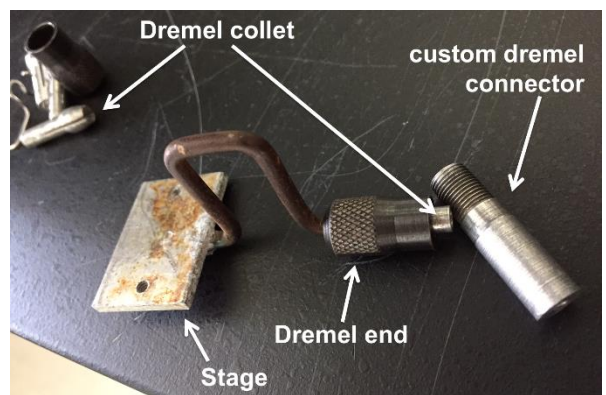


Attach the 1 N load cell to the transducer-base spacer. This is done by CAREFULLY threading the load cell onto the spacer. Thread the transducer until it is snug against the spacer.



Plug in the transducer to the back of the instron. It is pugged in where it says “Load cell” underneath it.

Attach the custom dremel connector onto the other end of the load cell CAREFULLY!!



Take the stage with the small “U” kink and thread on a dremel collet and dremel end. Now with these components on the stage, thread the other end of the dremel connector onto the dremel end to secure the stage onto the connector, and thus the load cell.



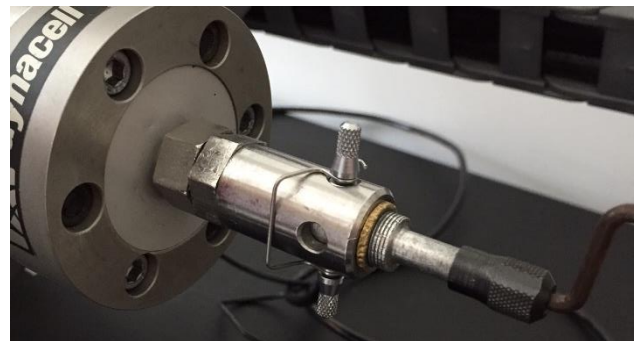
The right hand side of the set up is now complete.

Insert the custom dremel insert into the end of the actuator (left hand side of the setup)

Insert the pin through the hole of the actuator piece and the custom dremel insert. Use the clip to hold either end of the pin in place through the aligned holes of the connector and actuator.

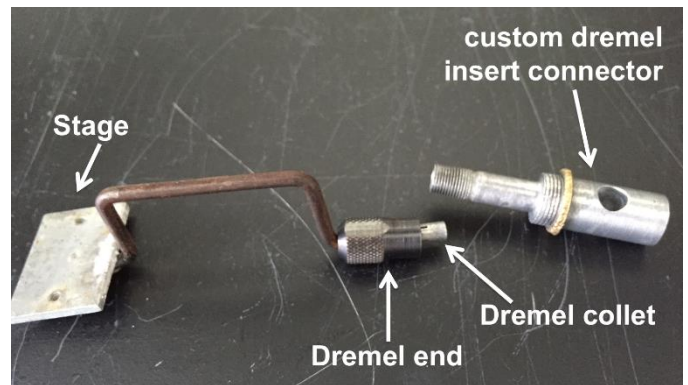


Tighten the gold ring on the connector until it holds the connector snug in place.



Place a dremel collet and dremel end over the stage with the longer “U” bend.

Thread the dremel end onto the connector



### INSTRUCTIONS – COMPUTER SETUP AND CALIBRATION:

Switch on the back of the large white INSTRON “computer,” located under the table

Open **Instron Console** on the desktop

\*\*\*NOTE: when calibrating the load cell, you want to calibrate it with the clips sitting on the stages\*\*\*

Click:

Load

Calibration

Calibration Wizard

Restore from Disk

VT 1N load cell 02 Jan 2014

Uncheck Lock calibration, Save calibration data

Check that Load primary limits are 1.05 N, and position primary limits are 29 mm

Open **Bluehill** from Desktop

Click TEST

Method: 170615fibrinscaffolds.im\_tens

Found in: \\research.wpi.edu\PinsLab\Anthony Campagna

For filename, name it the DATE the testing was done, and any distinctive features

Name each sample by the condition and the thread number

Input measured diameter average from hydrated threads.

“Next” takes you to the next test

“Return” once you are done testing

“RESET” allows you to reset gauge length (distance the stages will be apart)

- Do this at the position where the velum is sitting well aligned on the two stages, so that at the end of each test you can return to this starting position. The distance the stages should be apart is approximately 2.0 mm

“RETURN” allows you to return to the set gauge length.

#### SAVING FILES:

After 10 tests have been performed, the test will prompt you to save the work.

It will then allow you to end all testing, or continue testing with the same test method.

---

### **TO REPOSITION STAGES:**

To reposition the stages so they are the correct distance apart to place a vellum frame:

Loosen the black knob on top left of the the Instron to allow the whole system to move on the two large metal rungs. DO NOT FULLY REMOVE THE BLACK KNOB FROM THE MACHINE!

Manually move the system using the grey remote controller, and the black toggle button. First, the system will have to be switched from “0” to “1” in order to move it

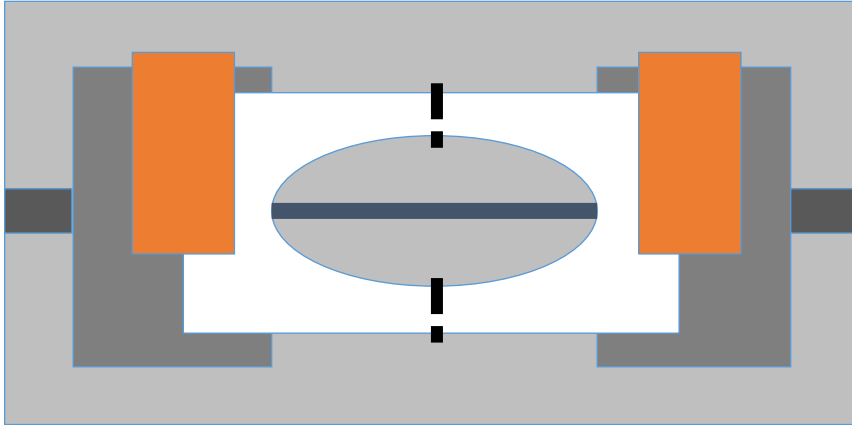
After it is moved to the desired distance, resecure the black knob so it is tight

### **SETTING UP VELLUM/THREAD:**

The stages (grey) are positioned apart so that the vellum frame (white) is positioned accordingly, where none of the film (blue) is on the stages.

Clamps (red) are then placed to secure the vellum frame in place on the stages

Before testing, the vellum frame is cut on both sides, indicated by dotted black lines in the figure below.

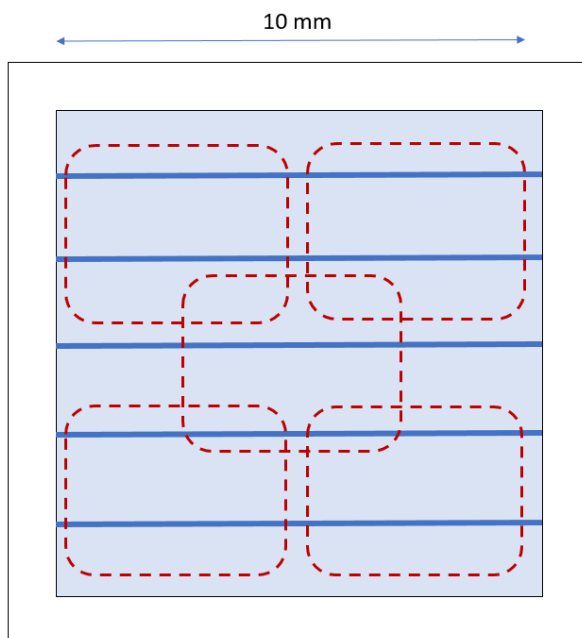


Top view of the vellum frame positioned on the stages. Dotted lines indicate where to cut the vellum frame

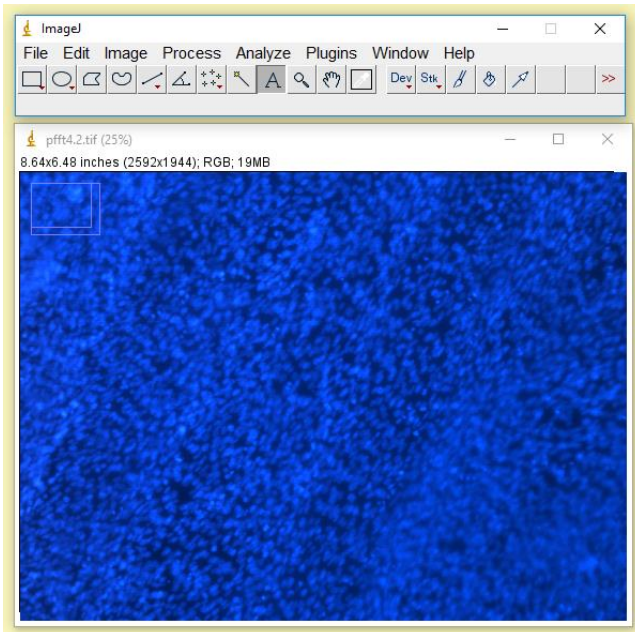
*\*All testing of scaffolds was performed hydrated and submerged in a PBS bath\**

### Alignment Analysis Protocol

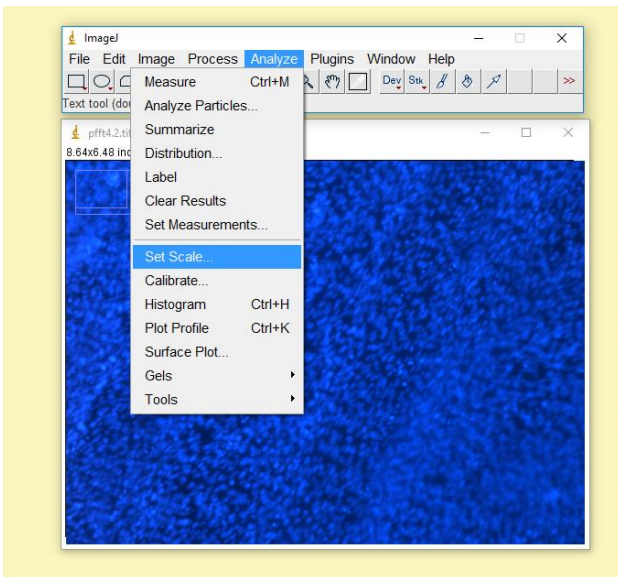
- Images the samples in a similar orientation as shown below.



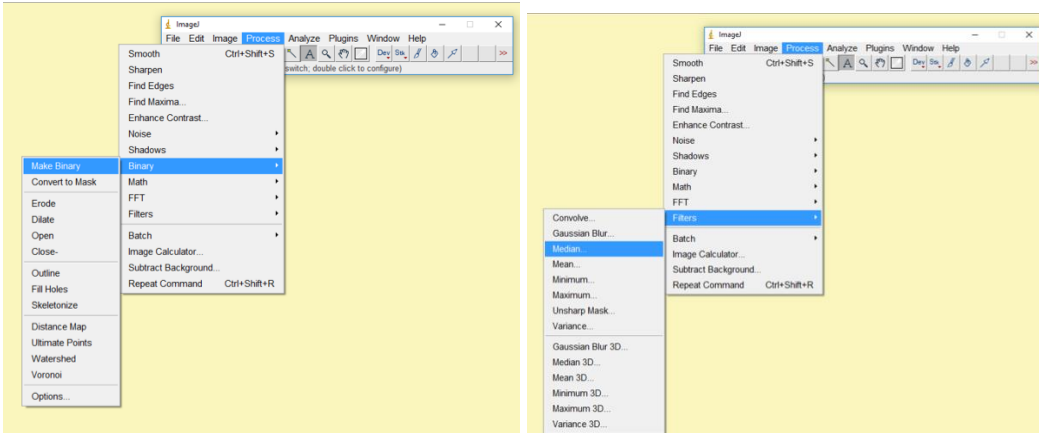
- Load image into ImageJ by either dropping the file into the ImageJ tab or opening it through the ImageJ system as shown below.



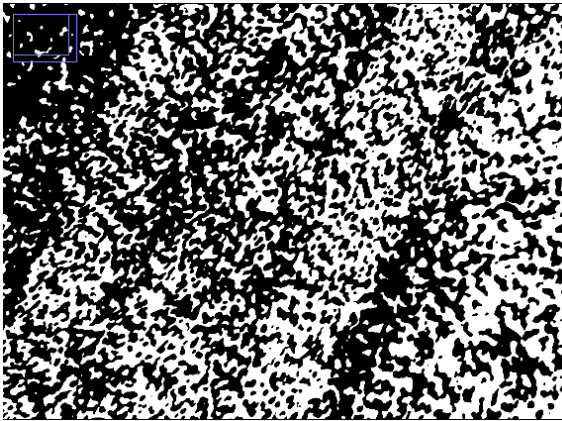
- Through the Analyze tab, set the scale of the image.



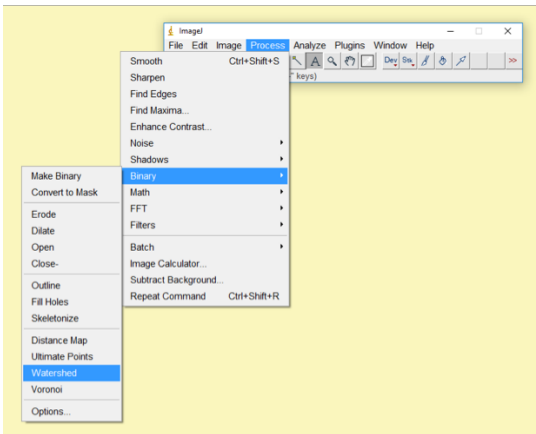
- Using the Process tab make the image binary and then add a median filter with a 5 pixel radius exclusion rule.



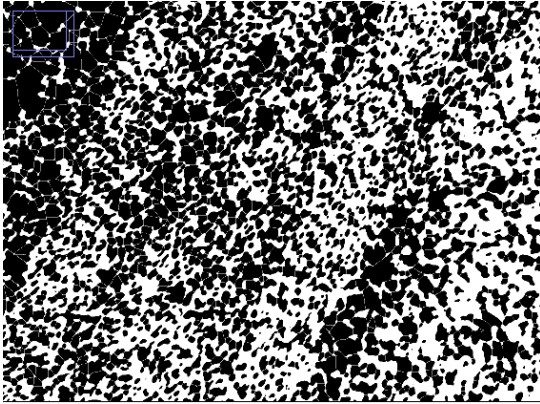
- These filters will produce an image similar to the one below.



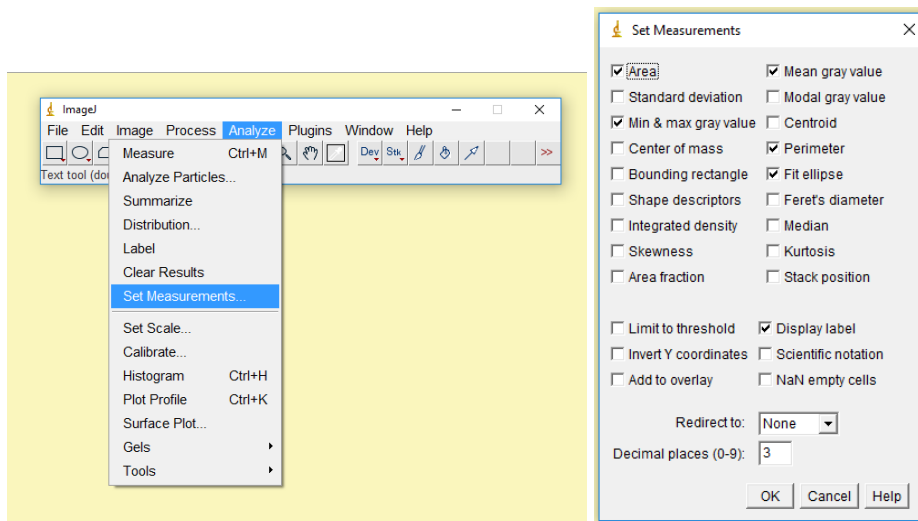
- Then through the Process tab make the image watershed to isolate each cell image.



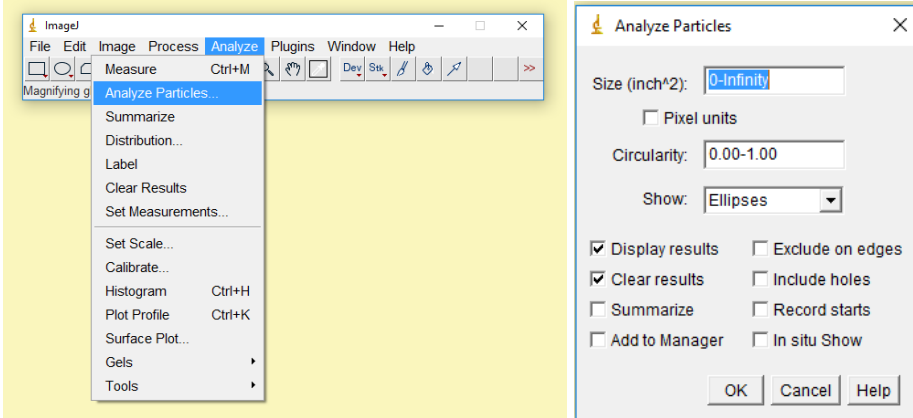
- This will produce an image as seen below.



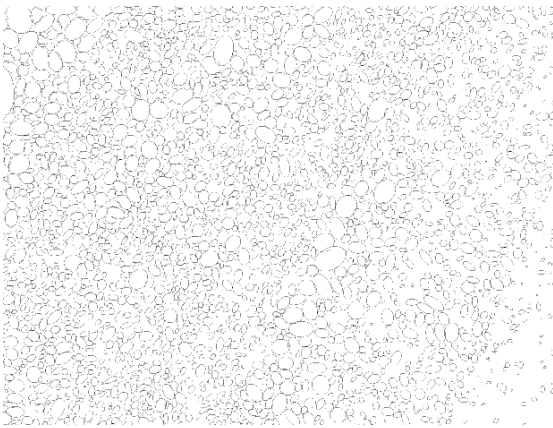
- Then use the Analyze tab and select ‘Set Measurements’. In the pop up window select ‘fit ellipse’.



- Then using the Analyze tab click on ‘Analyze Particles’ and select display results and show ellipses. The size textbox and circularity settings can be changed depending on the size of the cells in the image.



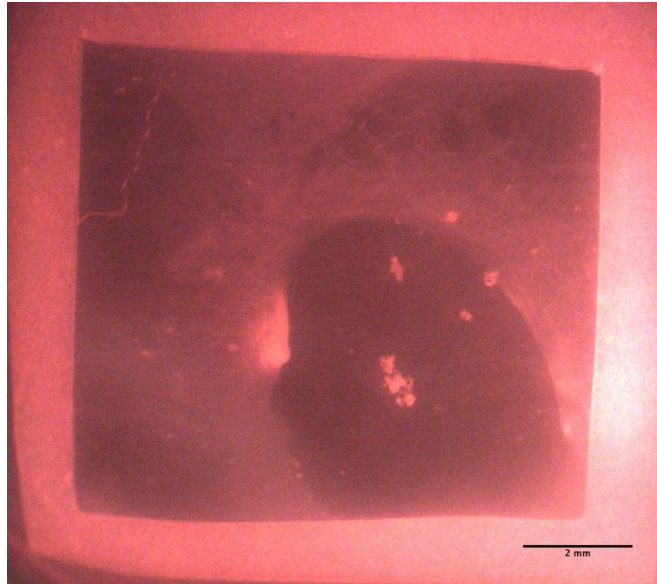
- This will produce an image as shown below and a data file output.



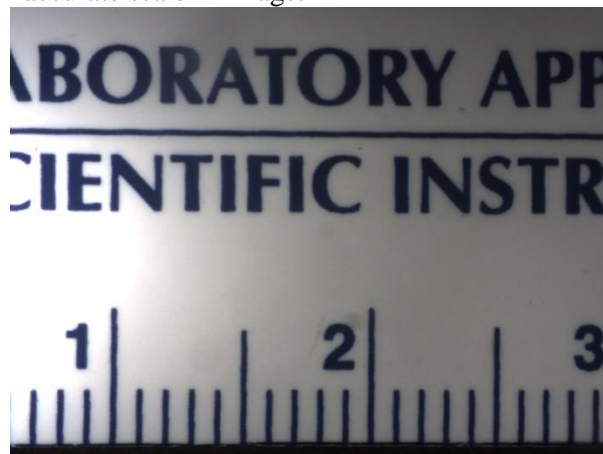
- Select the data in the pop-up window and transfer it to excel for data analysis.

## Degradation Analysis Protocol

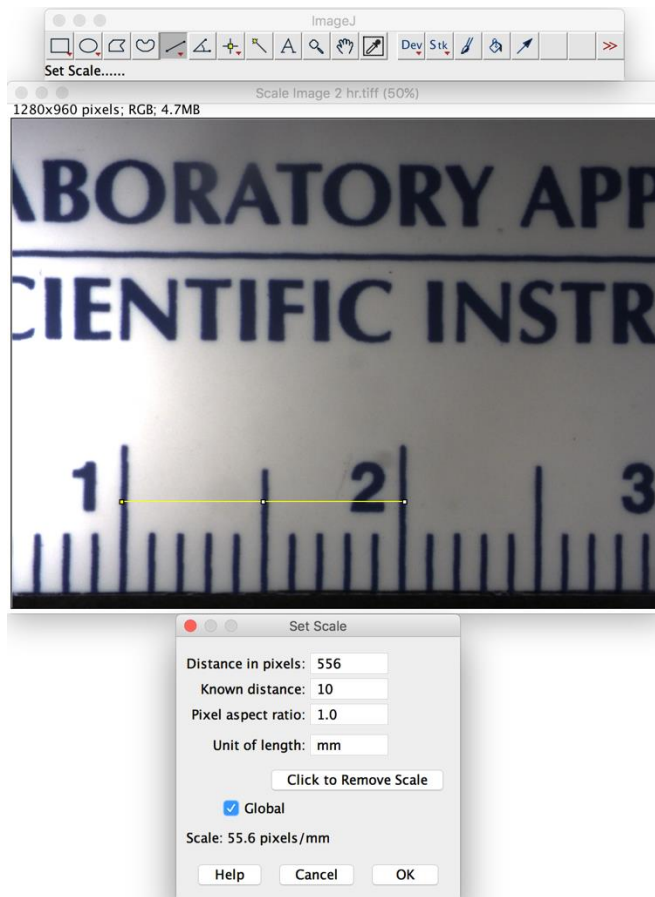
- Image the samples using the Zeiss microscope in Page's lab for the various timepoints as shown below.



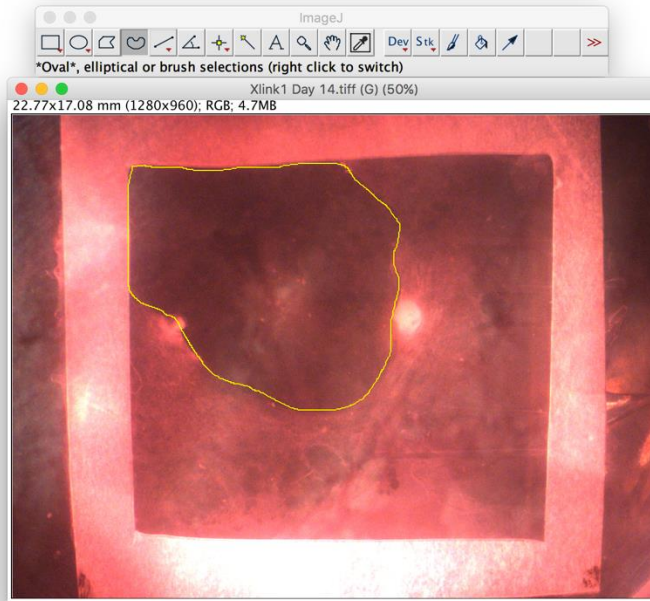
- After imaging all of the samples image a picture of a ruler for a scale image as shown below. This will allow for setting an accurate scale in ImageJ



- First load the scale image into Image as shown by either going through the open tab and searching for the image file or dropping the file into the ImageJ tab. Then using the straight line bar feature to draw a line for the known distance. Then under the analyze tab click the set scale option. Then enter the appropriate known distance and unit to set the scale. Ensure to set global so that the scale is the same when assessing the sample images. This is shown below.



- Now that the scale is set, open the samples as shown and using the free form line feature, draw around the area that was degraded on the sample as shown below.



- Then under the analyze tab, select measure and it will calculate the area of the drawn shape.

The screenshot shows the "Results" window in ImageJ. It contains a table with the following data:

	Area	Mean	Min	Max
1	66.346	79.838	44	209

## Appendix I: Raw Data Table for Alignment Analysis

<b>Film</b>													
	1	2	3	4	5	6	7	8	9	10	11	Total	
<b>Bin</b>	Cell #	%											
10	473	395	28	161	802	671	840	68	388	584	991	5401	13%
20	406	352	28	142	702	663	709	40	353	522	872	4789	12%
30	331	324	22	159	550	761	647	51	342	505	731	4423	11%
40	287	345	21	166	516	812	550	36	403	532	703	4371	11%
50	265	336	18	177	452	818	474	44	398	531	647	4160	10%
60	215	370	21	174	481	762	466	42	413	565	676	4185	10%
70	228	323	17	143	566	809	425	37	416	483	726	4173	10%
80	204	311	11	162	666	695	415	36	445	484	839	4268	11%
90	239	294	21	163	758	682	475	51	492	478	942	4595	11%
<b>Total</b>	2648	3050	187	1447	5493	6673	5001	405	3650	4684	7127	40365	

<b>Composite</b>											
	Sample 1	Sample 2	Sample 3	Sample 4	Sample 5	Sample 6	Sample 7	Sample 8	Sample 9	Total	
<b>Bin</b>	Cell #	Cell #	%								
10	70	289	111	1392	368	254	395	204	136	3219	15%
20	30	273	74	1446	296	106	349	246	140	2960	14%
30	46	245	70	1368	310	100	327	226	138	2830	13%
40	29	204	64	1131	268	96	318	172	135	2417	11%
50	22	196	60	857	217	100	324	267	135	2178	10%
60	33	177	53	812	183	63	309	195	222	2047	9%
70	40	212	47	796	200	88	257	199	205	2044	9%
80	31	215	55	556	190	92	399	365	203	2106	10%
90	25	135	81	583	186	129	389	152	187	1867	9%
<b>Total</b>	326	1946	615	8941	2218	1028	3067	2026	1501	21668	